BHABHA ATOMIC RESEARCH CENTRE STUDIES IN COLD FUSION

COLD FUSION

TECHNICAL NOTE

KEYWORDS: *palladium, fusion, electrolysis, deuterium, tritium, neutrons*

P. K. IYENGAR, M. SRINIVASAN, S. K. SIKKA, A. SHYAM, V. CHITRA, L. V. KULKARNI, R. K. ROUT, M. S. KRISHNAN, S. K. MALHOTRA, D. G. GAONKAR, H. K. SADHUKHAN, V. B. NAGVENKAR, M. G. NAYAR, S. K. MITRA, P. RAGHUNATHAN, S. B. DEGWEKAR, T. P. RADHAKRISHNAN, R. SUNDARESAN, J. ARUNACHALAM, V. S. RAJU, R. KALYANARAMAN, S. GANGADHARAN, G. VENKATESWARAN, P. N. MOORTHY, K. S. VENKATESWARLU, B. YUVARAJU, K. KISHORE, S. N. GUHA, M. S. PANAJKAR, K. A. RAO, P. RAJ, P. SURYANARAYANA, A. SATHYAMOORTHY, T. DATTA, H. BOSE, L. H. PRABHU, S. SANKARANARAYANAN, R. S. SHETIYA, N. VEERARAGHAVAN, T. S. MURTHY, B. K. SEN, P. V. JOSHI, K. G. B. SHARMA, T. B. JOSEPH, T. S. IYENGAR, V. K. SHRIKHANDE, K. C. MITTAL, S. C. MISRA, M. LAL, and P. S. RAO

Bhabha Atomic Research Centre, Trombay, Bombay 400 085, India

Received December 1, 1989
Accepted for Publication January 18, 1990

EDITOR'S COMMENT

George H. Miley

The following collection of technical notes on cold fusion were submitted by staff from the Bhabha Atomic Research Centre (BARC) in India. They have gone through the technical note review process and appear here as a collection of reports that provide insight into the breadth of the studies at BARC.

The preface that follows is an edited version of the inaugural talk delivered by P. K. Iyengar, director of BARC, at the meeting on cold fusion held in Trombay on May 18, 1989.

PREFACE

P. K. Iyengar

Energy production in the universe is mostly based on nuclear reactions, especially fusion reactions of light element nuclei. Energy production in the sun based on fusion of hydrogen, its isotopes, and elements up to carbon has been well theorized by now. It is natural to expect that there is a large variety of nuclear reactions that will lead to the production of nuclear energy. In fact, there is a whole gamut of fusion reactions in astrophysics that suggest various combinations of nuclear interactions and modes of decay for energy production. The collapse of binary stars and the transformation of neutron stars into black holes are the ultimate phases of stellar evolution and production of fusion energy. Even before the discovery of the neutron, scientists had predicted and even tried to prove that nuclear energy could be generated through fusion of hydrogen nuclei (protons). It was, however, only after detailed accelerator-based research in nuclear physics that the cross sections and Q values for these reactions became available. This led to many conjectures. Some of the candidate reactions considered for the generation of fusion energy are $(p + p)$, $(p + d)$, $(d + d)$, $(d + t)$, etc.

The familiarity of scientists with accelerator-based nuclear reactions, however, led them to believe that fusion reactions can take place only on the basis of overcoming the potential barrier caused by the electrostatic interaction. This demands that the particles have considerable relative velocity, and from the analogy of what is happening in the sun, thermonuclear fusion was considered to be the most appropriate technique for releasing fusion energy on a large scale. We are all aware of the many experimental attempts that have been made over the last four decades to obtain conditions appropriate for thermonuclear fusion. The principle of confinement of these hot plasmas by means of complex magnetic fields in special configurations was developed in the early 1950s. Of these, the tokamak has been a major success and has almost reached the stage of breakeven in energy production.

However, the large size and expensive equipment needed to attain even this breakeven stage have raised doubts about its commercial viability. The technique of generating temperatures of 100 million degrees using the principle of inertial confinement was first demonstrated in a thermonuclear bomb. The same principle has been borrowed and adapted in making fusion reactions possible in small pellets using lasers, electron beams, and heavy-ion beams. However, even this approach of releasing nuclear energy through a series of fusion microexplosions has not lived up to its early expectations as the power and energy of the driver beams for obtaining the

requisite pellet energy gain became uncomfortably high. Small, more elegant methods are therefore being attempted. Techniques such as Z pinches, combined magnetic, and inertial confinement schemes are under experimentation. As an interim measure, it has been suggested that fusion devices may be employed as a source of neutrons for producing fissile fuel for use in fission reactors. Thus, in the quest to establish the best method of producing fusion energy, there has been considerable innovation and exchange of new ideas during the last decades. However, new ideas are always welcome and must be tried.

Cold fusion is one such innovation that, on the face of it, looks so simple that it seems too good to be true. It has generated considerable speculation on the processes that cause fusion in the solid state at room temperatures. The basic problem is essentially to bring together ions of hydrogen isotopes at distances of a few fermis so that fusion takes place. It is worth recalling previous attempts to bring together hydrogen nuclei to distances at which the spontaneous fusion rate would increase considerably. The most effective method has been the replacement of the orbital electron of a molecular hydrogen ion by a μ meson or muon, as it is called. Because of its heavier mass, the muon is able to squeeze the nuclei into a more compact molecule and cause a fusion reaction. The muon is found to have an additional advantage: Because of its longer lifetime (2 μs), freed after a fusion reaction, it is able to catalyze more fusions. Almost 200 catalyzed fusions per muon have been experimentally observed in (d-t) mixtures to date. Some of the same scientists who were concerned with the physics of muon-catalyzed fusion have now reported cold fusion in a lattice of palladium.

In terms of understanding the physics behind cold fusion, one needs to discuss the lattice structure and its rearrangement when hydrogen is absorbed in palladium, titanium, or other alloys used for the storage of hydrogen. Because enormous quantities of hydrogen can be stored in these materials at densities comparable to or higher than that of liquid hydrogen, it was suggested that perhaps the internuclear distances could be reduced in such lattices. Many attempts have been made by theorists to evaluate the fusion rate in such lattices. Some of these are based on an extension of the well-known theory for muon-catalyzed fusion, wherein both the internuclear distances and the height of the potential barrier are varied. Both have the effect of increasing the fusion rate from 10^{-64}/s per ion pair in heavy water to something of the order of 10^{-23}/s per ion pair, which is required to explain the experimentally observed neutron production rate in cold fusion experiments. Whether it is possible to have such drastic changes in the fusion probability, which is essentially dictated by quantum mechanics considerations, is a matter of intense debate and discussion.

I would like to invite your attention to a novel application of the principles of quantum mechanics to such a problem. Several years ago, Rand McNally speculated on the feasibility of the occurrence of nuclear reactions at room temperature and was perhaps the first person to coin the phrase "cold fusion" as early as in 1983. To quote his own words: "The problem of neutron transfer in solid media is no longer an elementary binary collision process involving Coulomb barriers and brief collision times but rather one in which the nuclei are continuously in each other's proximity. Since ^{135}Xe has a slow neutron capture radius approaching that of the interatomic distance, the nuclear barrier would perhaps be grossly reduced. Thus, it is remotely possible that some combination of natural processes may permit barrier penetration to occur much more readily and a nuclear reaction to ensue." He also proposed the term "de Broglie interaction length" to emphasize that the de Broglie wavelength of particles with small kinetic energy is very long. The importance of the de Broglie interaction length can be seen in the extraordinarily high cross section for absorption of slow neutrons by certain nuclei. It is therefore of interest to know what the de Broglie interaction length of a deuteron with very small energy is in a palladium lattice. Furthermore, what happens to the charge distribution of such a deuteron extended in space and the effects of its polarization are too speculative. If the charge distribution has dimensions of the order of a de Broglie interaction length, then the potential barrier due to Coulomb interaction may perhaps become much smaller. If so, then fusion should be much more probable at very low temperatures.

From the experimental point of view, the proof of cold fusion must come from a demonstration of the production of neutrons, ^{3}He, ^{4}He, tritium, gamma rays, and other end products of nuclear transmutation reactions. Unfortunately, experiments performed so far have used very small electrodes and small cells, and there have not been sufficiently large experiments that can give unqualified proof of the number of neutrons or radioactivity produced from this process. Our attempts in different groups at Trombay have, however, all shown reliable data on neutron and tritium production. These are described in the various reports included in this technical note. It is interesting that fusion reactions also take place when deuterium ions are introduced into a metallic lattice by simply absorbing deuterium gas into titanium or palladium. The group at Frascati, Italy, first succeeded in producing neutrons by this method.

It is not our expectation that cold fusion will become an energy source tomorrow or the day after. After all, even in 1939 when neutron-induced fission in uranium was discovered, it took several years to find out how to set up a fission chain reaction and release fission energy on a large scale. Without detailed measurements of the number of neutrons produced in fission by the Columbia University group and Fermi's invention of the heterogeneous neutron multiplying system, the nuclear reactor would not have become a reality. Similarly, one has to explore and understand the basic mechanisms of fusion in a lattice and determine how this could be used either to produce energy directly or to produce neutrons and tritium in a sustained manner. It is too early to predict the time frame in which this will happen, but for those of us familiar with the historical evolution of nuclear technology, one can foresee how it can change our perspective drastically. It is therefore necessary for us to involve ourselves deeply in understanding the mysteries of this new phenomenon. The source of such energy, deuterium, is ordinary water, which is plentiful, and the technology to separate and concentrate deuterium from water is by now well established in our country.

I therefore end this preface by quoting from what Dr. Homi Bhabha said at the First International Conference on Peaceful Uses of Atomic Energy in 1955. He predicted that "in a couple of decades from now, fusion energy will become possible and that will ensure energy production for human needs as long as there is sea water on this earth." It is therefore a historical occasion for us to renew our efforts in research and development in an area so vital for human prosperity. I hope this technical note will stimulate the interest of scientists and engineers from various disciplines to channel their efforts in such a way that we lead in this emerging technology.

SUMMARY

P. K. Iyengar and M. Srinivasan

These reports are a compilation of the work carried out at Bhabha Atomic Research Centre (BARC), Trombay, during the first 6 months of the "cold fusion era," i.e., April to September 1989. Over 50 scientists and engineers, as well as many technicians, from more than ten divisions have been associated with these studies. This technical note investigates cold fusion based on electrolysis and summarizes work based on D_2 loading in the gas phase.

Several groups with expertise in various areas, such as hydriding of metals, electrochemistry, isotope exchange processes in the concentration of heavy water, and neutron and tritium measurements, devised and set up a variety of electrolytic cells. Table I summarizes some of the successful electrolysis experiments. Neutron and tritium production was confirmed in all these cells. However, many cells that were tested failed to give any positive results. These are not included in the table.

Our investigations positively confirm the occurrence of (*d-d*) fusion reactions in both electrolytic and gas-loaded palladium and titanium metal lattices at ambient temperatures. Neutron emission was observed at times even when the current to the electrolytic cell was switched off or, in the case of gas-loaded titanium targets, when no externally induced perturbation, such as heating, cooling, evacuation, etc., was effected. The main results of the BARC investigations are as follows:

1. Tritium is the primary end product of cold fusion reactions with the neutron-to-tritium yield ratio being $\sim 10^{-8}$. Thus, cold fusion may be characterized as being essentially "aneutronic."

2. Neutron emission from electrolytically loaded palladium and gas-loaded titanium is basically Poisson in nature; i.e., the neutrons are emitted one at a time. However, it is not clear whether the neutrons are generated in the (*d-d*) fusion reaction itself or whether they are produced in a secondary reaction involving the energetic protons or tritons. In this context, it would be of interest to investigate the possible presence of 14-MeV neutrons in cold fusion experiments.

3. About 10 to 25% of the neutrons produced appear to be generated in groups of over 100 neutrons each within <20 ms. Based on the neutron-to-tritium yield ratio of 10^{-8}, we conclude that a cascade representing more than 10^{+10} fusion reactions occurs in <20 ms. Since this appears very unlikely, lattice cracking, wherein the neutron-to-tritium branching ratio is close to unity, could be a source of these bunched neutron events.

4. Autoradiography of gas-loaded titanium and palladium targets demonstrated the presence of tritium. The experimentally deduced tritium/deuterium isotopic ratio in these targets is several orders of magnitude higher than in the initial D_2O and cannot be explained on the basis of preferential absorption of tritium by the titanium or palladium. The existence of highly localized regions (hot spots) on the target surface where tritium is concentrated, as well as the occurrence of spots along the periphery of the disk, illustrates the important role of lattice defect sites in the absorption process, at least in the case of titanium.

The very high probability for the tritium branch in cold (*d-d*) fusion reactions indicates processes of neutron transfer across the potential barrier, as postulated by Oppenheimer over 50 years ago. If neutron transfer takes place so easily, it may have many implications for the future of nuclear technology. The deuterium nuclide may very well do the work that free neutrons currently do in fission reactors.

TABLE I

Electrolytic Cell Experiments Conducted at BARC

Cathode material	Palladium-silver	Palladium-silver	Titanium	Palladium	Palladium	Palladium
Anode material	Nickel	Nickel	Stainless steel	Platinum	Platinum	Platinum
Geometry of cathode	Multiple tubes	Circular sheet	Rod	Hollow cylinder	Ring	Cube
Cathode pretreatment	Activated	---	---	---	Vacuum annealed	Vacuum heated
Electrolyte type	5 *M* NaOD	5 *M* NaOD	5 *M* NaOD	0.1 *M* LiOD	0.1 *M* LiOD	0.1 *M* LiOD
Volume (ml)	250	1000	135	45	250	150
Cell current (A)	60	65	40	1 to 2	1	0.6 to 0.8
Current density (mA/cm^2)	200	650	?	170	60	100 to 130
Tritium atoms	8×10^{15}	4×10^{15}	1.3×10^{14}	4×10^{14}	2×10^{11}	6.7×10^{11}
Neutron yield	8×10^{7}	4×10^{6}	1.3×10^{7}	3×10^{6}	1.8×10^{8}	1.1×10^{6}
Neutron-to-tritium ratio	10^{-8}	10^{-9}	10^{-7}	0.8×10^{-8}	0.9×10^{-3}	1.7×10^{-6}

PART A: ELECTROLYTIC CELL EXPERIMENTS

1. COLD FUSION EXPERIMENTS USING A COMMERCIAL PALLADIUM-NICKEL ELECTROLYZER

M. S. Krishnan,* S. K. Malhotra,* D. G. Gaonkar,*
M. Srinivasan,+ S. K. Sikka,+
A. Shyam,+ V. Chitra,+ T. S. Iyengar,†
and P. K. Iyengar‡

Introduction

The first reported observations of "cold fusion" during the electrolysis of heavy water[1,2] using palladium cathodes resulted in attempts at several laboratories to duplicate these experiments and, if possible, improve upon them. Electrolytic cold fusion investigations were initiated at Trombay in the first week of April 1989 as a collaborative effort between the Heavy Water and Neutron Physics Divisions of the Bhabha Atomic Research Centre (BARC). A commercial diffusion-type palladium-silver cathode/nickel anode hydrogen generator was used, loading NaOD as the electrolyte in place of the original NaOH. This report gives details of the electrolyzer characteristics, conditions of operation, and the neutron and tritium measurements.

*Heavy Water Division.
+Neutron Physics Division.
†Health Physics Division.
‡Director.

The Electrolyzer

The electrolyzer is a diffusion-type ultrapure electrolytic hydrogen generator.[a] A schematic of the electrolytic cell is shown in Fig. 1. The anode is made of nickel and the cathode consists of specially activated palladium-silver alloy membrane tubes. The nickel outer body of the cell and a central nickel pipe serve as coaxial anodes. The 16 cathode tubes are mounted with polytetrafluoroethylene (PTFE) spacers between the anode pipes as shown in Fig. 1 and have a total wet surface area of $\simeq 300$ cm^2. The cathode tubes are sealed at

[a]ELHYGEN Hydrogen Generator (Mark V), manufactured by the Milton Roy Company, Shannon Industrial Estate, Clare, Ireland.

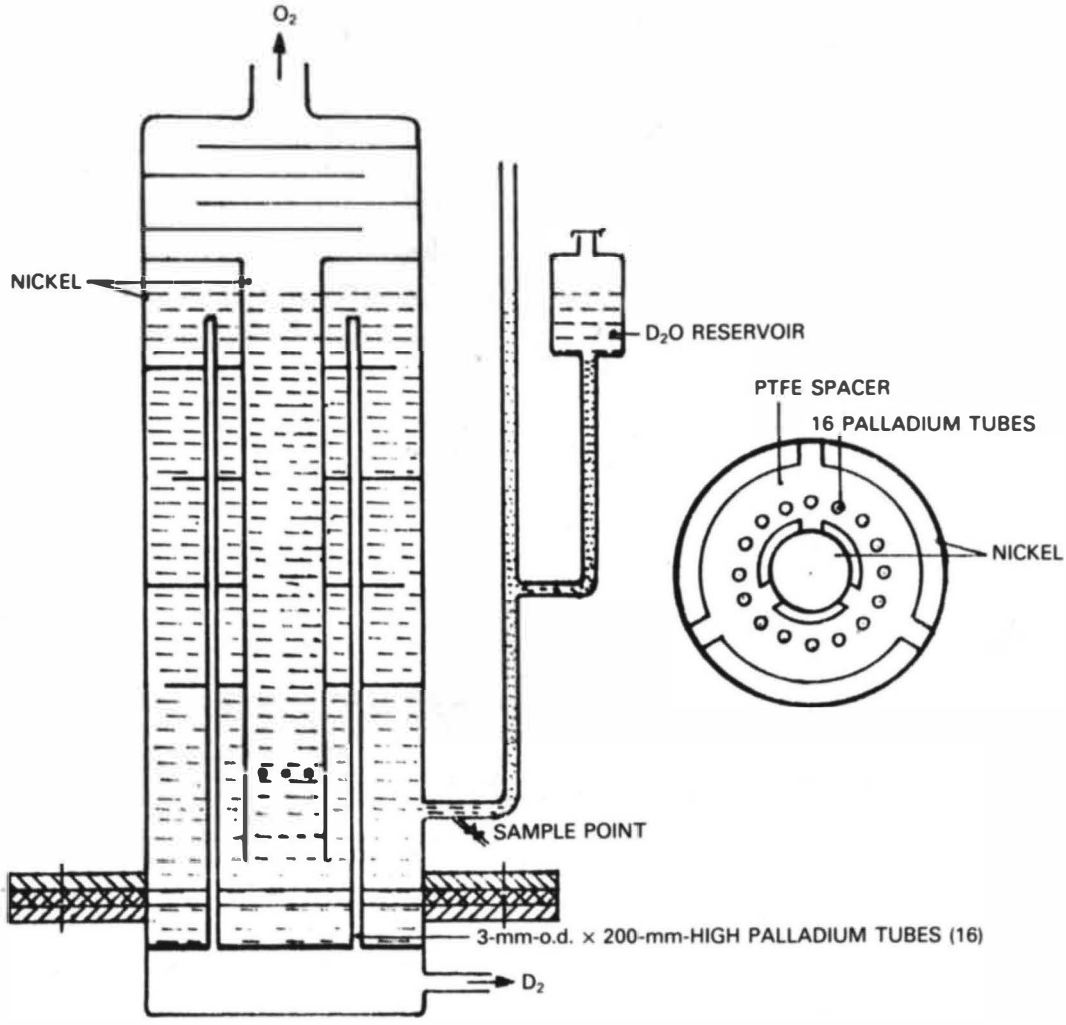

Fig. 1. Electrolytic cell and palladium tube arrangement.

the top, and they open at the bottom into a plenum through which the deuterium (or hydrogen) gas is drawn. The outlet of the gas plenum can be closed with a valve so that the deuterium pressure is allowed to build up. A pressure gauge reading up to 4 kg/cm^2 is provided. The important cell parameters are summarized in Table I.

The electrolyte is 20% NaOD in D_2O of >99.75% isotopic purity prepared by a reaction between moisture-free sodium and D_2O. The oxygen generated at the anodes during electrolysis escapes through a vent at the top of the cell. A set of baffle plates at the top prevents alkali carryover into the vent. The hydrogen and deuterium ions that impinge on the cathodes under the influence of the applied electric potential diffuse through the walls of the palladium-silver tubes and escape into the gas plenum. The ions recombine inside the tubes to form molecular deuterium, which is found to be of very high purity as analyzed by gas chromatography. The electrolyte level in the cell is maintained through a connected reservoir. The unit is completely automatic and is equipped with pressure control, a solenoid valve, electrolyte leak detector, low water level signal, and temperature control.

The built-in power supply is only capable of a current of ≃70 A. During the initial runs, this alone was used and operation was restricted to current values of 60 to 62 A. An important feature of the cell design, however, is its potentially high current-carrying capacity. The electrolyzer was connected to an external power supply capable of giving >100 A during subsequent runs. Current levels of ~100 A, however, were found to be possible only for short durations as the cell became overheated. To overcome this, a heat exchanger and a peristaltic pump were incorporated, enabling circulation of the electrolyte.

Neutron Monitoring

Initially, two types of neutron detectors were used to monitor the neutron yield from the electrolytic cell: a bank of three BF_3 counters embedded in a paraffin moderator block and an 80-mm-diam × 80-mm-high recoil NE-102A plastic scintillator sensitive to both fast neutrons and high-energy gammas. The detectors were mounted ~10 cm from the cell. The counting efficiency of these detectors was established using a calibrated plutonium-beryllium neutron source. The counting rates of the detector outputs were totaled for 5 min each and printed out continuously on a scroll printer. During the first run, there was no separate background neutron monitor. In subsequent runs, however, a bank of three ^{3}He detectors, also embedded in a paraffin block, was installed ~1.5 m from the cell to serve as a background monitor. A personal computer was used to graphically display the count rate variations and to accumulate and store the count data registered in 20-ms intervals for the neutron multiplicity distribution analysis as described in report A.4 of this technical note.

In some of the more recent runs, a bank of specially fabricated silver cathode GM tubes embedded in a paraffin slab was used as an activation detector for neutrons. This type of neutron detector is ideally suited for measuring the yield of a burst of neutrons produced in a time span of ~10 s or less. The neutron yield is deduced by counting the 24-s half-life of ^{110}Ag activity induced in the silver cathode. The threshold sensitivity of the system for the geometry used, determined using a calibrated plutonium-beryllium neutron source, was ≃3 × 10^5 neutrons.

Measurement of Tritium Levels in D_2O Electrolyte

The absolute levels of tritium in the D_2O electrolyte were measured by the Tritium Group of the Health Physics Division. Details of the liquid scintillation counting techniques along with precautions taken to minimize errors due to chemiluminiscence and other interference effects are discussed in report A.9 of this technical note. After the initial electrolysis runs, a valve was welded to the cell bottom to enable periodic sampling of the electrolytic solution for tritium assay.

Recently, two microprocessor-controlled on-line instruments for counting tritium activity using low-energy sensitive scintillation fibers were installed, one in the gas-phase analysis and the other for electrolytic solution counting. The development, testing, and calibration of these instruments were carried out by the Pollution Monitoring Section of BARC. These instruments employ two photomultiplier tubes each in coincidence to suppress noise effects.

Electrolysis Experiments and Observations

Run 1 (April 21, 1989)

The electrolytic cell was first operated with 20% NaOH in natural water as the electrolyte. This operation continued for ~48 h to collect background data. The cell was then drained, flushed with heavy water, and filled with 20% NaOD solution in D_2O. The cell was operated initially at 30 A; the current was later slowly raised to 60 A, corresponding to a current density of ~200 mA/cm^2. After operating under these conditions for ~3 h, both neutron counters showed bursts of neutron counts, well above background values, during some of the 5-min intervals. After a few more hours, both counting channels suddenly showed two very large peaks. At the time of the last peak, the current in the electrolyzer suddenly increased to ~120 A on its own and the electrolyzer immediately tripped. It was later found that the polyvinylchloride insulation of the electric connections between the dc power supply and the electrolyzer had melted, as had the soldering at the joint. The diodes of the power supply had also burned out, causing the trip.

The neutron count data of this run are presented in Table II and in Fig. 2. The counting efficiency of the BF_3 bank and the plastic scintillator was 0.06 and 0.4%, respectively. That both the counters showed identical behavior in spite of having very different neutron detection characteristics is noteworthy. The total number of neutrons generated during the 4 h of this run is estimated to have been ~4 × 10^7.

It is observed from the neutron count data of run 1 plotted in Fig. 2 that while the BF_3 bank recorded at least nine

TABLE I

Details of the Electrolytic Cell

Volume of palladium cathode (cm^3)	7
Mass of palladium (g)	82
Area of cathode (cm^2)	300
Current (A)	60
Current density (mA/cm^2)	=200
Electrolyte	20% NaOD in D_2O
Volume of electrolyte (ml)	250

TABLE II

Neutron Counts over Time

(April 21, 1989)

Interval duration (min)	5
Efficiency of BF_3 bank (%)	0.06
Efficiency of plastic scintillator (%)	0.4

	Neutron Counts			Neutron Counts	
Interval	BF_3	Plastic Scintillator	Interval	BF_3	Plastic Scintillator
1	74	683	26	78	636
2	74	659	27	64	606
3	55	605	28	62	640
4	68	672	29	61	659
5	75	686	30	55	603
6	79	693	31	68	631
7	54	650	32	58	755
8	73	612	33	65	647
9	77	641	34	1 680	2 827
10	167	727	35	174	788
11	54	643	36	254	1 176
12	124	769	37	269	977
13	74	663	38	329	1 290
14	64	629	39	113	624
15	429	1654	40	107	622
16	72	627	41	59	626
17	58	630	42	75	606
18	65	641	43	139	619
19	60	655	44	101	714
20	56	663	45	107	958
21	180	1086	46	74	656
22	367	1185	47	17 758	25 872
23	109	707	48	77	592
24	70	614	49	1 982	3 874
25	68	732	---	---	---

clearly visible peaks, the plastic scintillator missed some of the smaller peaks. This is obviously due to the higher background level of the plastic scintillator due to its sensitivity to gammas. The smaller peaks apparently were buried in the statistics of the background.

The ratio of the counts under the peaks in the two channels after subtracting the background varies between 1.3 and 2.8, which is considerably different from the value of ~6.7 expected from their efficiencies determined using a plutonium-beryllium neutron source. This discrepancy may be attributed to the following points: (a) The plastic scintillator is sensitive to the plutonium and beryllium gammas, indicating a higher sensitivity, and (b) the energy spectrum of cold fusion neutrons could be different from that of plutonium-beryllium source neutrons. Since the energy response characteristics of the plastic scintillator and BF_3 bank are different, the efficiency ratios for plutonium-beryllium neutrons and cold fusion neutrons could be quite different.

From a detailed analysis of the neutron multiplicity spectrum, it has been found that between 10 and 25% of the cold fusion neutrons are emitted in bunches of 100 or more. While the BF_3 bank can resolve and individually count a number of simultaneous incident neutrons, the plastic scintillator gives only a single pulse (although of a much larger height). In fact, by comparing the measured ratios of the counts under the peaks in the two channels with the expected efficiency ratio, one can approximately assess the fraction of the neutrons in each burst this is due to bunched neutronic events. In run 1, it is found that the larger peaks generally seem to contain a higher fraction of bunched events.

At the end of this experiment, a sample of the electrolyte indicated 1.5 μCi/ml of tritium activity in comparison to the initial stock heavy water value of 0.075 nCi/ml. This increase of a factor of ~20 000 is far beyond what can be accounted for by electrolytic enrichment alone.

Run 2 (June 12-16, 1989)

The second series of electrolysis runs commenced during the first week of June 1989. The cell was drained and flushed with heavy water many times for tritium decontamination. Fresh electrolyte solution prepared using new heavy water

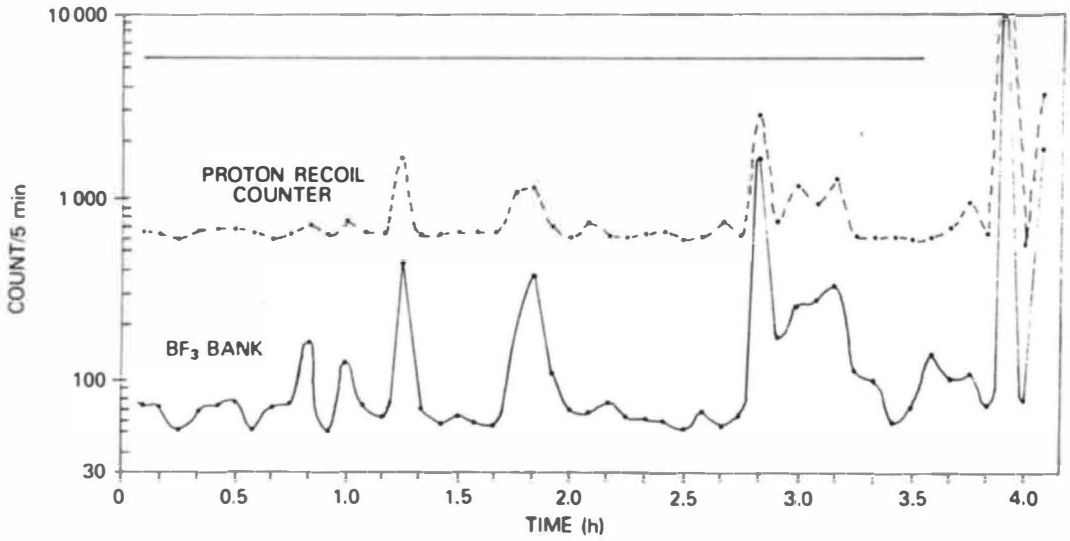

Fig. 2. Neutron count data from run 1.

was charged and left in the cell over the weekend. On June 12, a sample of this electrolyte gave a surprisingly high tritium level of ~0.32 nCi/ml. This is attributed to tritium left in the palladium-silver cathodes from run 1 that must have transferred back into the electrolyte by chemical exchange.

Electrolysis commenced at 1107. The cell was initially operated at currents of ~60 A (current density ~200 mA/cm^2). During this run, the BF_3 bank in paraffin was near the cell. A ^{3}He bank in paraffin ~1.5 m away served as background monitor. The first neutron burst of this run was recorded within ~0.5 h, at 1140. About 1 h later, two more 5-min counts indicated high neutron levels. No more neutron bursts were observed for the next few days, although cell operation was continued until 1745 on June 14 when the cell was turned off. Within a few hours, there was a neutron burst lasting 15 min. Samples of electrolyte were drawn periodically throughout this operation and sent for tritium analysis. The tritium content of the electrolyte did not show any increase. Rather, it decreased from 0.32 to 0.12 nCi/ml on June 15. This decrease is attributed to the fact that electrolyte containing 0.075 nCi/ml of tritium was added continuously to maintain the level of the electrolyte. This obviously diluted the tritium content in the electrolyte.

During the next 48 h, the neutron monitors did not show any increase in counts. On the night of June 16, more than 2 days after turning off the cell current, however, a large neutron burst was recorded that corresponded to a total neutron yield of well over 10^6 neutrons. Figure 3 shows a plot of neutron count variation during this burst. The detailed time structure of this burst is presented in Table VII of report A.4 of this technical note. A sample of electrolyte was drawn on June 23 to ensure that the maximum amount of tritium on the palladium cathodes would by then have exchanged with the bulk D_2O. This indicated a tritium level of 121 nCi/ml. The week-long experiment was terminated at this point, but the electrolyzer was left with the electrolyte in the cell and deuterium in the gas plenum at a pressure of 1 kg/cm^2 above atmospheric pressure. After ~1 month, when the electrolyte was removed and analyzed, the tritium level was found to have increased to 460 nCi/ml, corresponding to a fourfold rise in the tritium level. It is not clear whether this is due to additional fusion reactions occurring while the cell was quiescent or whether the earlier tritium buildup continued to leach out into the electrolyte.

Discussion

The results of these neutron and tritium measurements are tabulated in Table III. The observed tritium concentrations have been corrected for enrichment effects due to electrolytic separation of deuterium and tritium as well as evaporation losses. Note that tritium production is much higher than the neutron yield, although in "hot fusion" their probability is known to be approximately equal. Our experimental observation is that both neutron and tritium generation seem to be occurring simultaneously because no tritium and neutron peaks were observed for a long time, but the tritium level of the electrolyte increased multifold after a neutron burst was noticed. The observation in run 2 shows that both neutron peaks and tritium were recorded only ~30 h after the current had been turned off. An important observation of this work is that "spent" palladium electrodes seem to lose their ability to support cold fusion reactions, as can be seen from a comparison of the results of runs 1 and 2. In the latter case, the number of neutrons and tritium atoms produced has decreased. This observation calls for further investigations. A multidimensional characterization of freshly deuterated and spent palladium electrodes, such as measurement of the metallographic and lattice structure will go a long way in understanding this phenomenon and may shed considerable light on the mechanism of cold fusion.

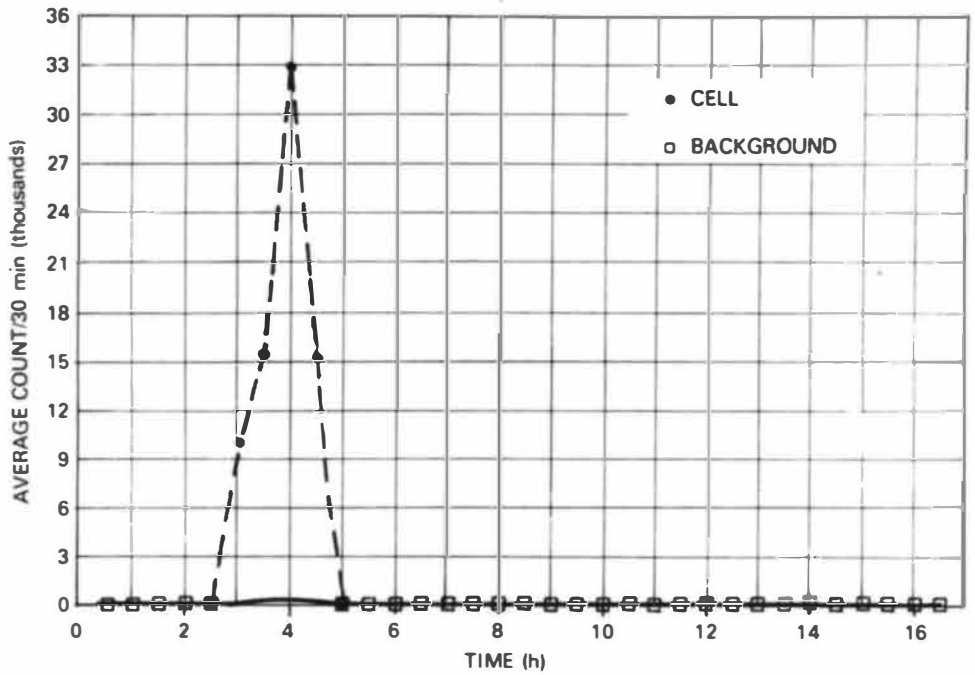

Fig. 3. Neutron yield variation during the burst on June 16, 1989.

TABLE III

Summary of Neutron and Tritium Yields

(Current density = 200 mA/cm^2)

Run	Duration of Electrolysis (h)	Total Neutron Yield	Atoms of Tritium Generated	Neutron to Tritium Yield Ratio
Run 1 (April 21, 1989)	72	4×10^7	8×10^{15}	0.5×10^{-8}
Run 2 (June 12-16, 1989)	54	9×10^6	5×10^{14}[a] 1.9×10^{15}[a]	$\sim 1.8 \times 10^{-8}$ 0.5×10^{-8}

[a]These were measured 30 h and 27 days, respectively, after the current had been turned off.

ACKNOWLEDGMENTS

The authors would like to acknowledge the unstinting cooperation received from several scientists in various aspects of these experiments. They are extremely thankful to each and every one of them. They include C. K. Pushpangathan, V. H. Patil, Arun Kumar, and N. P. Sethuram of the Heavy Water Division, and R. K. Rout and L. V. Kulkarni of the Neutron Physics Division. H. K. Sadhukhan, head of the Heavy Water Division, contributed immensely through fruitful discussions.

REFERENCES

1. M. FLEISCHMANN and S. PONS, "Electrochemically Induced Nuclear Fusion of Deuterium," *J. Electroanal. Chem.*, **261**, 301 (1989).

2. S. E. JONES et al., "Observation of Cold Nuclear Fusion in Condensed Matter," *Nature*, **338**, 737 (1989).

2. PRELIMINARY RESULTS OF COLO FUSION STUDIES USING A FIVE-MODULE HIGH-CURRENT ELECTROLYTIC CELL

M. G. Nayar,* S. K. Mitra,* P. Raghunathan,*
M. S. Krishnan,+ S. K. Malhotra,+ D. G. Gaonkar,+
A. Shyam,† and V. Chitra†

Introduction

In their first cold fusion paper,[1] Fleischmann and Pons suggested that an electrolytic cell with a large volume and surface area and a high current density may cause fusion reactions resulting in the production of significant amounts of heat and nuclear particles. The experiments reported here are the results of our early efforts to design and operate a high-current modular palladium-nickel electrolytic cell and look for cold fusion reactions.

Electrolyzer and Operation

A five-module cell with a bipolar filter press configuration using a palladium-silver alloy cathode (0.1 mm thick) and a porous nickel anode was fabricated. The electrodes have a circular plate geometry with a sectional area of $\simeq$78 cm^2. The five modules are connected in series and can be operated up to a current density of 1 A/cm^2 and temperatures of 100°C. The mixed gaseous products are carried out of the cell and recombined in a burner-condenser unit, and the resultant heavy water is recycled back to the electrolyzer. The electrolyte can be recirculated via a cooler to keep the operating temperature low enough to reduce evaporation losses. Figure 1 is a schematic of the modular cell. A flow diagram of the electrolyzer and accessories is shown in Fig. 2.

The D_2 and O_2 gases produced in the electrolyzer and evolving out in a mixed stream enter the recombination unit. This unit is essentially a burner complete with a self-igniter and a cooling arrangement so that the product of recombination, D_2O, is condensed and collected. Incremental quantities of oxygen can be continuously added to ensure the complete conversion of D_2 to D_2O.

The system was filled with freshly prepared NaOD in D_2O (20%) up to the preset mark in the level gauge. The electrolyzer was switched on and operated continuously at a current of 60 to 65 A (corresponding to an applied voltage of $\simeq$12.5 V) from May 5, 1989, onward, with a few hours of interruption due to failure of the dc power supply. The current was occasionally raised to 78 A. The characteristics of the cell are summarized in Table I.

The present operation was carried out to test the electrolyzer, recombination unit, and other subsystems. Sustained operation for extended periods of time, particularly in the closed-loop mode, was not carried out in this preliminary study.

TABLE I

Characteristics of the Five-Module Cell

Number of cathodes	5
Area of each cathode (cm^2)	$\simeq$78 per surface
Volume of each cathode (cm^3)	$\simeq$1
Total volume of electrolyte in system (cm^3)	1000
Current (A)	60 to 65 with occasional peaking at 78 A
Current density (mA/cm^2)	750

*Desalination Division.
+Heavy Water Division.
†Neutron Physics Division.

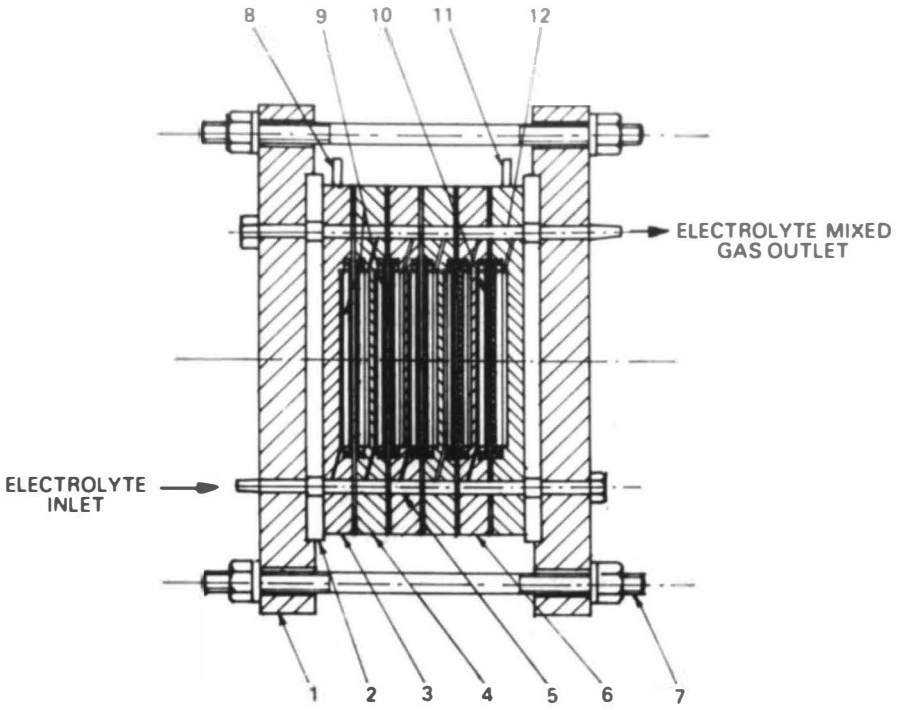

1 END FLANGE
2 INSULATOR
3 END PLATE
4 BIPOLAR PLATE
5 ELECTROLYTE INLET DUCTS
6 DIAPHRAGM GASKET
7 TIE ROD
8 ANODE TERMINAL
9 POROUS NICKEL ANODES
10 PALLADIUM-SILVER CATHODE
11 CATHODE TERMINAL
12 ELECTROLYTE AND GAS OUTLET DUCTS

Fig. 1. Five-module palladium-nickel electrolyzer.

Neutron and Tritium Measurements

The placement of neutron detectors around the cell was similar to that described in report A.1. Two neutron detectors, a bank of three BF_3 detectors embedded in paraffin, and an 80-mm-diam × 80-mm-high plastic fast neutron detector were used to monitor the neutron output. The count data were printed out on a scroll printer. The BF_3 channel counted for 110 s each while the plastic scintillator counted for 100 s each. Both counting intervals commenced at the same time. The cell had been operated continuously for 4 h when a large burst of neutrons overlapping two counting intervals was recorded in both detectors. Table II summarizes the neutron count data.

The tritium content of the electrolyte before and after electrolysis as analyzed by liquid scintillation counting techniques (see report A.9) was 0.055 and 190.3 nCi/ml, respectively. The significant quantities of tritium carried away by the combined D_2 and O_2 gas stream have not been included. Considering that the total volume of the electrolyte in the system including makeup was ~1 ℓ, this corresponds to a total tritium buildup of 190 μCi or 4×10^{15} atoms.

Conclusion

The electrolysis, though carried out only for limited periods, has shown conclusively that cold fusion occurs in this

TABLE II

Neutron Count Variations

BF_3 Channel (count/110 s)	Plastic Detector (count/100 s)
131	168
125	164
143	184
136	173
121	150
148	172
17 198[a]	1 563[a]
19 751[a]	21 113[a]
125	165
138	182
134	171

[a]The ratios of counts in the two channels were different in the two consecutive time intervals presumably because the single neutron burst is partitioned unequally in the two intervals. This is because the counting interval was 10 s longer in the BF_3 channel.

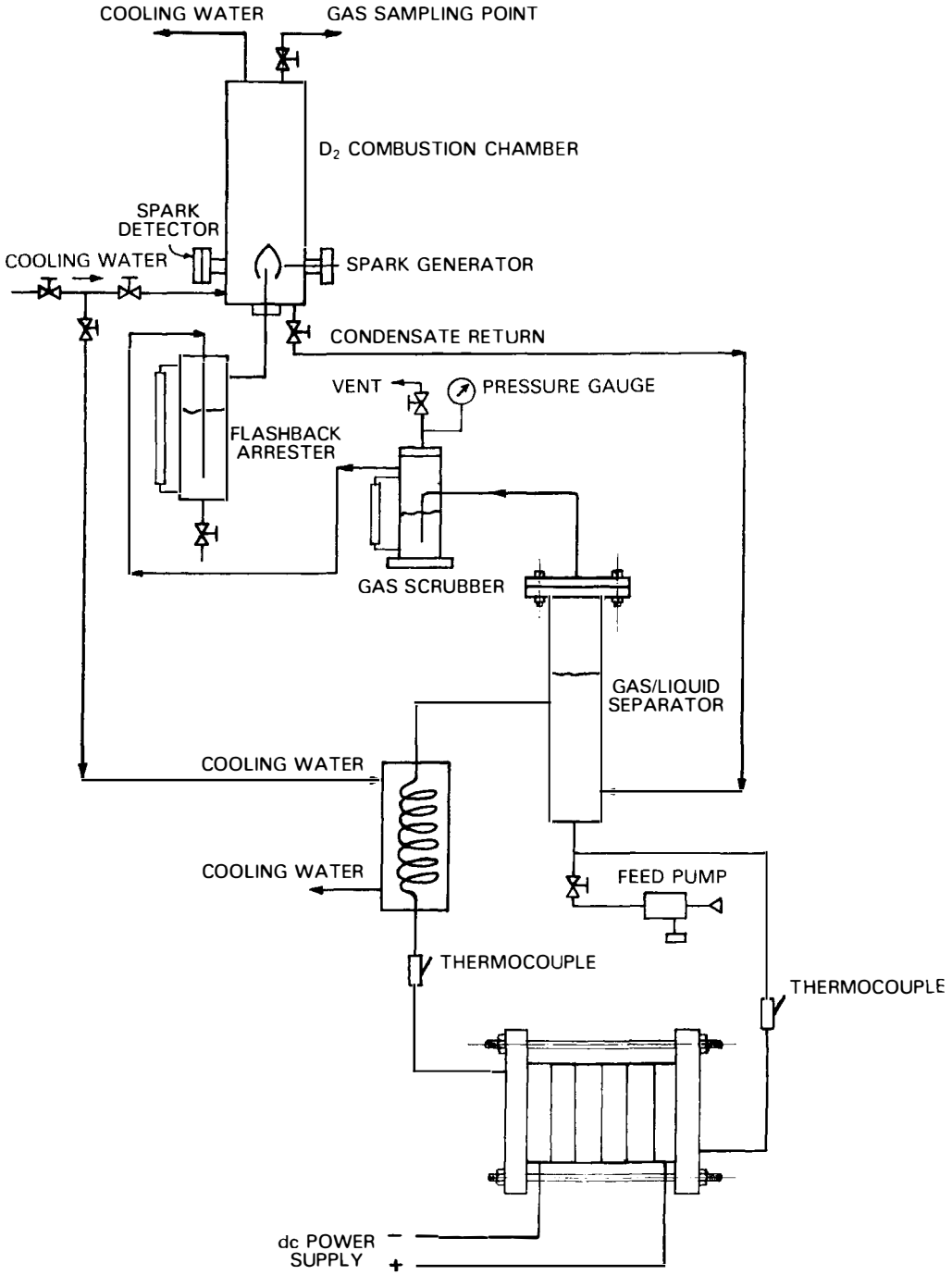

Fig. 2. Electrolyzer system for cold fusion studies.

system. This is obvious from the neutron bursts obtained (Table II) and the results of tritium analysis in the electrolyte. The latter results have shown an increase of >3500 times in the electrolyte after 50 h of operation.

From the efficiency of the neutron detectors and the neutron count data given in Table II, it is inferred that $\sim 5 \times 10^6$ neutrons were produced over a 100-s interval. The corresponding tritium yield was $\sim 4 \times 10^{15}$, suggesting a gross neutron-to-tritium yield ratio of $\sim 10^{-9}$. It must be emphasized, however, that a considerable quantity of tritium may have been carried away by the gas stream. Although efforts were made to recombine and recover the D_2O for tritium, they were not successful. The estimate of 10^{-9} for the neutron-to-tritium yield ratio may therefore be considered as a lower limit only.

These limited experimental studies have given enough experience to initiate a prolonged closed-cycle operation, where simultaneous counting of neutrons and monitoring of the

progressive buildup of tritium during electrolysis can be carried out.

ACKNOWLEDGMENTS

A number of scientists and engineers from the Desalination and Heavy Water Divisions contributed to the fabrication, installation, and operation of this cell. Their help is gratefully acknowledged.

REFERENCE

1. M. FLEISCHMANN and S. PONS, "Electrochemically Induced Nuclear Fusion of Deuterium," *J. Electroanal. Chem.*, **261**, 301 (1989).

3. OBSERVATION OF COLD FUSION IN A TITANIUM-STAINLESS STEEL ELECTROLYTIC CELL

M. S. Krishnan,* S. K. Malhotra,* D. G. Gaonkar,* M. G. Nayar,+ and A. Shyam†

Introduction

Since the two reports[1,2] of the occurrence of cold fusion, experiments have been initiated in a number of laboratories to study the electrolysis of D_2O using palladium as a cathode. In a few cases, titanium has also been used as a cathode. Titanium is a material of interest as it can form deuterides up to the composition of TiD_2 (against 0.6 in case of palladium). Titanium is also more easily available and less expensive in India. Three groups[3-5] have reported the use of titanium as the cathode in electrolytic experiments. Meanwhile, the use of titanium in deuterium gas-loading experiments has been reported[6] in which neutron bursts were observed under nonequilibrium conditions.

Having obtained very encouraging neutron and tritium yields with electrolytically loaded palladium (see report A.1), we decided to investigate titanium as a cathode material in the electrolysis of D_2O. The results of both neutron and tritium measurements are reported here. Unlike the palladium-nickel cell described in report A.1, which was a diffusion-type commercial hydrogen generator, the titanium electrolytic cell used for this work was a very simple design constructed from readily available materials.

Description of the Cell

A schematic of the cell is shown in Fig. 1. A 22-mm-diam × 150-mm-long cylindrical titanium rod constituted the cathode (104-cm^2 area), while a 4-cm-i.d. stainless steel outer tube served as the anode. The two electrodes were fixed coaxially with polytetrafluoroethylene (PTFE) spacers and gaskets. The interelectrode gap was 9 mm (surface to surface). As the cell does not have a provision for separating deuterium and oxygen, both gases were vented out the top. The cell also had a thermowell to measure the temperature of the electrolyte. A 5 *M* solution of NaOD in heavy water (isotopic purity of >99.8%) was used as the electrolyte, to achieve a high current density. An external dc power supply was used. The salient features of the electrolyzer are summarized in Table I.

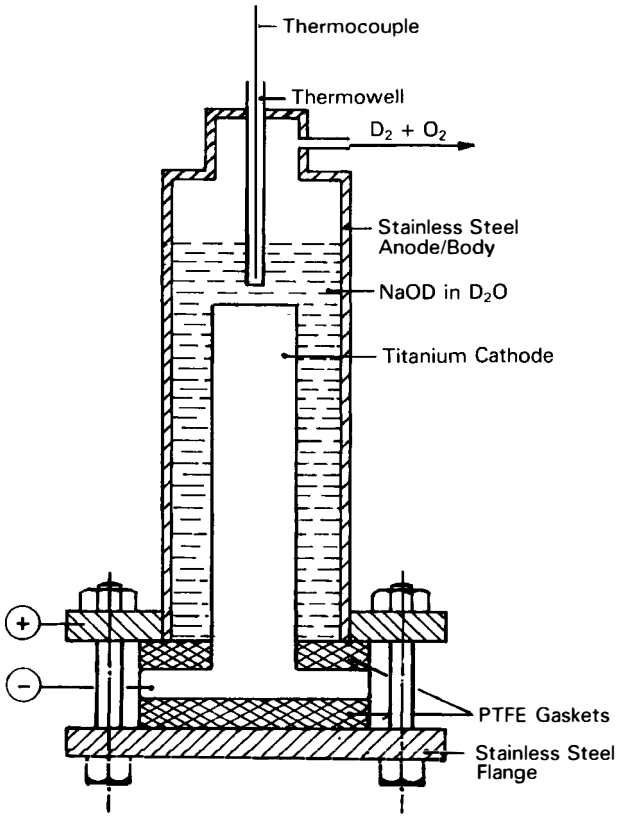

Fig. 1. Titanium-stainless steel electrolytic cell.

TABLE I

Salient Features of the Titanium-Stainless Steel Cell

Volume of titanium cathode (cm^3)	57
Area of cathode (cm^2)	104
Current (A)	40 to 60
Current density (mA/cm^2)	<600
Electrolyte	20% (5 *M*) NaOD in D_2O
Volume of electrolyte (cm^3)	150

Operation of the Cell

The electrolytic cell was first operated with 5 *M* NaOD in D_2O for ~8 h. Only temperature increase was recorded for this run. The current was raised slowly from 20 A (193 mA/cm^2 current density) to a maximum of ~40 A (~400 mA/cm^2 current density). The cell was then drained, flushed with distilled water several times, and operated for 12 h with an electrolyte of 5 *M* NaOH in H_2O. By this time, the neutron monitors were placed in position. Subsequently, the cell

*Heavy Water Division.
+Desalination Division.
†Neutron Physics Division.

was cleaned and rinsed, and a repeat run with 5 *M* NaOD in D_2O was conducted. As this cell does not have automatic electrolyte feed, the electrolysis was carried out as a batch process. After a few hours of operation, when the electrolyte level had decreased considerably, fresh electrolyte was added to make up the volume. The cell had operated for 8 h when the cathode was found to have attained a dull black coating, which when analyzed chemically was found to contain iron as the major component. The electrolyte solution also developed a pale greenish-yellow color because of the dissolution of iron from the anode. The cell is therefore being modified to have both the anode and the cathode made of titanium. In addition, the interelectrode gap between the anode and cathode is being reduced to attain larger current densities.

Neutron Measurements

A bank of three ^3He counters embedded in paraffin and a plastic scintillation detector were used for neutron measurements. The efficiency of the ^3He detectors was ~1%. The plastic scintillator was placed away from the cell and used as a background monitor. Background data were collected before electrolysis commenced. The background count in the ^3He channel was ≃240 count/10 s. Neutron measurements carried out with the cell operating with NaOH-H_2O were similar to the background data. But when the cell was operated with NaOD-D_2O, after ~3 h the level of the neutron count was higher (~590 count/10 s). No large bursts of neutrons were observed as in the palladium-nickel electrolyzer (report A.2). When higher counts were continuously indicated, the cell was turned off and the neutron count was observed to come down immediately, though it was still above background (~385 count/10 s). The experiment was finally terminated when the count level reverted to background, presumably due to fouling of the cathode surface by iron deposits. Figure 2 shows a representative plot of the data (10 min before and 5 min after switching off), showing the typical drop in the neutron count when the cell was switched off. The typical background count when the cell was removed is also indicated for comparison.

Tritium Measurements

At the end of ~8 h of electrolysis, the electrolyte was sampled and analyzed for tritium content. It was found to contain ~48 nCi/ml of tritium activity. This is almost three orders of magnitude higher than the tritium level of the stock heavy water used to prepare the electrolytic solution, which was ~0.05 nCi/ml. The tritium level in the electrolyte after ~12 h of operation with NaOH was only 0.0676 nCi/ml.

Conclusions

The results of the neutron and tritium measurements seem to strongly indicate that cold fusion also occurs in the titanium-deuterium system. When compared with palladium-deuterium systems where large neutron bursts are observed, neutrons are produced at a low but more or less steady rate in the present system. It is estimated from the neutron count data, the duration of cell operation (the integrated time during which the cell was active was ~150 min), and the efficiency of the neutron detectors (1%) that in all ~3×10^7 neutrons had been generated. The terminal tritium level in the electrolyte was ~48 nCi/ml. Since the cell volume is ~150 ml, the total tritium inventory in the cell corresponds to $48 \times 150 = 7.2$ μCi. After correcting for the tritium initially present in the D_2O both in the initial charge as well as makeup volumes, it is estimated that an excess of ~7 μCi of tritium was produced due to cold fusion reactions. Considering that the total number of neutrons generated was ~2×10^7, this leads to a neutron-to-tritium yield ratio of ~10^{-7}.

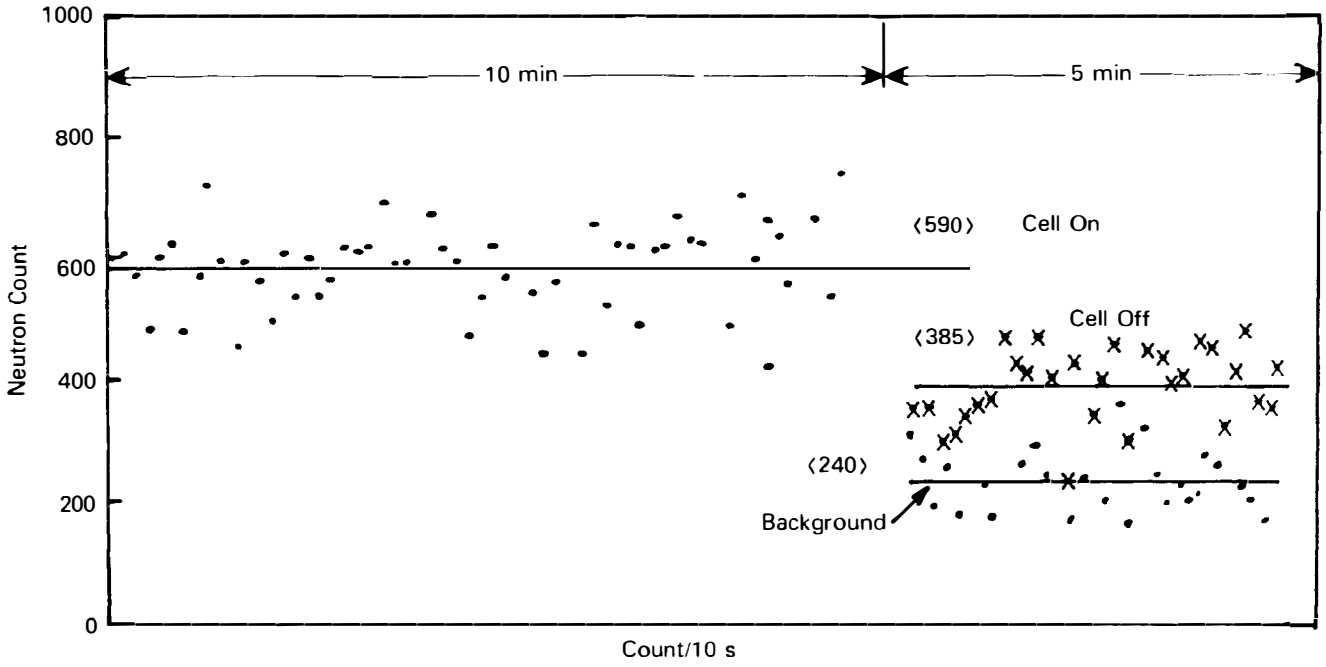

Fig. 2. Titanium-stainless steel cell: neutron count variation with cell turned on and off.

ACKNOWLEDGMENTS

The authors are very thankful to S. K. Mitra and V. Raghunathan of the Desalination Division and V. Chitra of the Neutron Physics Division for their help in the experimental work. We are also grateful to M. Srinivasan, H. K. Sadhukhan, M. P. S. Ramani, and P. K. Iyengar for their keen interest in this work.

REFERENCES

1. M. FLEISCHMANN and S. PONS, "Electrochemically Induced Nuclear Fusion of Deuterium," *J. Electroanal. Chem.*, **261**, 301 (1989).

2. S. E. JONES et al., "Observation of Cold Nuclear Fusion in Condensed Matter," *Nature*, **338**, 737 (1989).

3. C. K. MATHEWS et al., "On the Possibility of Nuclear Fusion by the Electrolysis of Heavy Water," *Indian J. Technol.*, **27**, 229 (1989).

4. K. S. V. SANTHANAM et al., "Electrochemically Initiated Cold Fusion of Deuterium," *Indian J. Technol.*, **27**, 175 (1989).

5. C. SANCHEZ et al., "Nuclear Products Detection During Electrolysis of Heavy Water with Ti and Pt Electrodes," to be published in *Solid State Comm.*

6. A. De NINNO et al., "Evidence of Emission of Neutrons from a Titanium-Deuterium System," *Europhys. Lett.*, **9**, 221 (1989).

4. MULTIPLICITY DISTRIBUTION OF NEUTRON EMISSION IN COLD FUSION EXPERIMENTS

A. Shyam,* M. Srinivasan,* S. B. Degwekar,+ and L. V. Kulkarni*

Introduction

Since the first announcements by Fleischmann and Pons[1] and shortly thereafter by Jones et al.[2] of the observation of cold fusion in palladium electrolytically loaded with deuterium, various theories and speculations have been offered as possible explanations. All the schemes proposed so far can be classified into two broad categories: (a) those that lead to (*d-d*) fusion reactions taking place one at a time, wherein occurrence of one fusion reaction does not directly influence the probability of occurrence of another [In this case, one can assign a certain probability per second per (*d-d*) pair for the reaction rate. A figure of 10^{-20}, for example, has been deduced by Jones et al.]; or (b) mechanisms that lead to a cascade or sharp bursts of fusion reactions.

One of the earliest speculations[3,4] attributed the cold fusion phenomenon to muon catalysis triggered by cosmic ray-produced muons: Each muon could in principle catalyze several hundred fusion reactions within a few microseconds. Another mechanism proposed was lattice crystal fracture or cracking, leading to acceleration of deuterons to energies of 20 to 50 keV in electric fields generated across fracture crevices. Such internally accelerated deuteron beams are then assumed to cause (*d-d*) reactions. Here again the fusion reactions may be expected to occur erratically, leading to bunched (*d-d*) reactions. A brief review of the phenomenology associated with lattice cracking is presented in Ref. 5.

Since neutrons are an end product of (*d-d*) fusion reactions, it may be expected that statistical analysis, such as measurement of the multiplicity spectrum of neutron emission, can give valuable insight into the possible origin of cold fusion reactions. The emission of neutrons in bunches of two or more can, for example, be observed by employing two (or more) fast neutron detectors and looking for coincidences among detected pulses within an interval of ~1 or 10 μs. Since the average background count rate is generally small, the chance coincidence rate due to background events would be negligible, making the task of establishing the occurrence of multiple neutron emission events quite simple.

Another method of detecting fast neutron multiplicity is to use a thermal neutron detector surrounded by a hydrogenous moderator such as paraffin. A bunch of fast neutrons simultaneously incident on this type of detector system would be temporally separated due to the statistical nature of the neutron slowing process and be detected as individual neutrons within a time span governed by the neutron die-away time in the moderator-detector assembly. This type of thermal neutron detector was used in the present studies. This report summarizes the results of the neutron multiplicity spectrum measurements carried out with the Milton Roy electrolytic cell (see report A.1) as well as D_2 gas-loaded titanium targets (see reports B.2 and B.3).

Theory of Multiplicity Analysis

If the events that produce neutrons are random in time and result in one neutron per event, then the number of counts observed in a time interval τ would be distributed according to the Poisson law as follows:

$$P_r = \frac{(N_0\tau)^r}{r!}\exp(-N_0\tau) \ , \qquad (1)$$

where

P_r = probability of obtaining r counts in time τ

N_0 = average count rate.

Thus, when the average count rate is small (when $N_0\tau \ll 1$), one can set $\exp(-N_0\tau) \simeq 1$. In this case, the probabilities of detecting one, two, and three neutrons in time interval τ are $(N_0\tau)$, $(N_0\tau)^2/2!$, and $(N_0\tau)^3/3!$, respectively. In particular, note that the ratio of doubles to singles is $(N_0\tau/2)$, while that of triples to doubles is $(N_0\tau/3)$, and so on.

On the other hand, if there are events that result in bunches of neutrons, say ν neutrons per bunch, then in a time interval τ that encompasses the nuclear event, the probability distribution P_r of counts would be given by a binomial distribution as follows:

$$P_r = \binom{\nu}{r}(1-\epsilon)^{\nu-r}\epsilon^r \ . \qquad (2)$$

It is assumed that interval τ is large compared to the neutron die-away time in the detection system. It is also assumed that the source event rate is so long that only one such event occurs in interval τ. Here ϵ is the overall counting efficiency. If S is the event rate of such multiple neutron-producing cascades, its contribution to the average count rate would be $S\nu\epsilon$.

Thus, we can now conceive of a situation where there is

*Neutron Physics Division.
+Reactor Physics Division.

a steady random background count rate of N_0 count/s on which is superimposed a signal event rate of S events producing ν neutrons each. In such a case, the average count rate in time τ can be expressed as

$$N\tau + S\epsilon\bar{\nu}\tau \ . \tag{3}$$

Likewise, the probability of registering two and three counts in time τ now comprises two components: one due to random background events and the other due to signal events releasing ν neutrons each. Table I summarizes the expressions for these probabilities. Note that while the probabilities of various multiplicities due to the random background depend on the product $N_0\tau$, that due to the bunched neutronic events depends mainly on ν and ϵ. In the limit of $\nu \gg 1$ and $\epsilon \ll 1$, the expressions simplify as shown in the last column of Table I. It is clear from this that the deciding quantity under these circumstances is the product $\nu\epsilon$.

Table II gives the expected frequency distributions of multiple neutron counts for typical values of N_0, ϵ, and ν. The counting time interval τ is kept fixed at 20 ms, while the

TABLE I

Expressions for Frequency Distributions of Neutron Counts for Random and Bunched Neutron-Producing Events

Multiplicity of Counts	Frequency			
	Random Events		Bunched Events	
		Approximate Values for $N_0\tau \ll 1$		Approximate Values for $\epsilon \ll 1$ and $\nu \gg 1$
0	$\frac{T}{\tau}\exp(-N_0\tau)$	$\frac{T}{\tau}(1-N_0\tau)$	$ST(1-\epsilon)^{\nu}$	$ST\exp(-\nu\epsilon)$
1	$\frac{T}{\tau}(N_0\tau)\exp(-N_0\tau)$	$\frac{T}{\tau}(N_0\tau)$	$ST\nu(1-\epsilon)^{\nu-1}\epsilon$	$ST(\nu\epsilon)\exp(-\nu\epsilon)$
2	$\frac{T}{\tau}\frac{(N_0\tau)^2}{2!}\exp(-N_0\tau)$	---	$ST\binom{\nu}{2}(1-\epsilon)^{\nu-2}\epsilon^2$	$ST\frac{(\nu\epsilon)^2}{2!}\exp(-\nu\epsilon)$
3	$\frac{T}{\tau}\frac{(N_0\tau)^3}{3!}\exp(-N_0\tau)$	---	$ST\binom{\nu}{3}(1-\epsilon)^{\nu-3}\epsilon^3$	$ST\frac{(\nu\epsilon)^3}{3!}\exp(-\nu\epsilon)$
4	$\frac{T}{\tau}\frac{(N_0\tau)^4}{4!}\exp(-N_0\tau)$	---	$ST\binom{\nu}{4}(1-\epsilon)^{\nu-4}\epsilon^4$	$ST\frac{(\nu\epsilon)^4}{4!}\exp(-\nu\epsilon)$
5	$\frac{T}{\tau}\frac{(N_0\tau)^5}{5!}\exp(-N_0\tau)$	---	$ST\binom{\nu}{5}(1-\epsilon)^{\nu-5}\epsilon^5$	$ST\frac{(\nu\epsilon)^5}{5!}\exp(-\nu\epsilon)$

TABLE II

Expected Frequency Distribution of Counts for Random and Bunched Neutronic Events for Typical Sets of Parameters

Multiplicity of Counts	Frequency of Counts in 20-ms Intervals for 10^5 Samples (8-h Real Time)					
	Poisson Events		Bunched Events ($S = 10^{-2}$/s)			
	$N_0 = 0.3$ count/s	$N_0 = 3.0$ count/s	$\nu = 100$, $\epsilon = 0.015$, $S\nu\epsilon = 0.015$	$\nu = 100$, $\epsilon = 0.005$, $S\nu\epsilon = 0.005$	$\nu = 500$, $\epsilon = 0.015$, $S\nu\epsilon = 0.075$	$\nu = 500$, $\epsilon = 0.005$, $S\nu\epsilon = 0.025$
0	99 940	99 402	99 984	99 992	99 980	99 980
1	60	597	6.6	6.1	0.07	4.0
2	$\sim 10^{-2}$	1.7	5.0	1.5	0.3	5.1
3	$< 10^{-5}$	$< 10^{-2}$	2.5	0.2	0.8	4.2
4	$\sim 10^{-9}$	$\sim 10^{-5}$	1.0	0.03	1.5	2.6
5	$\sim 10^{-13}$	$\sim 10^{-8}$	0.3	0.003	2.2	1.3

TABLE III

Summary of Multiplicity Distribution Analysis Runs

May–June 1989

	Cold Fusion Source					
	Background Study	Quiescent Milton Roy Cell	Milton Roy Cell		Deuterated Titanium-Zirconium Target	Deuterated Titanium Disk
Date	June 2–5	May 26–27	June 12–14	June 16	June 9–11	June 17–19
BF_3 bank (count/s)	0.023	---	0.12	0.2	0.2	0.06
^3He bank (count/s)	0.43	---	0.1/0.2	0.2	0.4	0.12
Detector viewing source	BF_3	BF_3	BF_3	BF_3	^3He	^3He
Peak signal count rate (count/s)	---	5.6 (average for 12 h)	0.5 to 1.7	20	---	1.8
Times background	---	---	4 to 14	~100	1.0	~15
Main characteristics	---	---	6 bursts	1 large 2-h (2×10^5 n)	---	1 large burst 85-min
Fraction of non-Poissonian neutrons (%)	---	~2	~25	~10	5	~16

bunched neutron producing event rate S is taken as 10^{-2}/s. The data presented are for a total of 10^5 sampling time intervals. It is clear that while the average count rate for Poisson events is much higher than for bunched events, the frequency of higher count multiplicities (>2) is much higher for the bunched events.

Experimental Details

Neutrons were counted by a bank of thermal neutron detectors embedded in paraffin. One bank comprised three BF_3 counters, while the other was made up of three ^3He counters. The neutron die-away time in each was ~25 μs. The BF_3 bank was mounted close to the palladium-nickel electrolytic cell and the ^3He bank was near the D_2 gas-loading apparatus, ~1.5 m away. While one counter bank was used as the signal counter in the experiment, the other bank served as background monitor and vice versa. The efficiency ϵ of detection for the cold fusion source neutrons was typically in the range of 0.5 to 1.5%, depending on the exact distance between the cold fusion source and the detector assembly as well as the pulse-height discriminator bias setting.

The outputs of both these counter banks were fed to scalers whose readings could be read by a personal computer (PC) at the end of each counting interval, which was controlled by the clock in the PC. By taking the difference in the scaler readings corresponding to the end of two consecutive counting intervals, the number of counts recorded in a given counting interval was computed and stored by the PC. It took the PC typically >250 ms to carry out these operations following each sampling time. Hence, a set of 1000 samples consumed a real time of ~5 min.

The selected counting interval was ~20 ms long. This is a compromise between the conflicting requirements of increasing the total number of counts accumulated to get good statistics and minimizing the chance coincidence probability for Poisson events. For the typical count rates during the neutron emission phase of the cold fusion experiments, 20 ms was a reasonably satisfactory choice. From such data accumulated over several hours, the frequency distribution of counts recorded in 20-ms intervals could be computed.

Results and Discussion

Table III summarizes the various neutron multiplicity spectrum measurements carried out during May–July 1989. The details of the commercial electrolyzer and its operation are described in report A.1. Likewise, the D_2 gas-loading experiments are summarized in reports B.2 and B.3. The

TABLE IV

Frequency Distribution of Background Counts*

Multiplicity of Counts	Frequency	
	BF_3 Bank	^3He Bank
0	750035	743948
1	339	6413
2	1	14
3	0	0
4 to 20	0	0
N_0 (count/s)	0.023	0.43
$N_0\tau$	5×10^{-4}	0.0086

*20-ms intervals over 63 h.

background counts were studied to ensure that the equipment was functioning satisfactorily. For this purpose, all potential cold fusion sources were removed from the room where the neutron detectors were located. Monitoring of background counts continued uninterrupted for 63 h over a weekend (1800 on June 2 to 0900 on June 5). During this run, the average background count rate in the BF_3 bank was ~0.023 count/s and in the ^3He bank ~0.43 count/s (the background rate in the BF_3 bank was intentionally adjusted to be lower by setting its pulse-height discriminator level high). Table IV presents the results of the frequency distribution of counts obtained in this long background run. It is heartening to note that not even once out of the ~750 000 odd samples were 3 or more counts registered by either of the detector banks as may be expected on the basis of Poisson distribution. The ratio of double to single frequency further conforms to Poisson statistics, indicating that the equipment was functioning properly. Sparking in any of the counters, for example, would have given rise to significant non-Poisson behavior.

Table V represents the results of our first attempt to measure multiplicity distributions of neutron signals. The data were accumulated overnight (1805 on May 26 to 0645 on May 27) with the BF_3 bank viewing the quiescent cell, with the cell current turned off. A plastic scintillator biased to register only neutrons of energy >9 MeV monitored cosmic-ray and other background events. The average count rate works out to 5.6 count/s. It is clear from the frequencies of doubles, triples, and higher multiplicities that there is considerable contribution from non-Poisson events. The table also gives the frequency distribution of the same count data whenever a pulse was also recorded by the plastic scintillator. From this, we conclude that only ~1% of the neutron events in the BF_3 bank can be attributed to cosmic-ray showers.

Table VI presents the frequency distribution results of the cell run of June 12–14. As noted in report A.1, six 5-min neutron bursts were recorded during this period: the first ~50 min after cell electrolysis commenced on June 12, the second and third ~1 h thereafter, and the remaining three a few hours after the cell current was switched off on the evening of June 14. During the burst phase, the count rates were in the range of ~0.5 to 1.7 count/s, which is ~4 to 14 times that of the background (~0.12 count/s). Note, however, that in four out of the six bursts observed, count multiplicities of 2, 3, 4, 5, and even 10 were recorded at least once each. This type of behavior indicates high-multiplicity neutron emission events. Throughout this run, which lasted several days, the background counter did not record any noticeable increase in counts.

Table VII summarizes the frequency distribution measured during the 2.5-h-long neutron burst recorded on June

TABLE V

Frequency Distribution of Counts with Quiescent Milton Roy Cell*

Multiplicity of Counts	Gross Frequency (BF_3 Bank)	Frequency in Samples in Which the Plastic Scintillator also Records a Pulse
1	11941	114
2	2760	31
3	111	0
4	19	0
5	2	0
6	13	0
7	9	0
8	3	0
9	5	0
10	1	0
11	0	0
12	1	0
13	0	0
14	0	0
15	1	0
16	0	0

*20-ms intervals over 12 h; total of 14 400 sampling intervals.

TABLE VI

Frequency Distribution of Counts for 20-ms Sampling Intervals During Periods of High Neutron Activity (June 12–14, 1989)

Multiplicity of Counts	Frequency						Total (A to F)	
	A	B	C	D	E	F	Observed	Expected
1	27	0	2	7	29	22	87	117
2	0	0	0	0	3	0	3	1
3	0	1	0	0	0	0	1	$<10^{-3}$
4	0	0	1	0	0	0	1	$\sim10^{-5}$
5	0	0	1	1	0	0	2	$\sim10^{-7}$
6	0	0	0	0	0	0	0	$\sim10^{-10}$
7	0	0	0	0	0	0	0	$<10^{-12}$
8	0	0	0	0	0	0	0	$\sim10^{-15}$
9	0	0	0	0	0	0	0	$\sim10^{-18}$
10	0	1	0	0	0	0	1	$<10^{-20}$

TABLE VII

Frequency Distribution of Counts for 20-ms Sampling Intervals During Periods of High Neutron Activity (June 16, 1989)

Multiplicity of Counts	Frequency													Total (B to M)	
	A	B	C	D	E	F	G	H	I	J	K	L	M	Observed	Expected
1	24	345	355	104	447	492	295	315	243	320	335	54	124	3429	3166
2	7	99	49	13	42	51	24	35	13	82	54	9	21	492	616
3	3	16	1	4	2	3	0	3	4	10	7	1	4	55	80
4	3	2	1	0	1	2	1	1	0	0	2	0	1	11	8
5	2	0	0	0	1	0	0	0	1	0	1	0	0	3	0.6
6	1	0	1	1	1	0	0	0	0	0	0	0	0	3	0.03
7	1	0	0	0	0	0	0	0	0	0	0	0	0	0	$\sim 10^{-3}$
8	1	0	0	0	0	0	0	0	0	0	0	0	0	0	$\sim 10^{-4}$
9	1	1	0	0	0	0	0	0	0	0	0	0	0	1	$\sim 10^{-6}$
10	1	0	0	0	0	0	0	0	0	0	0	0	0	0	$\sim 10^{-7}$
11	2	0	0	0	1	0	0	0	0	0	0	0	0	1	$< 10^{-8}$
12	2	0	0	0	0	0	0	0	0	0	0	0	0	0	$\sim 10^{-10}$
13	1	0	0	0	1	0	0	0	0	0	0	0	0	1	$< 10^{-11}$
14	0	0	0	0	0	0	0	0	0	0	0	0	0	0	$\sim 10^{-13}$
15	5	0	0	0	0	0	0	0	0	0	0	0	0	0	$\sim 10^{-14}$
16	2	0	0	0	0	0	0	0	0	0	0	0	0	0	$\sim 10^{-16}$
17	1	0	0	0	0	0	0	0	0	0	0	0	0	0	$\sim 10^{-18}$
18	1	0	0	0	0	0	0	0	0	0	0	0	0	0	$\sim 10^{-20}$
19	1	0	0	0	0	0	0	0	0	0	0	0	0	0	$\sim 10^{-21}$
20	0	0	0	0	0	0	0	0	0	0	0	0	0	0	$\sim 10^{-22}$

16 from 1900 onward with the electrolyzer (Fig. 3 of report A.1 gives a plot of the count rate variation during this burst). Note that the cell had not been operated for the previous ~52 h. The count rate during this wide neutron burst attained a value as high as 20 count/s at the peak. The background neutron monitor, which was only 1.5 m away, also indicated a small increase in count rate, confirming that the neutrons originated from the electrolytic cell. Careful scrutiny of these results indicates that the frequency distribution essentially corresponds to a Poisson distribution. However, the fact that multiplicities of 5 or more are recorded several times again points to the sporadic occurrence of multiple neutron emission events. Around 1950 (close to the peak), there were >20 such high-multiplicity cascade events within 5 min. (Note that in Table VII, set M corresponds to the early part of the burst and set A is near the peak with absolute time increasing from M to A.)

Tables VIII and IX summarize the results of multiplicity distribution measurements carried out with two D_2 gas-loaded titanium targets. During the weekend run of June 9–11, with 15 g of titanium-zirconium deuteride (see Table VIII), the average count rate measured was only 0.42 count/s. Since this corresponds to an $N_0\tau$ value of 0.008, we expect a doubles-to-singles ratio of only 0.004. While the high double events in both the background and signal counter can possibly be attributed to statistics, the 3 and 4 in the signal counts can be attributed only to high-multiplicity neutron emissions from the deuterated titanium-zirconium target. Absence of such high-multiplicity events in the background channel further strengthens this conjecture.

TABLE VIII

Frequency Distribution of Counts from Deuterated Titanium-Zirconium Target*

Multiplicity of Counts	Frequency	
	BF_3 Background	^3He Signal
0	67 778	67 493
1	281	557
2	5	11
3	0	5
4	0	2
5	0	0
6	0	0

*20-ms intervals.

Table IX presents a similar result from a titanium disk target. The gas-loading procedure for this target is described in report B.2, while the measurement of spatial distribution of tritium on the surface of this target by autoradiography is discussed in report B.3. The neutron active phase of this target lasted almost 85 min during which it is estimated to have emitted $\sim 5 \times 10^5$ neutrons (see Fig. 1). On the whole, this

TABLE IX

Frequency Distribution of Counts from a Deuterated Disk for 1000 Sampling Intervals of 20 ms During Periods of High Neutronic Activity

Multiplicity of Counts	Frequency																	Total (A to Q)	
	A	B	C	D	E	F	G	H	I	J	K	L	M	N	O	P	Q	Observed	Expected
1	11	9	7	8	4	9	0	20	32	50	36	37	42	26	38	33	23	385	440
2	0	0	0	0	0	0	1	0	1	1	0	0	2	1	2	2	0	10	6
3	0	1	0	0	0	0	2	0	0	0	0	0	0	0	0	0	0	3	0.05
4	0	0	1	1	0	0	1	0	0	0	0	0	1	0	0	0	0	4	10^{-4}
5	0	0	0	0	1	0	1	0	0	0	0	0	0	0	0	0	0	2	10^{-6}
6	0	0	0	0	0	1	1	0	0	0	0	0	0	0	0	0	0	2	10^{-8}

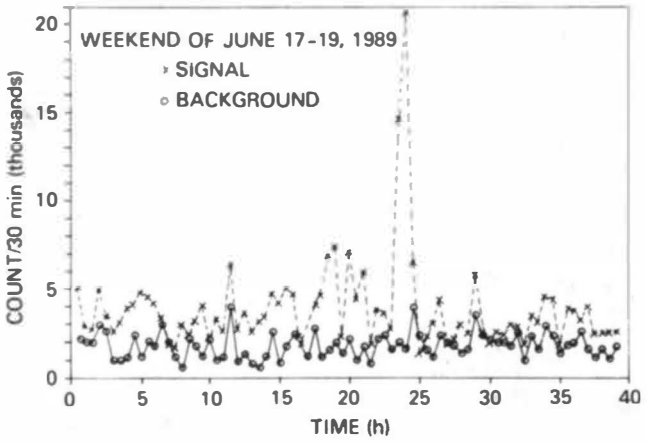

Fig. 1. Neutron count variation from deuterated titanium disk.

target also points to the occurrence of a significant number of high-multiplicity neutron emission events.

The last columns of Table VI, VII, and IX give the total frequency distributions for all the 5-min periods, i.e., the sum of all the columns. Also shown are the theoretical frequency distributions expected on the basis of Poisson statistics. Note that except for the background case (Table IV), in all the cold fusion measurements the frequencies fall according to the Poisson law for low-multiplicity events, but there is a distinct tendency for them to show a slight peak between the multiplicities of 4 and 6. If we assume that this peak is due to the superposition of bunched neutronic events on a Poisson background, we deduce the value of ν to be in the range of 400 to 600 since the peak of the binomial distribution occurs at the multiplicity value of $\nu\epsilon$ (see Table I) and ϵ values in the experiment are typically ~0.01. Furthermore, by comparing the observed frequencies with those shown in Table II, it appears that the average source event rate for such events during the neutron emitting phase is very roughly $\sim 10^{-2}$/s.

Summary and Conclusions

The multiplicity spectrum of neutron counts observed in 20-ms intervals was measured six times during cold fusion investigations: three with electrolytically loaded palladium electrodes, two with gas-loaded titanium targets, and once with the background. While the background counts display strictly Poisson statistics, in the three cases where a distinct excess over background neutron bursts was recorded, between 10 and 25% of the emitted neutrons appear to display high neutron multiplicity characteristics. The observed frequency distributions may be due to bunched neutronic events superimposed over a Poissonian background. Analysis of the data leads us to the conclusion that these bunched neutronic events occur on an average once every 100 s during the active period and typically produce ~400 to 600 neutrons per bunch, within a time span of <20 ms. Such occasional neutron bunches are also reported to have been observed by Menlove et al. at Los Alamos National Laboratory.[4]

If this is viewed in light of the experimentally deduced neutron-to-tritium branching ratio of 10^{-8}, we are obliged to come to the intriguing conclusion that, during bunched neutronic events, upward of 10^{10} fusion reactions occur in <20 ms (Ref. 6). As this appears very unlikely, the authors are inclined to believe that bunched neutronic events are not accompanied by tritium production with a yield ratio of 10^{8}, and hence lattice cracking where the branching ratio is close to unity would appear to be the most plausible cause for bunched neutron emission.

REFERENCES

1. M. FLEISCHMANN and S. PONS, "Electrochemically Induced Nuclear Fusion of Deuterium," *J. Electroanal. Chem.*, **261**, 301 (1989).

2. S. E. JONES et al., "Observation of Cold Nuclear Fusion in Condensed Matter," *Nature*, **338**, 737 (1989).

3. M. W. GUINAN, G. F. CHAPLINE, and R. W. MOIN, "Catalysis of Deuterium Fusion in Metal Hydrides by Cosmic Ray Muons," UCRL preprint 100881, Lawrence Berkeley Laboratory (1989).

4. *Proc. Workshop Cold Fusion Phenomena*, Santa Fe, New Mexico, May 23-25, 1989.

5. T. C. KAUSHIK, M. SRINIVASAN, and A. SHYAM, "Fracture Phenomena in Crystalline Solids: A Brief Review in the Context of Cold Fusion," BARC-1500, Bhabha Atomic Research Centre (1989).

6. P. K. IYENGAR, "BARC Cold Fusion Experiments," *Proc. 5th Int. Conf. Emerging Nuclear Energy Systems*, Karlsruhe, FRG, July 3-6, 1989, World Scientific, Singapore (1989).

5. SEARCH FOR ELECTROCHEMICALLY CATALYZED FUSION OF DEUTERONS IN A METAL LATTICE

T. P. Radhakrishnan,* R. Sundaresan,*
J. Arunachalam,* V. S. Raju,* R. Kalyanaraman,*
S. Gangadharan,* and P. K. Iyengar+

Introduction

Recently, Fleischmann and Pons[1] obtained evidence for the fusion of deuterons at low temperature through the electrolysis of deuterium oxide with a palladium cathode. It is believed that this can be achieved if the deuterium loading of the lattice exceeds the value for $PdD_{0.8}$. This report is a summary of the behavior of palladium and other metals during charging in alkaline heavy water.

Experimental

Materials, Reagents, and Apparatus

Electrodes of different metals were used, including a hollow palladium cylinder (5.87 cm^2, 0.4 mm thick), a palladium ring (14.5 cm^2, 2 mm thick), palladium foil (1.5 cm^2, 0.3 mm thick), titanium plate (8 cm^2, 0.5 mm thick), and a 10-cm^2, 10.5-g triangular piece of nickel-titanium alloy. Platinum gauze, a platinum disk, or a large piece of platinum foil was used as the anode. Heavy water (99.87% purity) and pure lithium metal were used to obtain 0.1 *M* LiOD. Iolar-2 N_2 or argon was used for deoxygenation and stirring. All electrodes were lightly abraded with emery, rinsed with acetone, and dried before use.

The electrolysis cells were made of quartz and the lids were of polytetrafluoroethylene or glass. Provisions and inlets for deoxygenation, addition and removal of solution, and temperature measurement were made. Loss of D_2O due to evaporation and electrolysis was compensated.

Equipment

Galvanostatic sources and current pulsing units were made in the laboratory. A digital panel meter was used for voltage measurements. Neutron counting and tritium activity studies were carried out. The setup is shown in Fig. 1.

Results

Differential Enthalpimetric Studies

Twin cells were composed of a palladium cathode (5.9 cm^2) and a platinum gauze anode in one cell (cell I) coupled in series with a platinum cathode (5.9 cm^2) and platinum gauze anode in another cell (cell II). This was used to assess the magnitude of heat effects due to reactions such as deuterium adsorption on the electrode, recombination, and dissolution in the lattice. The cells were insulated by a dewar, and 45 ml of 0.1 *M* LiOD was taken in quartz cells. The temperatures were monitored by matched thermistors using a bridge circuit and with thermometers. The temperatures of the two cells during charging are shown in Fig. 2. The temperature of cell II remained nearly constant, whereas the temperature of cell I increased to a high value. The temperature rise in cell I is due to absorption, dissolution, and interaction of deuterons in the palladium lattice.

Calorimetric Measurements of Enthalpy Changes

A modified isoperibol solution calorimeter with an accurate thermistor bridge was used. The cell and its contents were enclosed in a tight-fitting dewar and immersed in a thermostat at 25°C for thermal insulation. Electrodes made of a hollow cylindrical palladium cathode (5.48 cm^2) and a platinum sheet anode with 50 ml, 0.1 *M* LiOD were used. Iolar-2 argon was used for deoxygenation, and the solution was stirred

*Analytical Chemistry Division.
+Director.

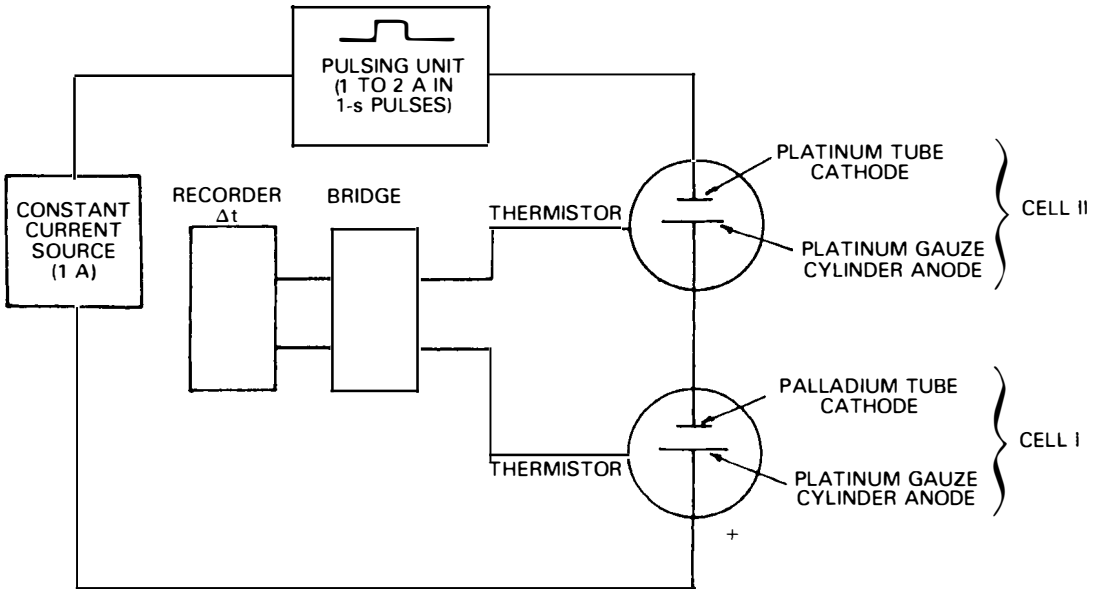

Fig. 1. Experimental setup.

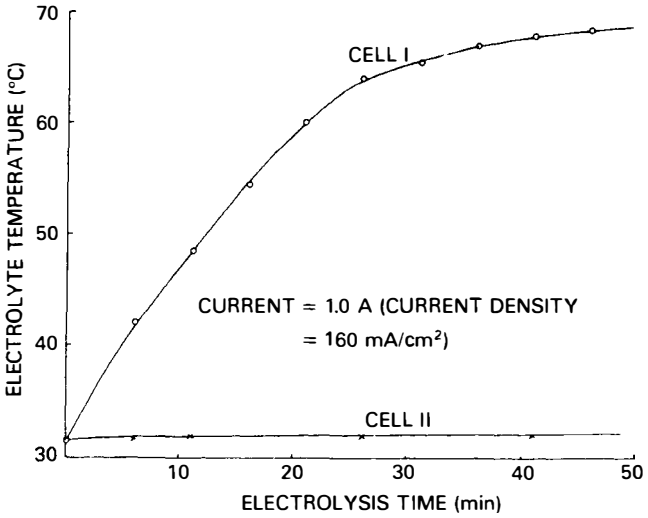

Fig. 2. Time dependence of temperature.

mechanically. Charging was effected at different current densities, and the terminal voltage in each case was noted. The solution temperature was monitored by the thermistor probe and bridge and by a sensitive thermometer. The temperature increase as a function of time at different current densities is shown in Fig. 3. The heat capacity of the cell and its components was determined by electrical calibration, and corrections for heat losses were applied on the basis of Newton's law of cooling (Fig. 4). The results are included in Table I.

Extended Electrolysis with Current Pulsing

Cylinder Electrode. A hollow cylindrical palladium cathode (5.9 cm^2) and a platinum gauze anode were used and 0.1 *M* LiOD was electrolyzed in a quartz cell with nitrogen bubbling. Initially, a constant 1-A current was used. When the temperature reached 60°C, pulsing was commenced between 1 and 2 A at 1-s intervals. The temperature was controlled at 63°C by forced circulation of air. Neutron flux measurements were made, and D_2O was added for makeup. After 41.8 h,

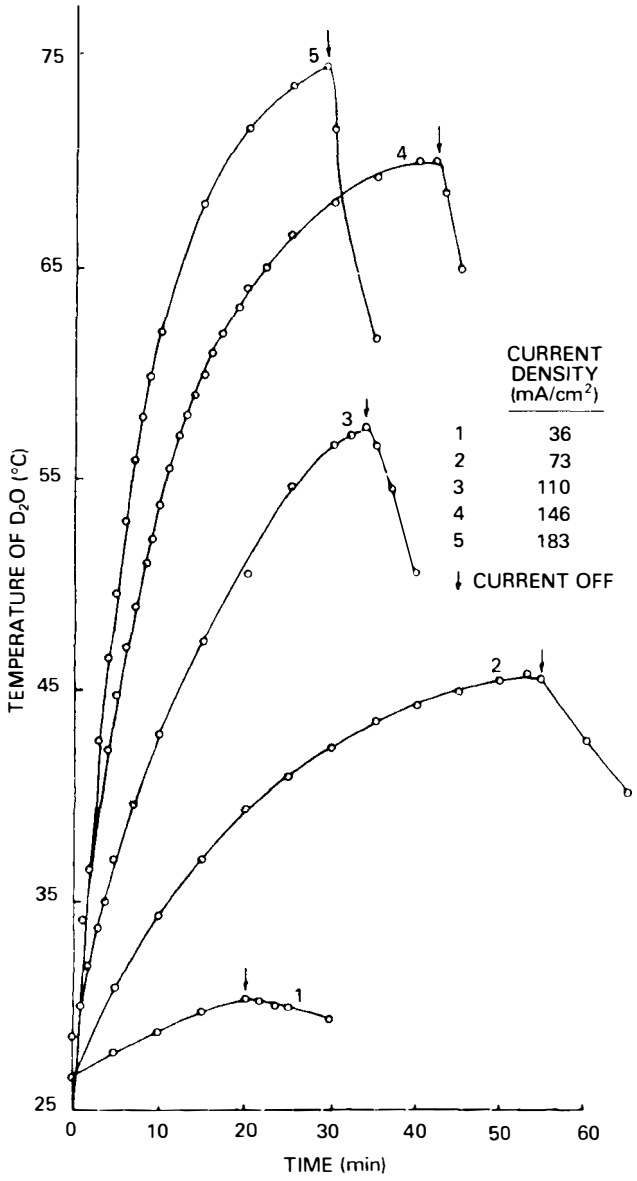

Fig. 3. Temperature changes during charging.

TABLE I

Excess Enthalpy Generated During Electrolysis of LiOD

Current Density (mA/cm^2)	Energy Input, *Ei* (W)	Measured *H* (W)	Excess Enthalpy (in % breakeven)	
			$\frac{\Delta H \text{ measured}}{(E-1.54)i} \times 100$	$\frac{\Delta H \text{ measured}}{Ei} \times 100$
36	1.25	1.00	105	80
73	3.96	3.13	94	79
110	7.30	5.60	88	77
146	10.47	6.95	75	66
183	15.46	10.79	78	70

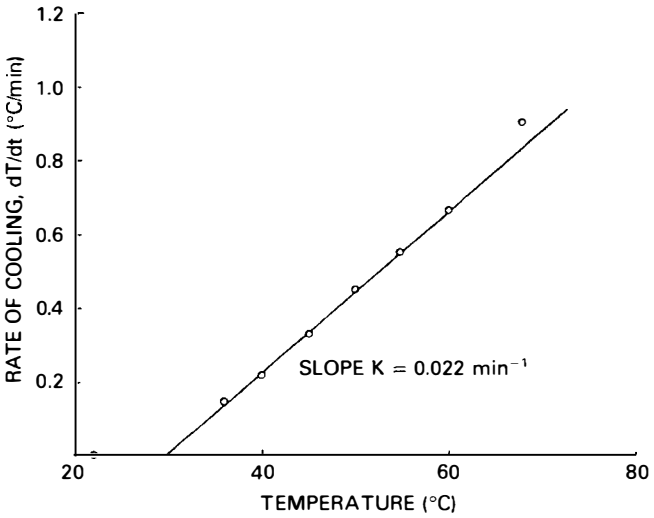

Fig. 4. Relationship between temperature and rate of cooling.

during which 52.2 A·h was consumed, the electrolysis was terminated. Measurement of tritium buildup in the final solution showed 3.75 μCi.

Ring Electrode. Sixty-five ml of 0.1 *M* LiOD in D_2O was electrolyzed in a quartz cell using a palladium-ring cathode (14.5 cm^2) and two platinum disks as the anode. At low current densities, the cell voltage was observed as a function of current, as shown in Fig. 5. Later, electrolysis was continued for 9 days with current pulsing between 1 and 2 A (80 h), 3 and 4 A (20 h), and 4 and 4.5 A (7 h), consuming a total of 296 A·h. Neutron activity and capture gamma measurements were made throughout the duration of electrolysis. At the conclusion of the electrolysis, tritium content in the solution was found to be 16.25 μCi.

The above experiment was repeated using 0.1 *M* NaOD, and a total of 231 A·h was consumed during 77 h. Neutron counting and tritium activity measurements were carried out.

The same ring electrode, after degassing in vacuum, was subjected to 844 A·h charging in 382 h in 65 ml of deaerated 0.1 *M* LiOD. There was no significant tritium buildup in solution. The electrode was greyish black in color.

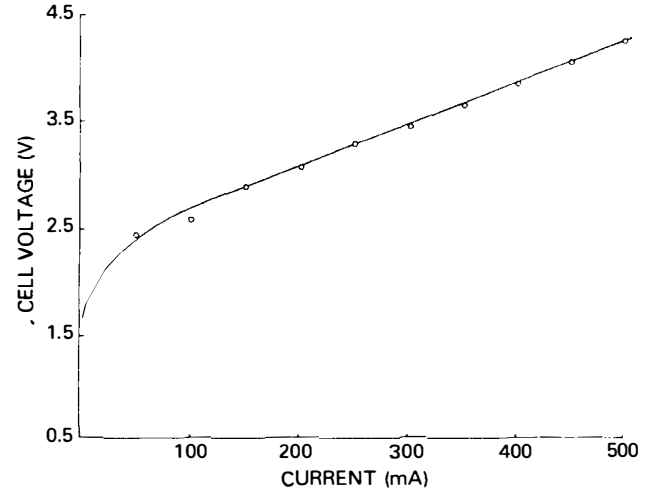

Fig. 5. Cell terminal voltage as a function of cell current.

Nickel-Titanium Electrode. A nickel-titanium cathode (10 cm^2) was used in 0.1 *M* LiOD with a total charge of 135 A·h over 111 h. Appreciable neutron activity was observed. The cathode flaked and disintegrated to powder.

Titanium Electrode. A titanium sheet cathode (8 cm^2) and platinum sheet anode were used in the electrolysis of 1 *M* NaCl in D_2O at 34 $mA \cdot cm^{-2}$. The terminal voltage was 4.4 V and temperature rose from 27 to 36.6°C in 53 min. Prolonged electrolysis did not show any significant increase in temperature.

Nuclear Measurements

Four different types of measurements were made to identify the emission of neutrons from the electrolysis cells.

1. Detection and direct measurement of neutrons were based on the use of ^3He detectors arranged in a well counter as well as a ^6Li-enriched scintillation detector. The detectors were calibrated by an americium-beryllium source. Nearly complete rejection of high-energy gamma rays was ensured by proper discrimination of the 2.5-MeV ^{60}Co sum peak using a ^{60}Co source.

2. Detection of high-energy capture gamma rays of gadolinium, platinum, and palladium was achieved by using a Ge(Li) or high-purity germanium (HPGe) detector.

3. Measurement of low-energy capture gamma rays of energies 199, 944, and 1186 keV was carried out with a HPGe detector.

4. Gross counting of gamma rays of energy >3 MeV was effected by means of a properly shielded 3- × 3-in. NaI(Tl) detector.

All the above measurements were done in combination to yield cross-validated results. However, in some cells, only a single type of measurement could be made.

Neutron counting was performed both in the multichannel scaling (MCS) mode [using a personal computer (PC)-based 8-kbyte multichannel analyzer (MCA) system] and in the pulse-height analyzer (PHA) mode whenever possible. Different dwell times ranging from 0.5 to 60 s were selected in the MCS mode to check whether neutron emission was continuous or in "bursts." The complete counting setup is given in Fig. 6.

Hollow Palladium Cylinder Cathode (Run 3.1). The 1186-keV gamma-ray activity was measured every 100 s for >24 h. In Fig. 7, three definite "spikes" can be identified. The duration of the bursts was 14 to 20 min.

Palladium Ring Cell (Run 3.2.1). A time-correlated analysis of the neutron counts in the ^6Li scintillation counter and measurement of gamma rays of energy >3 MeV in the NaI(Tl) detector was carried out (Fig. 8). The correlation coefficient for the 50 observations was 0.26, which is significant at the 5% level.

Nickel-Titanium Cathode Cell (Run 3.3). Neutron counting was carried out using ^3He as well as ^6Li scintillation detectors with the former in both the MCS and integral modes and the latter in the MCS mode. The cell was run initially at 1-A current. When the current was increased to 2 to 2.5 A,

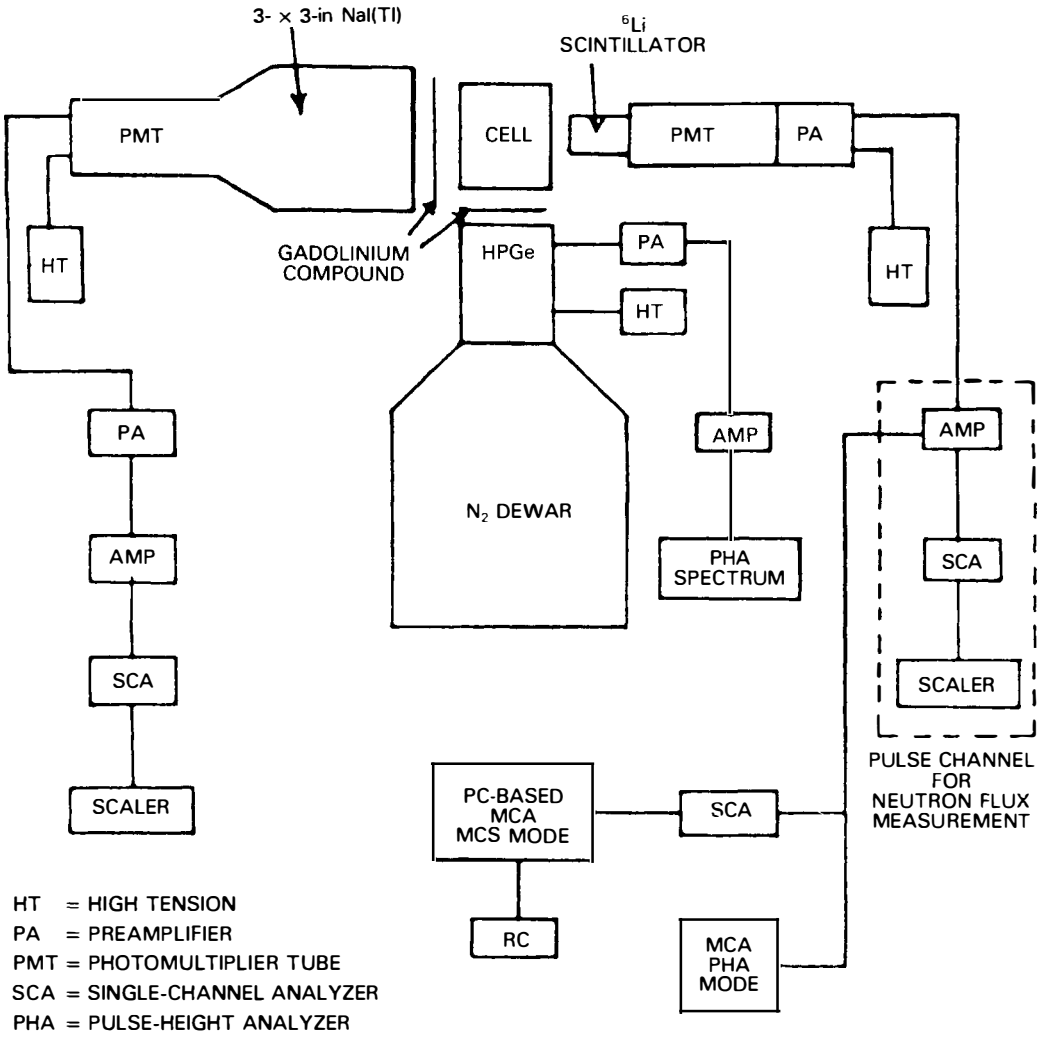

Fig. 6. Counting setup for neutrons and gamma rays.

three well-defined spikes were registered in the MCS mode, as shown in Fig. 9.

The count rates of the ^{3}He and ^{6}Li scintillators are not correlated in any significant manner, possibly because of the different efficiencies and geometries. However, tiny spikes are registered in the ^{3}He detector.

Palladium Ring Cell (Run 3.2.3). Several spectra for the low-energy capture gamma rays were detected using a HPGe detector for 10000 to 50000 s. In some spectra, 199-, 944- and 1186-keV capture gamma rays could be identified, though they were not traceable in other spectra. As the accumulated count rates for these energies are rather small, it appears that neutron emission is low and not continuous.

Discussion

Electrolysis of alkaline heavy water results in the splitting of D_2O with evolution of deuterium at the cathode and oxygen at the anode. The electrode process involves charge transfer, adsorption of the intermediates, subsequent reaction, and gas evolution.[2] On the palladium electrode, the discharge reaction in alkaline solution is followed by a rate-determining recombination of adsorbed deuterium atoms at low overpotential, whereas at high overpotential an electrochemical desorption reaction is favored. In the case of a nickel-titanium cathode, the discharge reaction is always accompanied by rate-determining electrochemical desorption reaction.

The uptake of deuterium by metals during charging depends on the reaction

$$MD_{ads} \rightarrow MD_{abs} \rightarrow MD_{lattice} , \quad (1)$$

and is therefore governed by the fraction of the electrode surface covered by adsorbed deuterium, solubility of deuterium in the metal, and its diffusivity. The observed rise in temperature of the electrolyte is not due to the exothermic dissolution of deuterium in palladium, nickel-titanium, and titanium or due to other chemical factors.

The measured overpotential is composed of ohmic, activation, adsorption, diffusion, and concentration overpotential terms. The ohmic resistance and polarization resistance cause Joule heating and thereby contribute to the observed changes in enthalpy. Had the cell systems been reversible and

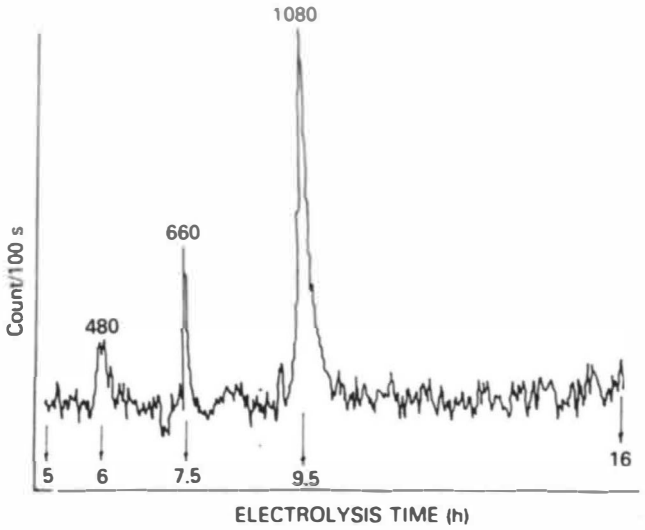

Fig. 7. The 1186-keV capture gamma ray of gadolinium: NaI(Tl) detector.

the polarization is reversed, the electrode reactions at the palladium and platinum electrodes should also be reversed. In the upper limit, the maximum Joule heating is the product of the cell voltage E and cell current i. In the case of palladium-platinum electrodes, the minimum voltage or back electromagnetic force for electrolysis of D_2O was calculated from thermodynamic data as 1.54 V. Therefore, the electrical power available for Joule heating is $(E - 1.54)i$, and this is the lower limit. The enthalpy changes calculated for different current densities and the ratio of thermal output to the power input, expressed as percent breakeven, are included in Table I.

The predominant process during dc polarization is the electrolysis of D_2O and has been checked by measuring the volume of D_2 and O_2 mixture liberated in a fixed electrolysis time using a precision integral flowmeter and by gas chromatographic analysis of the composition of the gas mixture. As excess heat is liberated over and above electrolysis, it is clear that some other reactions are responsible for the excess enthalpy observed. Pauling[3] ascribed the excess heat to the formation of palladium deuteride. However, Bockris et al.[4] have shown that exothermic effects due to solution of deuterium in palladium, recombination of deuterium atoms, formation of D_2O, etc., cannot account for the observed heat evolution. Normal chemical reactions cannot account for the generation of neutrons or the production of tritium during charging of palladium with deuterons. As has been pointed out by Fleischmann and Pons,[1] the results can be rationalized and understood on the basis of cold fusion reactions occurring between deuterons in the palladium lattice as indicated below:

$$ {}^{2}_{1}\mathrm{D} + {}^{2}_{1}\mathrm{D} \rightarrow {}^{3}_{1}\mathrm{H} + {}^{1}_{1}\mathrm{H} \qquad (2) $$

$$ {}^{2}_{1}\mathrm{D} + {}^{2}_{1}\mathrm{D} \rightarrow {}^{3}_{2}\mathrm{He} + {}^{1}_{0}n \ . \qquad (3) $$

In the present work, the emission of neutrons, reasonably above the background level, and the buildup of significant tritium activity in excess of the blank value have been confirmed in four different electrolysis experiments. In certain experiments, neither the evidence for significant neutron emission nor any appreciable buildup of tritium activity was observed. It is likely that in such cases charging was not sufficient to ensure optimum loading of the lattice with deuterons to induce fusion. However, it appears that in addition to reaction channels (2) and (3), the possible occurrence of a nonemitting nuclear process cannot be precluded. This reaction can be written as

$$ \mathrm{Pd} + {}^{2}_{1}\mathrm{D} + {}^{2}_{1}\mathrm{D} \xrightarrow[catalyzed]{lattice} {}^{4}_{2}\mathrm{He} + \mathrm{Pd}^{*} \ , \qquad (4) $$

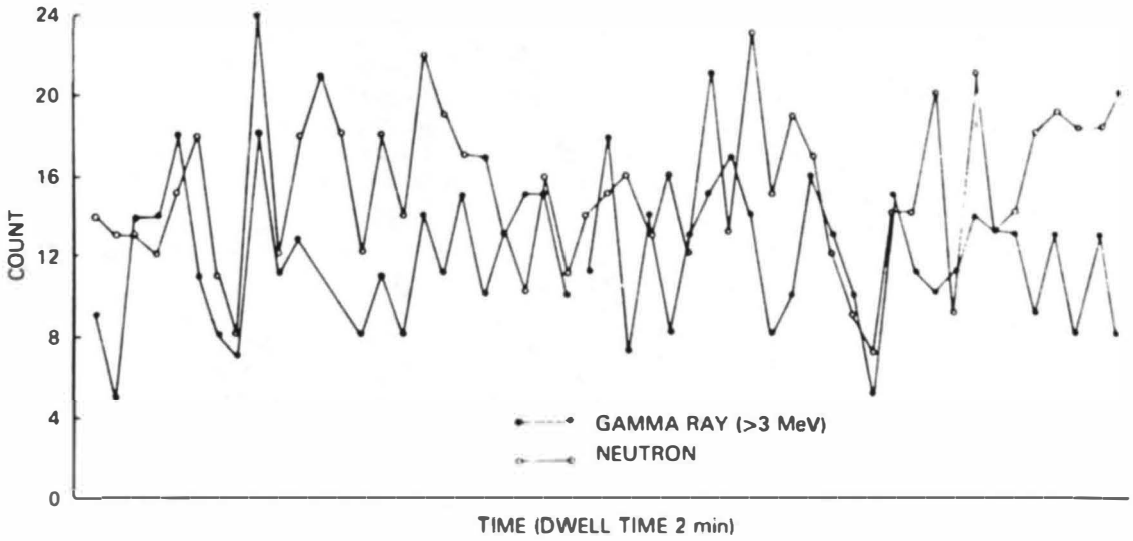

Fig. 8. Time correlation of neutron and gamma-ray activities.

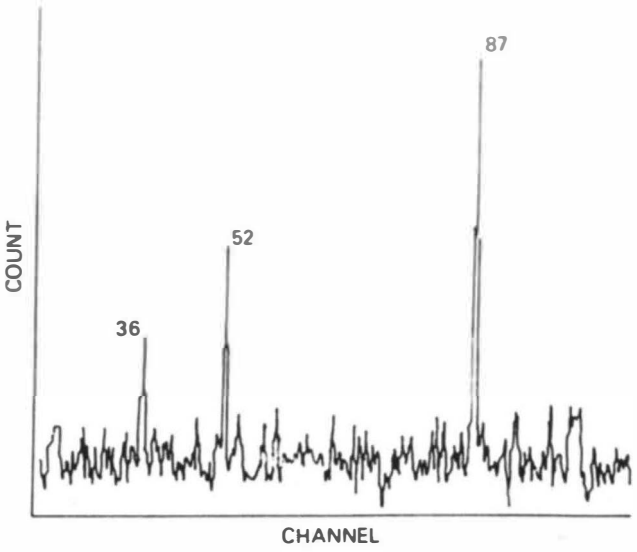

Fig. 9. Distribution of neutron counts.

which implies that the lattice is excited to a higher energy level to conserve both momentum and energy. It is likely that during the subsequent lattice relaxation, the excess energy stored in the lattice is liberated as heat.[5] This mechanism would lead to the formation and buildup of helium inside the metal and can possibly account for the observed low yield of neutrons or tritium in certain experiments. Accurate mass spectroscopic analysis of the ^3He:^4He ratio in the cathode material is needed to substantiate this view. In conclusion, it is necessary to examine in detail the different parameters and optimize important factors such as the metallurgical history and pretreatment of the cathode, solution chemistry, surface chemistry, and electrochemistry to achieve reproducible fusion through electrochemical charging of metals in heavy water.

ACKNOWLEDGMENTS

The authors are grateful to R. M. Iyer, director of the Chemical Group, for his keen interest and encouragement. Acknowledgments are due to T. S. Murthy, director of the Isotope Group, for kindly providing the data on tritium analysis. Support from S. P. Chaganty of the Electronics Division for scintillation detector and associated electronics facility, J. D. Gupta and Suman Kumari of the Computer Division for the 8 K PC-based MCA system, and M. R. Iyer of the Health Physics Division for the ^3He well counter and MCS mode acquisition setup are gratefully acknowledged. In particular, we wish to acknowledge the painstaking efforts and support of the following scientists in providing the reliable data cited in this work: (a) continuous nuclear data acquisition: G. Leela, Anna John, S. Sanjeevkumar, Sunil Jai Kumar, Rakesh Verma, D. Shreevalsan Nair, and S. C. Hodawadekar; (b) nuclear and electrochemical instrumentation: K. C. Thomas, J. R. Kale, R. G. Dalavi, and A. W. Sahani; (c) calorimetric measurements: S. S. Sawant.

REFERENCES

1. M. FLEISCHMANN and S. PONS, "Electrochemically Induced Nuclear Fusion of Deuterium," *J. Electroanal. Chem.*, **261**, 301 (1989).

2. T. P. RADHAKRISHNAN, "Electrochemical Kinetics in Metal-Hydrogen Systems," *Proc. Interdisciplinary Mtg. Hydrogen in Metals*, Bombay, India, February 19–20, 1980, p. 148.

3. L. PAULING, "Explanations of Cold Fusion," *Nature*, **339**, 105 (1989).

4. J. O'M. BOCKRIS, N. PACKHAM, O. VELEV, G. LIN, M. SZKLARZCYCK, and R. KAINTHLA, *Proc. Workshop Cold Fusion Phenomena*, Santa Fe, New Mexico, May 23–25, 1989.

5. J. S. COHEN and J. D. DAVIES, "The Cold Fusion Family," *Nature*, **338**, 705 (1989).

6. TRITIUM GENERATION DURING ELECTROLYSIS EXPERIMENTS

T. P. Radhakrishnan,* R. Sundaresan,* S. Gangadharan,* B. K. Sen,+ and T. S. Murthy+

Introduction

In continuation of the earlier work carried out in connection with the investigations for electrochemically induced fusion of deuterons using a palladium cathode and a platinum anode, a series of experiments was carried out. The following is a summary of the results and observations for two of these experiments.

The PDC-II Experiment

This experiment ran from July 10–25, 1989. A cylindrical palladium cathode was used that had not been used earlier for any tritium work. It had been used, however, in the analysis of hydrogen gas samples and hydrogen purification. It was cleaned by degassing, using solvents such as acetone, and was heat treated at 300°C under vacuum for 2 h. Its dimensions were as follows: 0.45 mm thick, 6.37-cm^2 area, 0.143-cm^3 volume, 1.7-g weight, and 1 cm long. This was spot welded to a platinum rod. The 25-cm^2 anode was made of platinum gauze.

Cell and Accessories

The ~100-ml cell was made of quartz. The Pyrex glass lid had cones for the thermometer and the cathode, an entry port for sparging solutions with pure argon gas, and a vent for released gases. The cell was cooled by an external fan.

The evaporated heavy water from the cell was refluxed back into the cell with a water condenser, and the vapor that escaped from the condenser was collected in a moisture trap that was cooled with ice. The argon, deuterium, and oxygen gases were passed through a column of catalyst, which recombined the deuterium and oxygen into D_2O. The gases that emerged after recombination were passed through a water trap without further provision for recombination.

Nuclear-grade heavy water with an isotopic purity of 99.87% and an initial tritium content of 170 dpm/ml (0.076×10^{-3} μCi/ml) was used in the cell. The 60 ml of electrolyte was prepared 0.1 N to LiOD by using lithium metal. Iolar-2 argon was used as the carrier gas.

*Analytical Chemistry Division.
+Isotope Division.

Measurement Techniques

A calibrated thermometer was used to measure temperature. A galvanostatic power source with provisions for current pulsing was used for electrochemical measurements. Terminal voltage was measured by a digital panel meter. An LKB model 1215 RACKBETA-II system was used for tritium counting.

Sampling

Two-millilitre samples were drawn from the cell during the experiment to assess the tritium content. Aliquots from these samples were drawn and added to a 10-ml "Instagel Cocktail." Measured amounts of tritiated water from National Bureau of Standards (NBS) cells were added to 10 ml of Instagel for reference. A blank sample was also prepared with tritium-free groundwater in Instagel. Samples of the double-distilled water used to dilute and make the samples were also counted. Where interesting results were obtained, the full tritium spectrum was obtained and compared with the NBS tritium samples. When the samples had significant activity, known amounts of the samples were distilled and the resulting water was also counted.

During electrolysis, the cell level was maintained at a constant volume of 60 ml by periodically adding pure D_2O. The alkalinity was maintained at 0.1 *N* by occasional additions of LiOD.

Electrolysis

In the beginning, electrolysis was conducted at a constant 1-A current for 40 h; later, the electrolysis was done using pulses of varying current. Pulsing was done only during the day; at night, electrolysis was done at a constant current.

Degassing Procedure

At the end of the electrolysis, the cathode was transferred to a quartz heating tube and connected to a vacuum assembly. The moisture was removed from the electrode surface by heating it to 80 to 110°C and condensing in a cold trap. The oxygen and nitrogen gases were then recovered by standard getters. The electrode was gradually heated further, and the gas released was purified and absorbed in a pyrophoric uranium trap. The electrode was maintained at 550°C for 2 h, until there was no further release of gas. Deuterium gas was released from the pyrophoric trap, diluted with ~2.5 ℓ of hydrogen, and converted into water by circulating it through a heated copper oxide bed. This water was taken for tritium sampling.

Observations

See Table I for a summary of this experiment. There was a 25-min power failure between 1155 and 1220 on July 11.

The first sample was collected after 75 A·h for tritium assay. It gave 1.59 μCi/ml of D_2O. The cell volume of D_2O at this time was 60 ml (the total D_2O volume was 100 ml: 60-ml cell volume and 40-ml makeup volume). The tritium activity accounted would be 95.4 μCi. The excess tritium produced at the end of 75 A·h works out to be 1.25×10^4 times.

The second sample was drawn at 235.65 A·h. The assay of the sample showed that the activity was now 0.76 μCi/ml. The experiment was continued to 433 A·h, and samples were taken at 273.3, 381.5, and 433.32 A·h.

On July 26 at ~1015, the lid of the electrolytic cell was removed along with the anode and the thermometer. The experiment was stopped and a new lid was placed with the cathode inside the cell. An oxygen-argon mixture was bubbled through the cell, and the final sample was taken on July 28 and assayed for tritium (0.31 μCi/ml).

During electrolysis, 55.53 μCi of activity was recovered, 0.71 μCi was recovered from the vapor condensate and the recombination trap after electrolysis, and electrode degassing yielded 0.03 μCi; thus, a total of 56.27 μCi was recovered.

From the total of 256 ml of D_2O used (60 ml initially, 196-ml makeup volume), 132 ml was recovered and accounted for at the end of the experiment. The total tritium activity from the 256 ml of D_2O was 0.02 μCi.

In conclusion, at the end of 75 A·h, the electrolysis had generated ~95.4 μCi of excess tritium (12 500 times the input); however, at the end of the electrolysis (433.32 A·h), the total excess tritium recovered was 56.27 μCi.

The PDC-III Experiment

This experiment ran from September 9–14, 1989. The same cylindrical palladium cathode was used as for PDC-II. The cathode was treated to remove any deuterium and tritium. It was placed in the quartz assembly connected to the high-vacuum line and slowly heated. The cathode was heated under a continuous vacuum from room temperature to 850°C. When the temperature exceeded 750°C, a black deposit formed on the cooler parts of the quartz assembly. Heating was then continued at 850°C for 2 h more. No further deposit was released at this temperature.

The cathode was brought to room temperature, and the vacuum line was filled with deuterium gas at 1 cm of mercury pressure. The cathode was then slowly brought to 800°C and maintained at this temperature for 3 h. After this deuterium reduction process, the deuterium gas was removed and heating continued for 3 h under a continuous vacuum. The cathode was then checked for any further release of gas, but no further degassing was observed. However, the black coating released from the cathode turned into a silvery white deposit. The cathode itself was shining silvery white after this process and was thus used for the experiment.

A platinum gauze (25-cm^2) anode similar to the one in PDC-II was used.

Cell and Accessories

The cell and accessories were similar to those used in PDC-II, except for the following:

1. A standard palladium catalyst was used for recombination.

2. An additional recombination stage consisting of a copper oxide column was used to convert oxygen-depleted deuterium gas into D_2O.

Sampling and Measuring Techniques

The same kind of electrolyte and 80 ml of the same grade of heavy water were used. The sampling and measurement techniques were also the same as in PDC-II.

TABLE I

Summary of the PDC-II Experiment

Electrolysis	Dates	A·h
Constant current mode	July 10–12, 1989	40.33
Pulsing current mode (during day)	July 12–25, 1989	133.99
Constant current mode (during night)	July 12–25, 1989	248.85
Total		423.17

Tritium Levels in D_2O During Electrolysis

Volume of D_2O/0.1 LiOD electrolyte (ml)	60
Tritium activity in blank D_2O/LiOD [μCi/ml (dpm)]	0.076×10^{-3} (170)

Date	Sample	Cumulative A·h	Cumulative D_2O Added (ml)	Tritium Activity (μCi/ml D_2O)	Excess Tritium (times)
July 13, 1989	PDC-II-1	75	40	1.59	1.25×10^4
July 19, 1989	PDC-II-2	235.6	111	0.76	3.5×10^3
July 20, 1989	PDC-II-3	273.3	131	0.62	2.56×10^3
July 24, 1989	PDC-II-4	381.5	176	0.39	1.31×10^3
July 25, 1989	No sample	423.17	196	---	
July 26, 1989	No sample	433.32	196	---	
July 28, 1989	PDC-II-5	433.32	196	0.31	0.95×10^3

Tritium Activity in the Overall Experiment

Source	Volume (ml)	Total Activity (μCi)
Total input of tritium activity	256	0.02
Output		
End electrolysis D_2O cell sample recovered (PDC-II-5)	52	15.96
Vapor and condensate recovered	16	11.87
Deoxo-recombined D_2O recovered after termination of electrolysis	16 + 52	20.82
Vapor and condensate II recovered	0.5	0.14
Deoxo-recombined D_2O II recovered	2.8	0.57
Bubbler (H_2O)	16	1.16
Electrode gas control extracts after the electrolysis	---	0.03
Samples drawn during electrolysis	8	5.72
Total output		56.27

Note: Excess tritium recovered = $56.25/0.02 = 2.812 \times 10^3$ times.

Twelve samples were taken during this experiment. Other samples for tritium counting were collected from various stages of recombination from the catalyst, the water bubbler solution, and the degassed electrode.

Electrolysis

The electrolysis procedure was similar to that used for PDC-II, except that pulsing was introduced after 67 A·h of electrolysis under constant current. Pulsing was continued during the day and night for the entire experiment.

On September 13, electrolysis was returned to a constant 2-A current for 3 h, followed by pulsing at 2 to 4 A until the end of the experiment.

Observations

Table II summarizes this experiment. There was a power failure between 1300 and 1350 on September 8. A total of 185 ml of D_2O was used: 80 ml in the cell and 105 ml of makeup.

Nine cell solution samples were collected between September 7–13 to monitor tritium activity. The tritium content in the cell did not increase during this time; there was a marginal decrease in the samples taken on September 13 compared to those taken on September 12. The experiment was continued with a higher pulsing parameter as in the Fleischmann and Pons experiment; constant current was run for 3 h and pulsing for 2 h.

On September 14, at about 1000, there was a change in

TABLE II

A Summary of Electrolysis for PDC-III

Electrolysis	Dates	A·h
Constant current mode	September 6–9, 1989	71.75
Pulsing current mode	September 9–14, 1989	214.87
Total		286.62

Tritium Levels in D_2O During Electrolysis

Volume of D_2O/0.1 *M* LiOD electrolyte (ml)	80
Tritium activity in blank D_2O (dpm)	166 ± 4
Tritium activity in blank D_2O/LiOD [μCi/ml (dpm)]	0.075×10^{-3} (166 ± 4)

Date	Sample	Cumulative A·h	Cumulative D_2O Added (ml)	Tritium Activity (dpm/ml)
September 7, 1989	PDC-III-4	18.0		195 ± 4
September 8, 1989	PDC-III-5	42.0	15	276 ± 8
September 8, 1989	PDC-III-6	Current stopped	---	263 ± 8
September 9, 1989	PDC-III-7	65.67	30	249 ± 8
September 10, 1989	PDC-III-8	106.12	45	216 ± 4
September 11, 1989	PDC-III-9	137.87	53	248 ± 10
September 12, 1989	PDC-III-10	170.22	65	256 ± 10
September 12, 1989	PDC-III-11	185.87	75	260 ± 5
September 13, 1989	PDC-III-12	218	80	250 ± 5
September 14, 1989[a]	No sample	286.2	105	End of experiment

Tritium Activity in the Overall Experiment

Source	Volume (ml)	Total Activity (dpm)
Total input of tritium activity	185	30710 (0.0138 μCi)
Output		
Cell wash/broken quartz pieces	2	8592
Vapor and condensate recovered	2.5 + 5.0	114025
Palladium catalyst recombined	70 + 20	68605
D_2O recovered		
D_2O recovered after copper oxide	1 + 1.1	4285
Bubbler (H_2O)	---	3068
Electrode gas content extracted after explosion	---	5530
Samples drawn during electrolysis	18	4426
End electrolysis D_2O cell sample[b]	---	---
Total output		208531 (0.0939 μCi)

Note: Excess tritium recovered = 177821/30710 = 0.080 μCi = 5.79 times.

[a]There was an explosion and all the D_2O in the cell was lost; therefore, no sample could be taken.
[b]Calculation of total tritium activity does not take into account 80 ml of D_2O spilled due to the explosion.

the cell behavior. The bottom of the cell shattered due to an explosion. Before the explosion, the cell temperature shot up from 71 to 80°C and the bubbling rate was low.

Due to the explosion at the end of the experiment, the entire ~80 ml of electrolyte solution was lost and no sample could be collected for tritium assay. The upper part of the cell and the broken pieces were washed and a sample collected for counting. The D_2O condensate and the recombined water from the palladium catalyst, copper oxide, and the bubbler solutions were taken for tritium assay.

The total tritium activity from all the samples accounted for 208 531 dpm, while the total input tritium activity was

30 170 dpm. The activity in the cell solution could not be accounted for, as it was lost. However, even this 208 531 dpm of activity shows excess tritium of 5.79 times.

In addition, had the cell solution not been lost, a significant amount of tritium also could have been recovered. A large tritium activity was not produced in the cell until September 13, even at 218 A·h. Excess tritium was produced only between September 13–14 (between 218 and 286.2 A·h), whereas in the PDC-II experiment, excess activity was generated at ~75 A·h in 3 days of electrolysis.

Results of the Metallographic Examination of the Cathode

The palladium cathode underwent a metallographic examination at the Physical Metallurgy Division by means of

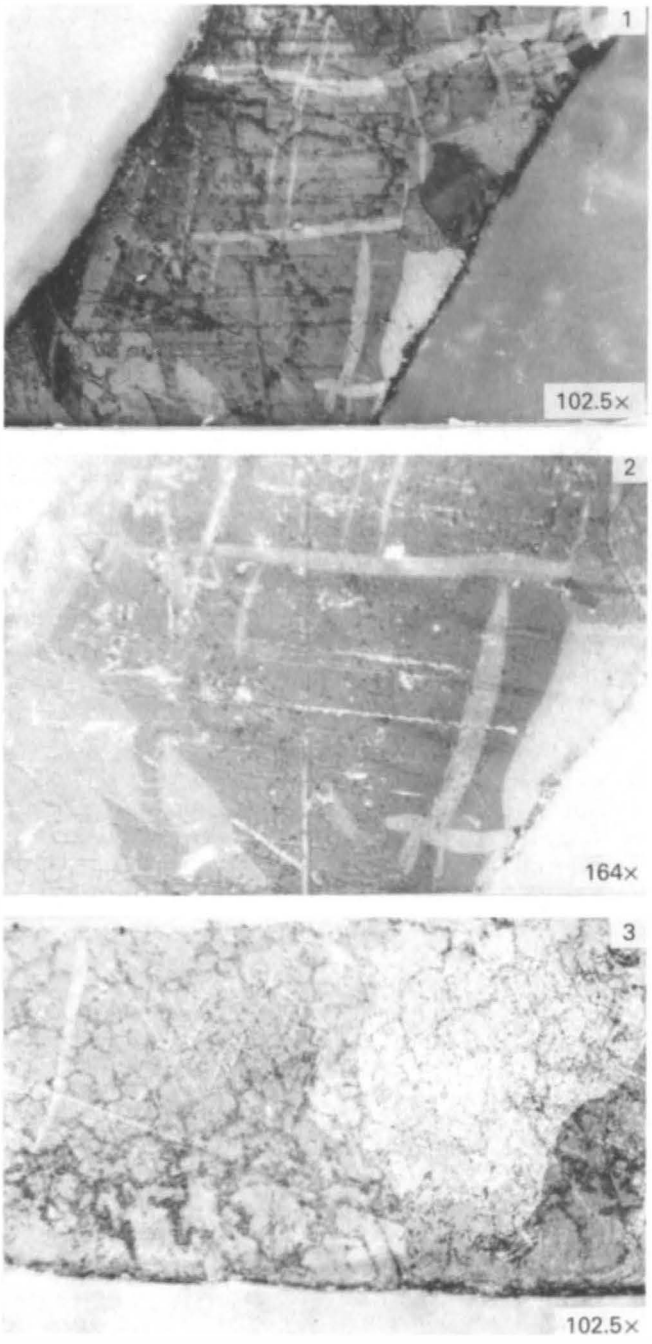

Fig. 1. Deuterium-loaded palladium sample 1: after explosion.

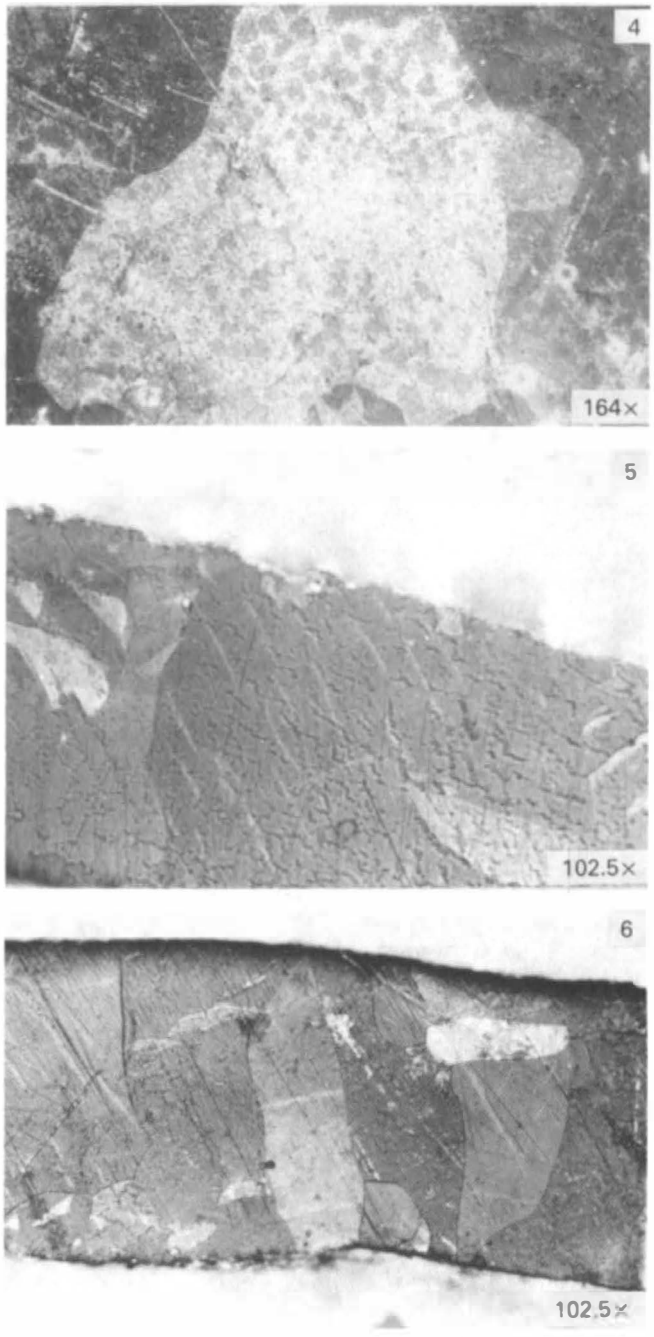

Fig. 2. Deuterium-loaded palladium sample 1: another view.

polarized light microscopy after embedding and mounting the electrode with an acrylic polymer resin. The examination showed extensive twinning within the palladium grains with a wormlike structure. This is suggestive of an intensive shock-wave impact on the metal. Microphotographs of the two samples are shown in Figs. 1, 2, and 3.

The cathode was then cleaned with acetone and tetrahydrofurane to remove the polymer coating. On degassing, the electrode released ~1.2 ml of gas, which accounted for 5530 dpm of tritium activity. If the electrode had been degassed before the metallographic examination, the tritium content would have been significantly higher.

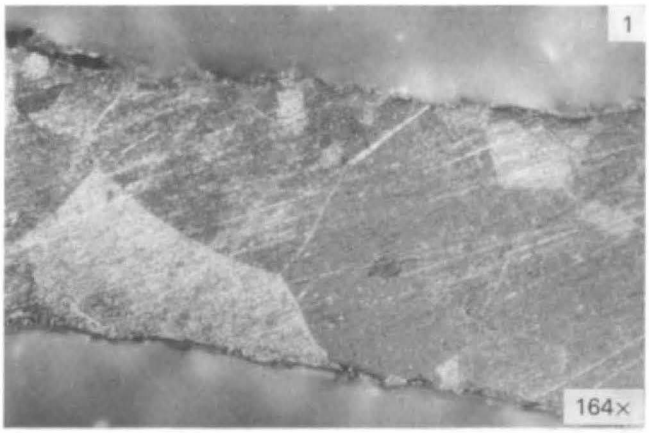

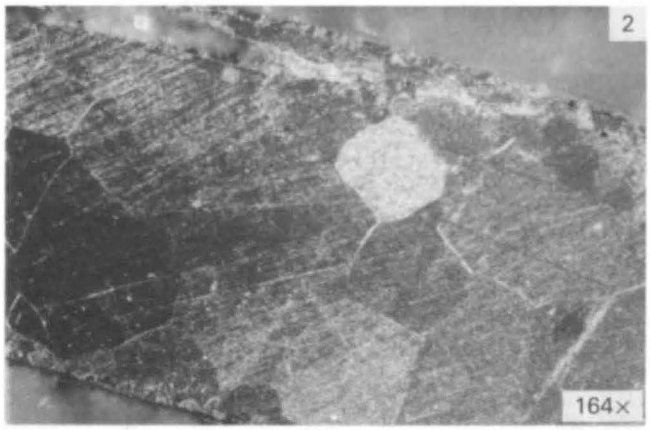

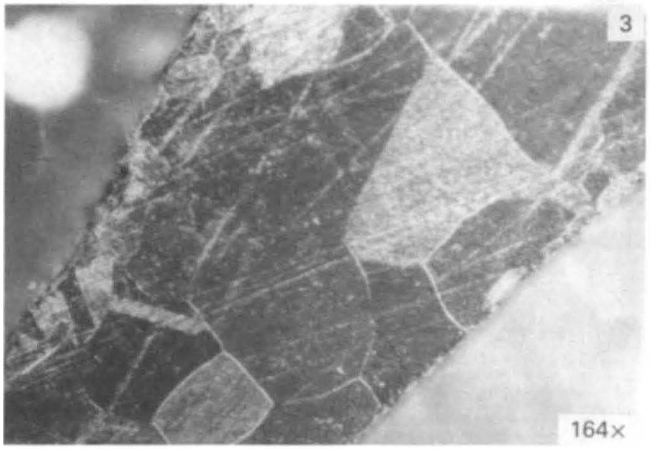

Fig. 3. Palladium sample 2, annealed at 550°C for 2 h, without deuterium loading.

ACKNOWLEDGMENTS

Acknowledgments are due to P. K. Iyengar, director of Bhabha Atomic Research Centre, for his keen interest in this work. Acknowledgments are also due to G. E. Prasad and M. K. Asundi, head of the Physical Metallurgy Division, for carrying out the metallographic investigations.

7. BURST NEUTRON EMISSION AND TRITIUM GENERATION FROM A PALLADIUM CATHODE ELECTROLYTICALLY LOADED WITH DEUTERIUM

G. Venkateswaran,* P. N. Moorthy,*
K. S. Venkateswarlu,* S. N. Guha,+ B. Yuvaraju,*
T. Datta,† T. S. Iyengar,‡ M. S. Panajkar,+
K. A. Rao+ and K. Kishore*

Introduction

There have been many recent reports on the observation of neutrons, tritium, and excess heat output from palladium and titanium cathodes electrolytically charged with deuterium.[1-4] Steady neutron count rates observed during the operation of electrolytic cells containing these cathodes and platinum anodes were in some cases only 1.5 to 3 times the background rate,[3,4] whereas in other cases a much higher steady emission rate (10^4 s) was observed. In some earlier experiments at Bhabha Atomic Research Centre, neutron bursts two orders of magnitude larger than the background were reported from electrolytic cells.[5] The possible nuclear reaction responsible for the emission of neutrons has been inferred to be the "cold fusion" of deuterium atoms (existing as D^+) in the metallic lattice of the cathode:

$$ {}^{2}_{1}\mathrm{D} + {}^{2}_{1}\mathrm{D} \rightarrow [{}^{4}_{2}\mathrm{He}]^* \rightarrow {}^{3}_{2}\mathrm{He} + {}^{1}_{0}n \ . \qquad (1) $$

We report here a large burst emission of neutrons (signal-to-background ratio as high as 2000) from a thin ring-shaped palladium cathode during the electrolysis of heavy water at relatively low cell currents and tritium generation as measured in the electrolyte and in the water recombined from the absorbed gas recovered from the cathode.

Experimental

The electrolytic cell design was optimized with respect to observation of fusion products rather than the accurate measurement of excess heat output. This is because the quantity of heat required to raise the temperature of 1 g of D_2O by even 1 K demands the occurrence of $\sim 10^{13}$ fusions; hence, heat measurement appears to be an insensitive method of confirming whether or not cold fusion occurs in the cathode. Figure 1 is a schematic of the experimental setup. The electrolytic vessel (volume ~250 cm^3) was made of quartz with a gastight nylon cap. The cap had a number of penetrations for

*Applied Chemistry Division.
+Chemistry Division.
†Radiochemistry Division.
‡Health Physics Division.

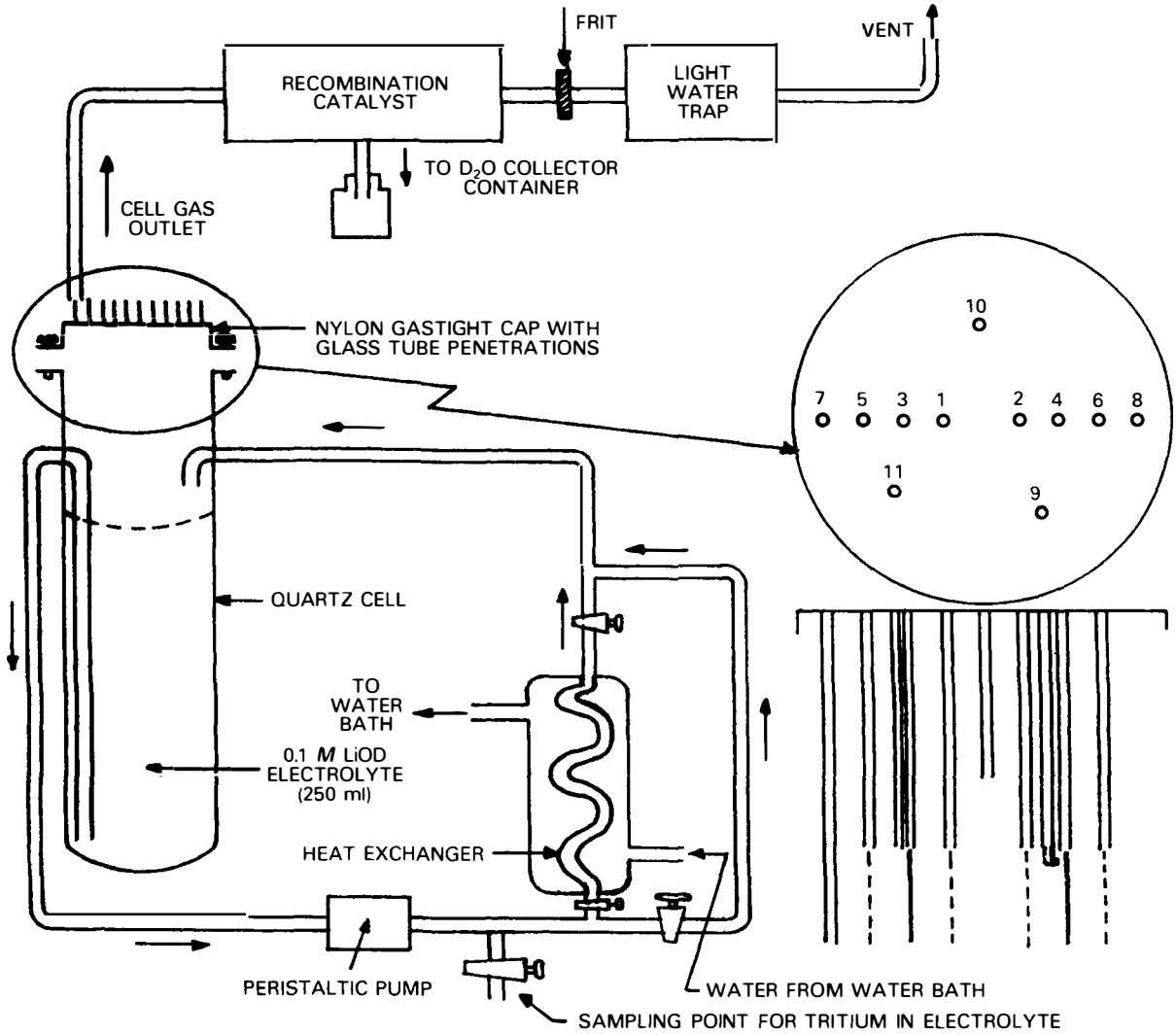

Fig. 1. Schematic of experimental setup.

inserting electrode lead wires, thermocouple, reference electrode, and purge gas inlet and outlet tubes. These tubes were made of Corning glass.

The palladium cathode was a hollow ring 2.5 cm in diameter, 1 cm high, and ~0.1 cm thick (surface area = 18 cm^2). It was pretreated by vacuum degassing ($<10^{-3}$ mm Hg) at 1073 K for ~10 h in three heating-cooling cycles (~3.3 h/cycle). The bulk density of the cathode was determined to be 12 g/cm^3. The ring cathode could be charged with deuterium from both sides as it was surrounded from inside and outside by platinum gauze anodes. The anodes were loosely sandwiched between pairs of Nafion membrane to prevent oxygen evolved at the anode from diffusing to the cathode surface.

The electrolyte was D_2O of 99.86% isotopic purity containing 0.1 mol/dm^3 LiOD and was kept under constant circulation at a flow rate of 10 cm^3/min using a peristaltic pump. The D_2O used to prepare the initial LiOD solution and subsequent makeup during the electrolysis came from a single stock of D_2O. A heat exchanger in the circulation path along with a thermostated water bath (273 to 373 K) maintained the temperature of the electrolyte (and hence the electrode) at any desired value in this range. Nitrogen gas was bubbled through the cell to reduce the dissolved oxygen level in the electrolyte. A saturated calomel electrode, along with a luggin probe containing 0.1 mol/dm^3 LiOD/D_2O dipped in the electrolyte, was used as a reference electrode to monitor the single electrode potential of the cathode. Periodic

monitoring of the cathode potential was carried out both when the working electrode was under polarized conditions and when the polarization voltage was momentarily switched off.

The well-type neutron detector assembly consisted of 24 ^{3}He detectors embedded in paraffin and held between aluminum cylinders for thermalization of the neutrons. This configuration gave 8.6% efficiency. The output from the detector-preamplifier-active filter amplifier tie-up was fed in parallel to a scaler with a preset time, to an oscilloscope and a personal computer operated in an 8-K multichannel scaling (MCS) mode with a dwell time of 40 s per channel. The MCS mode was used specifically for detecting any small burst release of neutrons that could otherwise be averaged out in a longer preset time. Typically, preset time counting was done for 6000-s periods, but during the intense burst release of neutrons, the preset time was reduced to ~1000 s to avoid scaler overflow. Any extraneous signals, such as those emanating from the operation of pump motors, drilling machines, tesla coils, piezoelectric gas lighter, and fluorescent lamps going off and on, were thoroughly checked. The counter was found to have good stability and was immune to such electrical disturbances. A constant background of ~1.6 count/s was registered without the electrolytic cell in operation for 10 days before being set up inside the counter well and also during electrolysis when there was no burst emission of neutrons.

Accumulation of tritium in the electrolyte was monitored by withdrawing 1-cm^3 samples from the cell at ~6-day intervals and measuring the tritium content using a gel liquid scintillation "cocktail" and a Packard counting system. The counting efficiency was ~25%. A chemiluminescence effect due to the presence of LiOD was seen in the samples, and counting continued until such effects died down completely and stable count rates were obtained.

During certain periods of electrolysis, the electrolytic gases from the cell were recombined over a platinum/polyester fabric catalyst and collected in a cold trap. The resulting D_2O was checked for the presence of tritium. Loss of D_2O due to electrolysis and evaporation was made up by periodic addition of pure D_2O, while losses due to sampling were made up by adding 0.1 mol/dm^3 LiOD solution in D_2O. The D_2O used for the experiment and for replenishment was from a single stock of heavy water. The temperature of the electrolyte was monitored by a Chromel-Alumel thermocouple encased in a glass tube inserted in the solution.

The cell was run for 32 days, mostly at a current density of ~60 mA/cm^2. At the end of the electrolysis run, the palladium cathode was disassembled from the cell and the connecting leads and dried. The absorbed gases from the cathode were recovered by heating it at 680 K in an evacuated chamber. From the pressure/volume relationship and gas chromatographic analysis of the deuterium content, the volume of absorbed D_2 gas was computed to be 320 cm^3 at standard temperature and pressure (STP). This gas was then equilibrated over copper oxide at 680 K until there was no further reduction in volume, and the water formed (less than ~0.3 cm^3) was collected in a thimble cooled to liquid N_2 temperature. This water was also counted for tritium.

Results

Burst Neutron Emission

Up to day 14 of electrolysis (using ~2.24×10^6 C), only background neutron counts were observed and again after day 17 (~2.5×10^6 C) until the end of the run, day 32 (a total of ~3.65×10^6 C), only background counts were seen. During the neutron emission period (days 15, 16, and 17), the bursts were intense up to ~14 h into the emission with intervening quiescent periods (in which counts were close to background) varying from as short as ~120 s to as long as 3 h. In the later stages, the burst intensity decreased, but the bursts became so frequent near the end that they appeared to be continuous. The maximum burst signal (at ~14 h into the emission) corresponded to 142 000 counts in a 40-s time channel compared to 50 to 70 counts registered for the background. This corresponds to a maximum signal-to-background ratio of ~2000. Using the 8.6% efficiency of the neutron counter, the total number of neutrons emitted in these bursts works out to 1.8×10^8 in ~40 h, which corresponds to a pseudo-average emission rate of 1.3×10^3 n/s.

The electrolyte temperature was varied in the initial stages of the run by changing the voltage applied to the cell or the set temperature of the thermostatic water bath. Ten hours before the burst emission and during the burst emission, the temperature of the electrolyte was not altered and it remained between 296 and 300 K. Electrolyte temperature during the entire electrolysis time remained >293 K.

Figure 2 shows the observed burst neutron emission that lasted for ~40 h during the 32-day operation of the cell. This figure represents 4000 data points collected in the MCS mode, each point being the neutron counts in a 40-s time channel. A portion of the steady background counts recorded before the beginning of the burst emission is included to show the burst intensities in relation to this background. Figure 3 shows observed burst neutron emission in a ten-times expanded time axis.

Tritium in Electrolyte and Electrode

Tritium counting of samples (Table I) drawn 5 to 17 days after the burst neutron emission (samples 4, 5, and 6 in Table I) showed an increase from 0.4 to 1.3 Bq/cm^3. Low-level counting methods (60-min count) coupled with a stable system background yielded a standard deviation of only 3% on the count rates. The cell electrolyte volume being 250 cm^3, an increase of 0.4 to 1.3 Bq/cm^3 in tritium activity shows an extra input of tritium of 100 to 325 Bq, amounting to 5.6 to 18.0×10^{10} extra tritium atoms accumulating in the electrolyte, probably as DTO. It is known that at temperatures

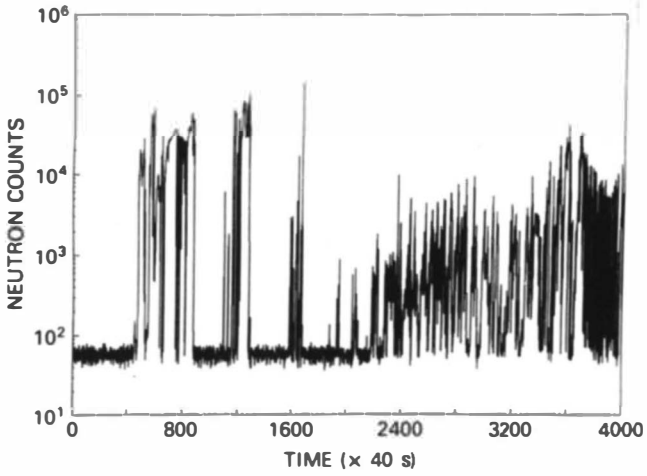

Fig. 2. Burst neutron emission in MCS mode over time.

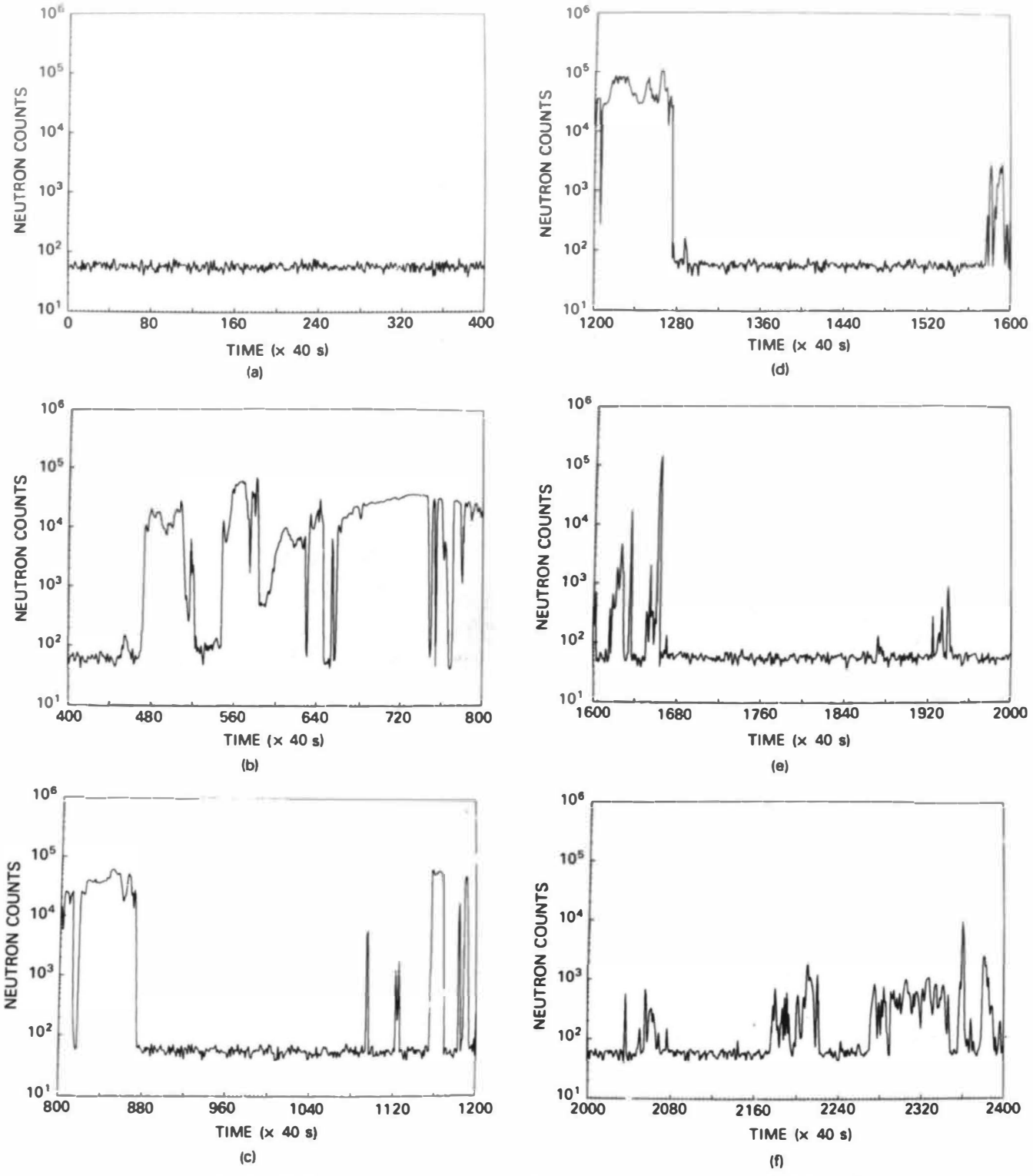

Figs. 3a–3f. Burst neutron emission in MCS mode over time on an expanded time axis.

>293 K, electrolysis of D_2O does not result in significant enrichment of tritium in the electrolyte.[5] In the present experiment, electrolytic gases recombined over a catalyst and counted for tritium showed tritium escaping from the cell. Hence, the observed excess of tritium activity points to an extra source of tritium on the conservative side; i.e., not accounting for the tritium that is carried away in the gas stream during the electrolysis.

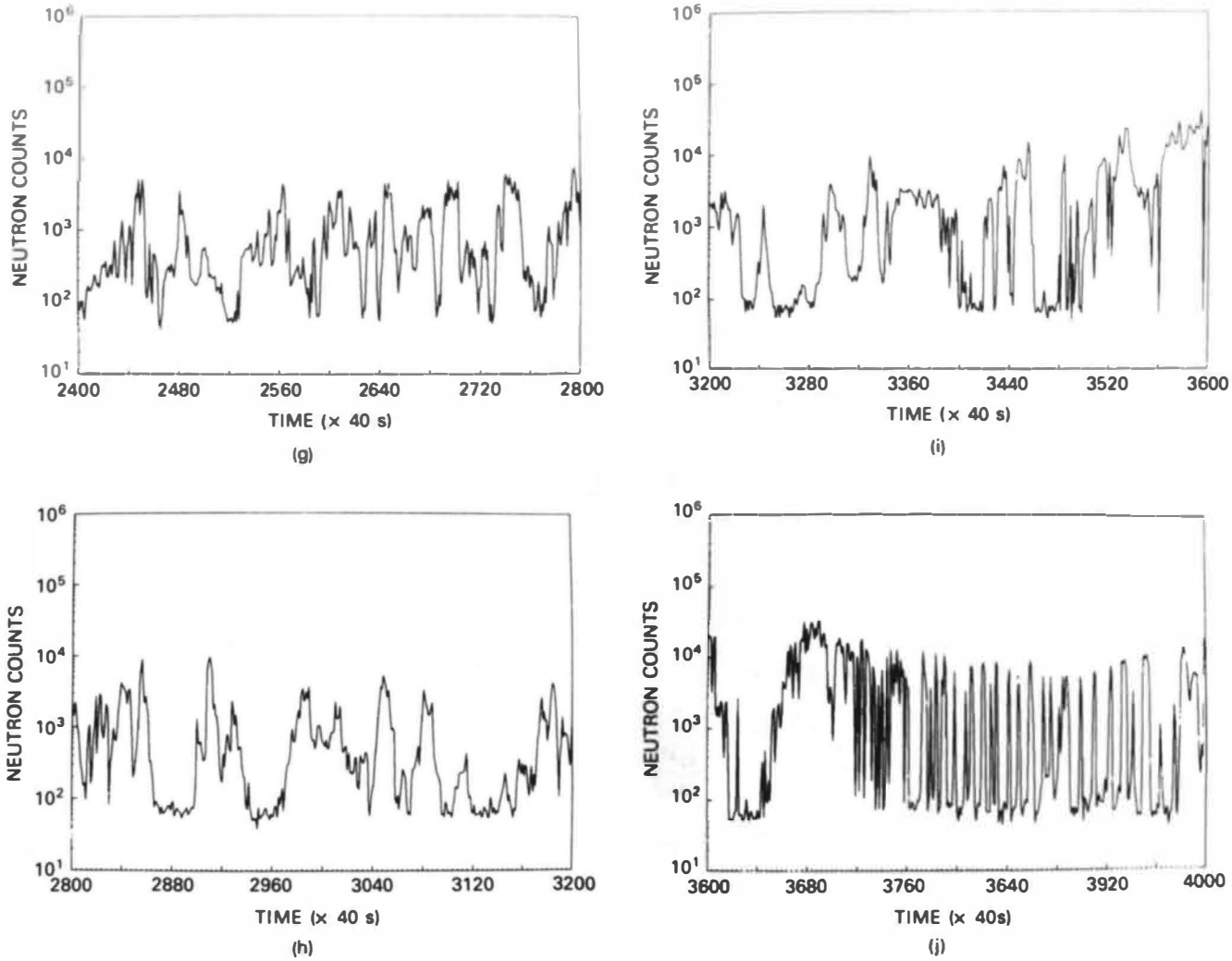

Figs. 3g–3j. Burst neutron emission in MCS mode over time on an expanded time axis.

Degassing of the palladium cathode at 680 K at the end of the experiment yielded 320 cm^3 of D_2 gas at STP. By reaction of this gas over copper oxide turnings at 680 K and quantitatively collecting the recombined water, counting for tritium showed 5.4 Bq (3×10^9 atoms of tritium) accumulating in the palladium cathode.

Electrode Potential

Figure 4 indicates the variation of cathode potential and neutron emission rate (deduced from the scaler counts obtained with preset time) with time. A potential of −1.0 V against saturated calomel electrode (SCE) when the polarization voltage was switched off indicates that the electrode in a 0.1 mol/dm^3 alkali concentration behaves as a near-hydrogen (in the present case, deuterium) electrode. Monitoring potentials some hours into the burst emission period revealed fluctuations in the working electrode potentials. The neutron count rate peaks seem to coincide with the shift of potentials to more positive values by as much as 0.7 V in the cell when off and by 3 V when on.

Heat Output

No discernible extra heating over the background Joule heating was observed in this experiment.

Discussion

This study has shown that monitoring neutrons is a much more sensitive method than monitoring tritium for identifying whether cold fusion occurs or not, especially when the fusion events generating tritium are not very high. This is because of the small decay constant of tritium, which requires an accumulation of 10^9 atoms to register 1 Bq of tritium activity. In the present case, although the neutron-emitting events computed from the integrated neutron counts amounted to only 10^8, compared to $\sim 10^{10}$ to 10^{11} events computed from tritium data, the neutron emission occurred with large spikes and bursts. Thus, 10^{11} events through the tritium channel were inferred from an increase of 1.3 Bq/cm^3 extra tritium activity observed at the end of the experiment. Since only 5.4 Bq of tritium was in the palladium cathode at the end of the experiment, it looks as if the tritium generated (~325 Bq)

TABLE I

Tritium Content in the Electrolyte of Palladium-Platinum Electrolysis Cell

Sample	Duration of Electrolysis (days)	Cumulative Coulombs Used ($\times 10^{-6}$)	Tritium Activity (Bq/ml)[a]
1	0	0	3.65
2	7	1.07	3.32
3	16	2.36	3.65
4	20	2.72	4.94
5	26	3.21	4.24
6	32	3.55	5.20

[a]Standard deviation = ±3%.

mostly diffuses into the electrolyte rather than being retained in the palladium matrix, which is somewhat akin to the neutron emission, and suggests the possibility of fusion events occurring close to the surface. From the variation in tritium activity at different times during the course of electrolysis (Table I), it appears that tritium input into the electrolyte started after the burst neutron emission occurred. This is because the day 16 sample that was taken during the burst neutron emission registered the same tritium activity as the sample taken in the initial stages of the run. During the tritium generation period (days 17–32), however, there was no neutron emission over the background rate.

From the volume of D_2 gas trapped inside the palladium electrode (320 cm^3 at STP actually collected), the composition of the palladium deuteride that would have given rise to the burst neutron emission was inferred to be between $PdD_{0.3-0.4}$. Using the known diffusion coefficients of deuterium ($<1 \times 10^{-7}$ cm^2/s), it was computed that deuterium atoms can enter the 1-mm-thick cathode and come out the other side in ~30 h, thus pointing to the attainment of at least a $PdD_{0.25}$ configuration in ~1 day. But, as shown by the D_2 gas trapped in the cathode at the end of the experiment (day 32), only at the end of the 32 days does this composition seem to have been reached. The reason for this could be the loose blackish coating formed on the palladium cathode during the experiment, which perhaps acted as a diffusion barrier for the entry of deuterium atoms. Analysis of this coating revealed that it was platinum that might have arisen from anodic dissolution of platinum at the applied cell voltages (which were higher than the reversible Pt/Pt^{2+} potential). The reason the burst neutron emission was not sustained for >3 days may be summarized as follows: Those sites in the palladium matrix in which fusion of deuterium atoms occurred might have been the really active sites. Once the deuterium atoms were depleted from those sites, further replenishment did not take place possibly because of the barrier coating,

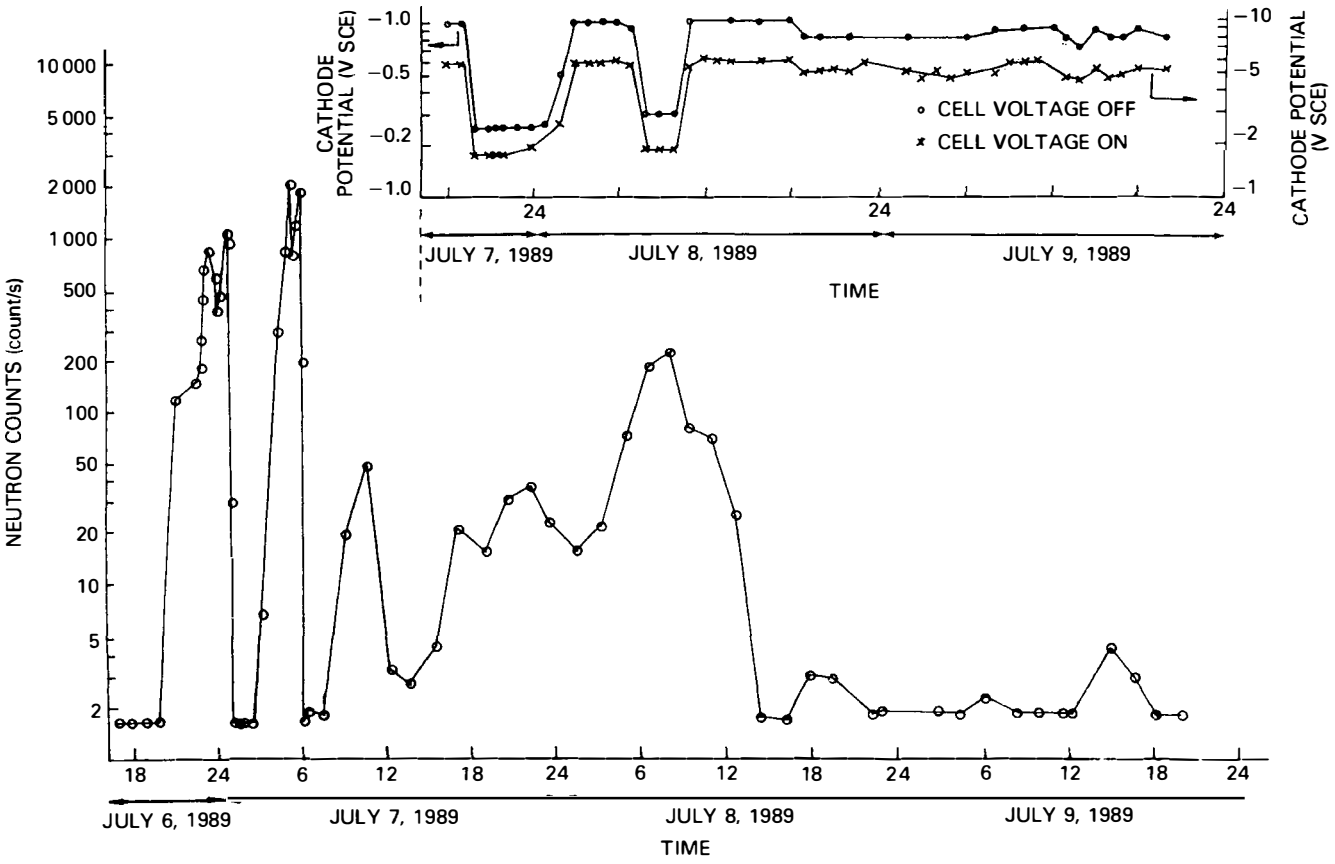

Fig. 4. Burst neutron emission rate and cathode potential variation.

which only favored molecular D_2 formation from the cathode surface with no further entry of deuterium atoms into the matrix.

A palladium electrode dipped in an alkaline solution and on whose surface D_2 is evolving is expected to behave as a normal OD^-/D_2 electrode, registering a potential of -1.01 V SCE. However, since palladium absorbs deuterium, the overpotential for D_2 evolution is expected to increase and the polarization voltage must be adequate to evolve D_2 on the electrode surface by electrolysis. In the present study, however, even after charging the palladium for a number of days, the overpotential obtained was negligible, although degassing the cathode at the end of the experiment showed that it had absorbed 320 cm^3 of D_2 gas at STP. The shift to more positive potential values by as much as 0.7 V in the cell coinciding with the neutron count rate peaks indicates possible depletion of deuterium gas at the surface of the electrode. Thus, monitoring the cathode potential has shed some light on what happens to a palladium electrode that has absorbed deuterium.

In general, very few groups have been able to reproduce the large heat output reported by Fleischmann and Pons[1] and Mathews et al.[4] Even to match a cooling rate of 0.1 K/min in a cell of the dimensions reported here, it would require fusions occurring at a steady rate of $\sim 10^{10}$/s. As discussed above, the observed neutron bursts revealed that the fusions do not occur at a steady rate of the desired magnitude, and hence, it is no wonder that the excess heat output went undetected. In our laboratory, we carried out several runs on electrolytic cells using palladium cathodes of various shapes and dimensions (including a 1-cm-diam × 1-cm-long solid cylinder) and platinum anodes in 0.1 mol/dm^3 of $LiOD/D_2O$ along with control palladium cathodes and platinum anodes in 0.1 dm^3 of $LiOH/H_2O$ to observe the excess heat output. We did not, however, observe excess heat within the limits of the uncertainty of our calorimetry, which is estimated to be about ±10%.

Conclusions

This study has shown evidence for cold fusion phenomenon in an electrolytically charged palladium matrix in terms of neutron and tritium production. The tritium channel seems to be favored over the neutron channel. During our experiment, a total of 10^{11} fusion events leading to tritium generation were observed, whereas the neutron channel accounted for only 10^8 fusion events. No significant heat output over Joule heating could be observed. This study also revealed that the effect is small and not sustained. Sustained energy production from cold fusion of deuterium in an electrolytically charged palladium matrix may require more systematic exploration to identify the various parameters governing the process, not the least important among which is the proper pretreatment of the electrode.

ACKNOWLEDGMENTS

We are thankful to R. M. Iyer, director of the Chemical Group, and J. P. Mittal, head of the Chemistry Division, for their encouragement and support for this work; to S. D. Soman, director of the Health and Safety Group, for his guidance in tritium analysis; and to P. R. Natarajan, head of the Radiochemistry Division, for making available the neutron counting setup. We are grateful to R. H. Iyer and J. K. Samuel of the Radiochemistry Division for useful discussions and V. N. Rao of the Chemistry Division for providing the necessary instrumentation for electrode potential measurements. The authors wish to thank Balhans Jayswal of the Computer Division for helping to plot with optimum resolution the large number of neutron count data gathered in the MCS mode. We gratefully appreciate the tireless devotion and patience with which the following personnel from the Water Chemistry and Chemistry Divisions kept these experiments continuously running over the long time period: B. R. Ambekar, T. P. Balan, A. D. Belapurkar, K. B. Bhatt, K. N. Bhide, A. S. Gokhale, Hari Mohan, D. R. Joshi, P. S. Joshi, K. N. G. Kaimal, S. B. Karweer, A. S. Kerkar, M. Kumar, H. S. Mahal, Mani Maran, N. Manoj, M. O. Mathews, R. K. Misra, A. Satyamoorthy, and K. N. Shelar.

REFERENCES

1. M. FLEISCHMANN and S. PONS, "Electrochemically Induced Nuclear Fusion of Deuterium," *J. Electroanal. Chem.*, **261**, 301 (1989).

2. S. E. JONES et al., "Observation of Cold Nuclear Fusion in Condensed Matter," *Nature*, **338**, 737 (1989).

3. K. S. V. SANTHANAM et al., "Electrochemically Initiated Cold Fusion of Deuterium," *Indian J. Technol.*, **27**, 175 (1989).

4. C. K. MATHEWS et al., "On the Possibility of Nuclear Fusion by Electrolysis of Heavy Water," *Indian J. Technol.*, **27**, 229 (1989).

5. P. K. IYENGAR, "Cold Fusion Results in BARC Experiments," *Proc. 5th Int. Conf. Emerging Nuclear Energy Systems*, Karlsruhe, FRG, July 3–6, 1989, World Scientific, Singapore (1989).

8. VERIFICATION STUDIES ON ELECTROCHEMICALLY INDUCED FUSION OF DEUTERONS IN PALLADIUM CATHODES

H. Bose,* L. H. Prabhu,* S. Sankaranarayanan,*
R. S. Shetiya,* N. Veeraraghavan,* P. V. Joshi,+
T. S. Murthy,+ B. K. Sen,+ and K. G. B. Sharma+

Introduction

In continuation of the work carried out earlier on electrochemically induced fusion of deuterons, a series of experiments was carried out using a palladium cathode and a platinum wire gauze anode. Some of the main features of the experiments were as follows:

1. The electrolysis experiments were conducted using 0.1 *M* LiOD solution in D_2O using a 1- × 1- × 1-cm cube of palladium as the cathode and platinum wire gauze as the anode.

2. The experiment lasted for 7 weeks during which data on heat measurements, tritium production, and neutron emission were collected.

3. The amount of deuterium loading on the palladium electrode was measured at the end of the experiment.

4. Blank experiments with a stainless steel cathode instead of palladium and H_2O instead of D_2O were also carried out.

*Reactor Operations and Maintenance Group.
+Isotope Division.

Experimental

Cathode

The spectrographic analysis showed the palladium content of the palladium cube cathode to be 98.2%. The impurities were mainly copper, calcium, iron, lead, and nickel. The cathode was heated under vacuum and cleaned electrochemically before use. After use in the electrolysis experiments, these cathodes were generally degassed at high temperatures (850°C) and heated in vacuum for a few hours for reuse. A 1- × 1- × 1-cm cube of stainless steel (Type 304L – 72% Fe, 18% Cr, 8% Ni) was used as a cathode in the blank experiments after polishing the surface and cleaning with distilled water.

Electrolyte

The volume of solution used in the electrolysis cell was 140 ml. The electrolyte solution of 0.1 *M* LiOD in D_2O was prepared by dissolving lithium metal in D_2O with an isotopic purity of >99.86%. For some of the blank experiments with H_2O, the electrolyte solution of 0.1 *M* LiOH in H_2O was prepared by dissolving lithium metal in pure double-distilled water.

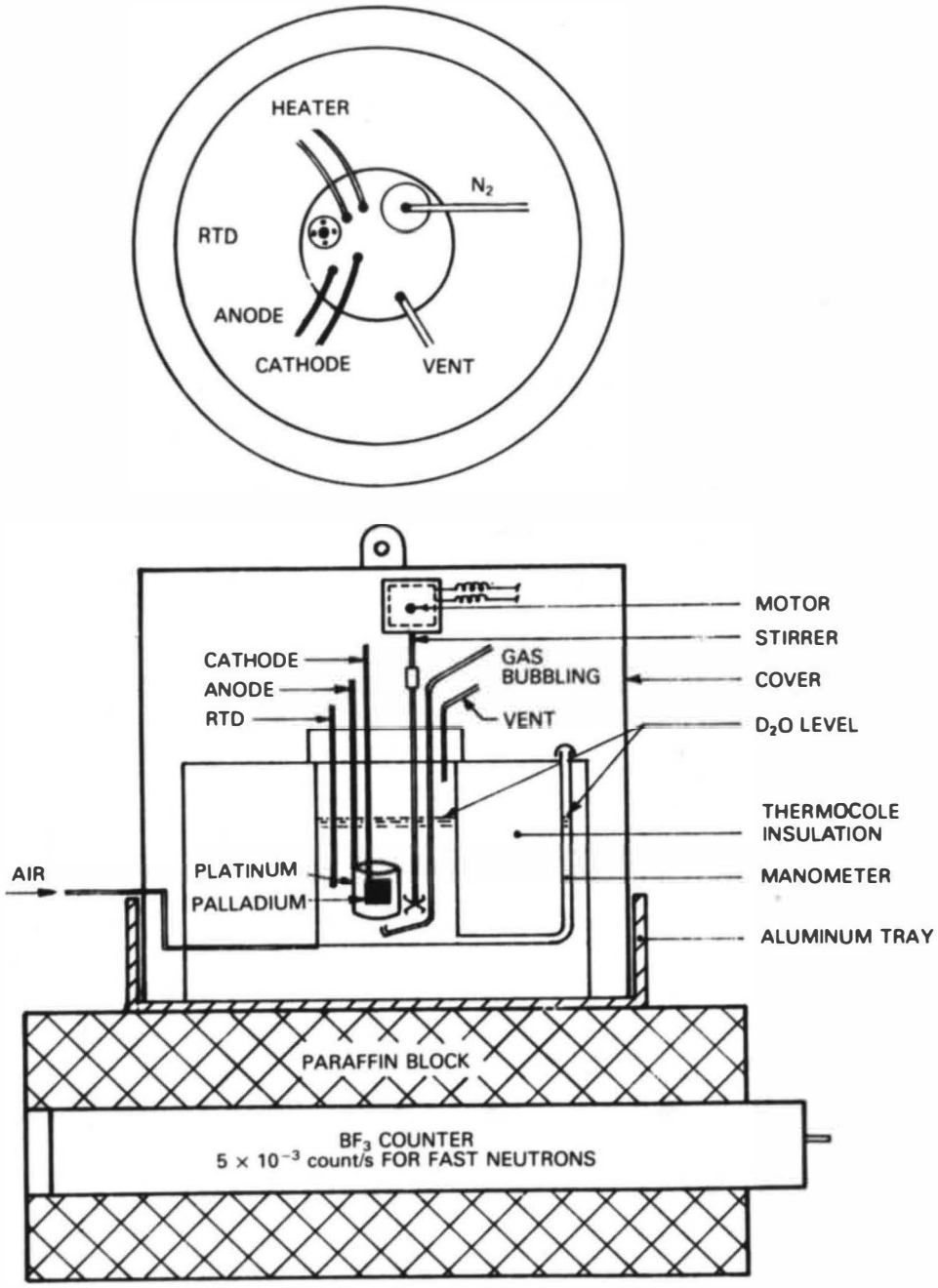

Fig. 1. Electrolysis cell.

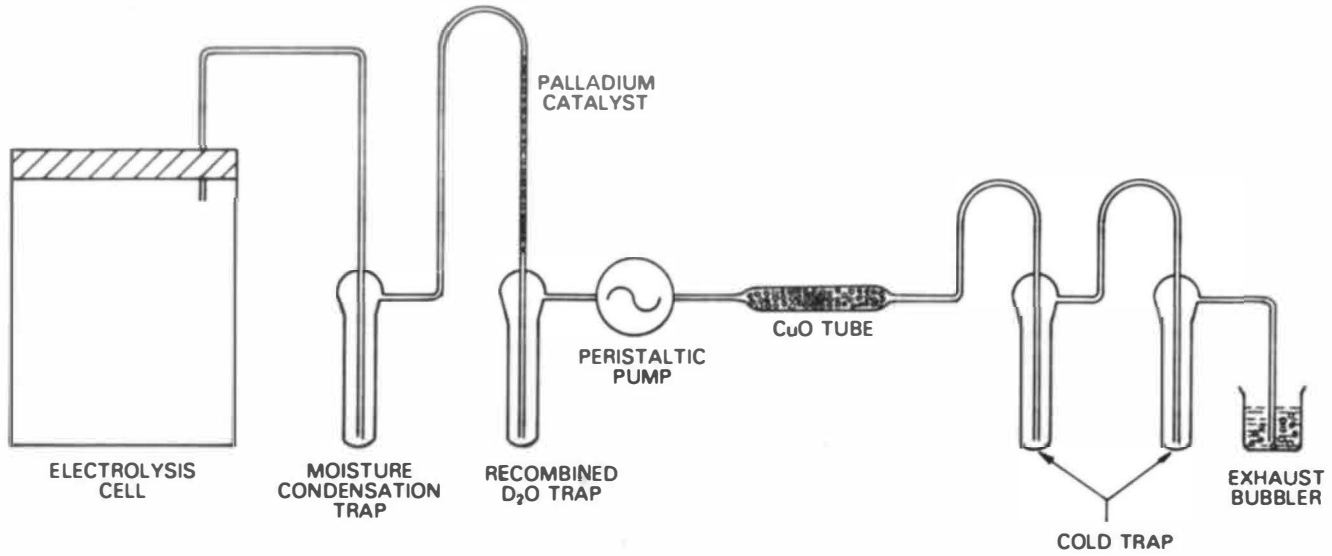

Fig. 2. Assembly for converting $D_2 + O_2$ or D_2 to D_2O.

Experimental Assembly

Figure 1 is a schematic of the assembly. The experimental assembly was covered with thermocole insulation open to ambient air while data on heat measurements were collected. Subsequently, the cell was cooled only by air. During the later part of the electrolysis, the cell was cooled by cold water.

Figure 2 shows the details of the assembly used for recovery and conversion of gases (D_2 and O_2) liberated during the electrolysis. A palladium catalyst was used to recombine D_2 and O_2, and hot copper oxide was used to convert D_2 into D_2O. The recovery assembly enabled assessment of the recombination of D_2 and O_2 emerging from the electrolytic cell and estimation of the absorbed D_2 gas liberated from the palladium cathode after the electrolysis was terminated.

A resistance wire heater was placed in the cell to collect data on electrical heating without electrolysis. The temperature of the electrolyte solution was monitored by a resistance temperature detector (RTD) placed in the cell, and it was recorded continuously on a chart. During the heat measurements, a mechanical stirrer was used to mix the electrolyte. Subsequently, the cell was stirred by bubbling nitrogen gas from a cylinder.

Electrolysis

Electrolysis was done at constant current and variable voltage. At the end of 1365 A·h, current was changed to the pulsing mode (0.5 A for 1 s followed by 2.5 A for 1.5 s) for ~3 h and then to 0.5 A for 1 s followed by 4.5 A for 1.5 s. After ~10 min under this mode, an explosion occurred inside the cell, resulting in the cell lid being thrown out with the electrode assembly. The electrodes were intact but were found to be electrically shorting. Electrolysis was terminated and the D_2 gas released by the palladium electrode was passed through the palladium catalyst and copper oxide for conversion of D_2 to D_2O.

Neutron Detection

For neutron detection, a BF_3 neutron detector with a counting efficiency of 5×10^{-3} count/s per fast neutron was placed below the electrolysis cell. An additional BF_3 detector was placed ~2 m away from the cell to monitor background neutrons.

Sampling and Assay

The cell electrolyte and the D_2O collected in the various cold traps in the attached assembly were periodically sampled during the experiment, for tritium measurement. The D_2 gas released by the palladium electrode (after conversion to D_2O) was also analyzed for tritium content. All the tritium measurements were done using an LKB model 1215 RACKBETA-II system.

Blank Experiments

Blank experiments were carried out following a similar procedure using a combination of palladium and stainless steel cathodes, D_2O and H_2O electrolyte solutions (see Table I). Each blank experiment lasted ~16 to 20 h.

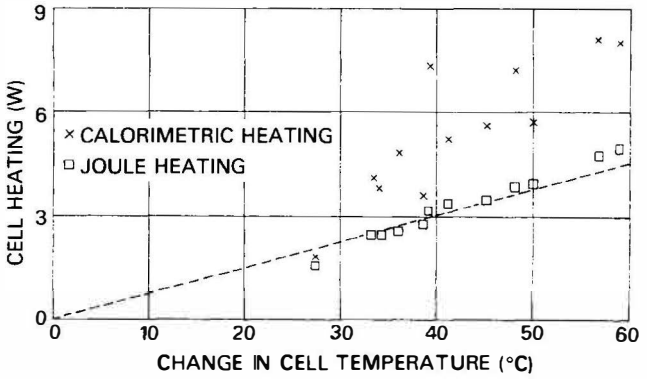

Fig. 3. Experiments with palladium or stainless steel cathodes in D_2O or H_2O.

Heat Measurements

For measurement of the heating rate in the electrolysis cells, the cell temperature rise over time was collected for different current density values until the cells attained thermal equilibrium. Steady-state cell temperatures at different stages of electrolysis with increasing deuterium loading in the palladium were also collected.

Figure 3 gives the variation of equilibrated cell temperature rise with Joule heating of the cell. The cell thermal sensitivity, expressed as the ratio of steady-state cell temperature rise (with respect to heat sink temperature) to Joule heat input power, remained almost constant in all the experiments with palladium or stainless steel as cathodes and D_2O or H_2O solutions of lithium as electrolyte. This seems to indicate that the electrolysis cells behaved similarly so far as their heat production characteristics are concerned. However, this observation does not specifically resolve the presence or absence of excess heating in the cells. To examine this aspect further, the cell temperature over time data were analyzed using a nonlinear least-squares fit algorithm to obtain the cell calorimetric heating rate using a "time-constant" method. The calculation method was verified to yield satisfactory results (within ~10%) for simulated electrical resistance heating measurements of a typical cell configuration. Results showed that, compared to the Joule heating, the calorimetric heating was consistently higher within experimental and calculational errors for all the cells, as shown in Fig. 3.

Table I summarizes the results. The ratio of the calculated cell calorimetric heating to the Joule heating rates varied

TABLE 1

Analysis of Cell Heating Rates

Serial Number	Date	Cathode	Electrolyte	Cathode Current (mA)	Cell Parameters[a]	
					T_{cell} (°C)	ΔT_{cell} (°C)
1	June 30, 1989	Palladium	D_2O	600	59.4	33.4
2	July 6, 1989	Palladium	D_2O	700	65.0	39.0
3	July 10, 1989	Palladium	D_2O	800	75.8	49.8
4	July 11, 1989	Palladium	D_2O	900	82.6	56.6
5	August 31, 1989	Palladium	D_2O	900	68.1	41.1
6	August 22, 1989	Stainless steel	D_2O	700	51.4	27.4
7	August 23, 1989	Stainless steel	D_2O	900	62.5	38.5
8	August 24, 1989	Stainless steel	D_2O	1400	81.7	58.7
9	September 6, 1989	Stainless steel	H_2O	900	59.0	36.0
10	September 7, 1989	Stainless steel	H_2O	1130	69.0	45.0
11	September 4, 1989	Palladium	H_2O	900	58.0	34.0
12	September 5, 1989	Palladium	H_2O	1250	72.0	48.0

Serial Number	Cell Heating Rate (W)			Calorimetric Heating / Joule Heating	Maximum[c] Error (°C)
	Electrical	Joule	Calorimetric		
1	3.5	2.5	4.1	1.64	1.4
2	4.2	3.2	7.3	2.28	−2.1
3	5.2	4.0	5.7	1.43	−2.1
4	6.2	4.8	8.1	1.69	−2.4
5	4.8	3.4	5.2	1.53	1.7
6	2.6	1.6	1.8	1.13[b]	−1.9
7	4.2	2.8	3.6	1.29[b]	0.7
8	7.2	5.0	8.0	1.60[b]	1.3
9	3.9	2.6	4.8	1.85[b]	0.8
10	5.2	3.5	5.6	1.60[b]	1.3
11	3.8	2.5	3.8	1.52[b]	−0.9
12	5.8	3.9	7.2	1.85[b]	−0.8

[a]The cells were operated at the indicated constant currents; T_{cell} denotes stabilized cell temperature and ΔT_{cell} denotes temperature rise with respect to ambient air heat sink.

[b]For Pd-H_2O, stainless steel-D_2O, and stainless steel-H_2O cells, linear least-squares fit gives $(P_{calo}/P_{joule}) = 0.00057$ (mA) + 0.976 with a standard deviation of 11.7%.

[c]Denotes maximum deviation in cell temperature computed with least-squares-fitted parameters and corresponding observed cell temperature.

between 1.4 and 2.3 for the Pd-D_2O system, 1.1 and 1.6 for stainless steel-D_2O systems, 1.5 and 1.9 for Pd-H_2O systems, and 1.6 and 1.9 for stainless steel-H_2O systems. (It was also experimentally established that the D_2 and O_2 gases do not recombine significantly within the cell volume, which could lead to the cell calorimetric heating rate being higher than the Joule heating rate.)

For the Pd-D_2O cell, the computed excess over Joule heating rates was used to estimate the extent of known nuclear fusion reaction rates. To allow for possible heating contributions from chemical reactions in the Pd-D_2O cell, the excess over Joule heating rates computed for the blank experiments with Pd-H_2O, stainless steel-D_2O, and stainless steel-H_2O cells were least-squares fitted as a straightline function of cell current. Due to the similarity in cell geometry and cell contents, the least-squares fit results were assumed to be applicable to the Pd-D_2O cell as well.

If one assumes that the "extra" excess-over-Joule-heating rates thus obtained for the Pd-D_2O cells for various cell currents is due to known nuclear fusion reactions with deuterons, then the fusion rates per second per (d-d) pair would be $\sim 7.3 \times 10^{-11}$ assuming the $D(d,n)^3He$ reaction, 6.2×10^{-11} for the $D(d,p)T$ reaction, and 1.0×10^{-11} for the $D(d,\gamma)^4He$ reaction.

When the main Pd-D_2O experiment was conducted with current pulsing and a low heat sink temperature environment, the cell experienced a temperature transient of ~25°C over a period of 8 min. The cell underwent a mild explosion that dismantled the cell configuration.

Subsequently, experiments with near-simulated heat transfer conditions (as in the main experiments before the temperature transient) with low heat sink temperatures were done.

Typically for an electrical power input of ~40 W, these experiments showed the following:

1. The cell temperature stabilizes at ~27°C in ~15 min with a low heat sink (water bath) temperature of 4°C.
2. When the heat sink water was drained (as happened during the explosion), the cell temperature increased at the rate of ~2°C/min.
3. A low-temperature heat sink in the form of ordinary ice (as observed before the explosion) was not enough to reduce the cell temperature substantially.

Furthermore, with an electrical power input of ~115 W into the cell (as existed during the current pulsing conditions), the cell temperature could rise by ~6.5°C/min even with a low (water bath) heat sink temperature of 4 to 5°C.

These experiments thus showed that the observed cell temperature transient could be due to inadequate heat transfer from the cell surfaces or high electrical energy input into the cell during the pulsing experiments. The reason for the mild explosion, however, has not been understood.

Tritium Formation

For a proper assessment of excess tritium production in the electrolysis cell, known data for the input tritium in the total D_2O used in the experiment and for the tritium analyzed in the various samples, including that from the palladium electrode, were used. Table II gives the tritium results. For the unaccounted D_2O (D_2O that could not be accounted for by makeup and recovery in the daily D_2O material balance), a tritium value as shown in Table II was taken, based on the tritium value experimentally obtained for the recovered D_2O. Thus, it is seen that a net tritium excess corresponding to 50% of the total input tritium was observed. The measured excess tritium production of 0.0348 μCi for the main electrolysis experiment corresponds to an average fusion rate of 2.3×10^{-18} fusions per (d-d) pair per second assuming $D(d,p)T$ is the only reaction.

TABLE II

Tritium Balance

	Tritium Results (μCi)
Total tritium input	0.06578
Tritium recovered in the experiment	
Tritium in the electrolysis cell at the end	0.02876
Tritium in the vapor condensate	0.00234
Tritium from recombined gases	0.02297
Tritium from D_2O formed in the copper oxide	0.00060
Tritium from electrode degassing	0.00922
Tritium in samples during electrolysis	0.00747
Tritium in unaccounted D_2O lost during the experiment	0.02926
Total tritium recovered	0.10062
Excess tritium	0.03484

Neutron Emission

In the initial stages of electrolysis with the Pd-D_2O cell, 17 neutron bursts lasting for 2 to 55 min each were observed. The integrated neutron emission in the bursts varied from 5.1×10^3 (burst period = 2 min) to 5.4×10^5 (burst period = 8 min). The recorded background neutron level was ~20 n/s during these measurements. However, there was no indication of neutron emission later in spite of the increased deuterium loading of the palladium. In fact, analysis of absorbed deuterium in the palladium electrode after the termination of the experiment gave a value of D/Pd > 2.2, which showed that the electrode was saturated with deuterium. The measured number of neutrons emitted in the bursts observed in the main experiment indicated an average fusion rate of 2.2×10^{-21} fusions per (d-d) pair per second assuming $D(d,n)^3He$ is the only reaction.

Observations

The following observations were made from these experiments:

1. The fusion rates calculated for the experiment via known nuclear reactions do not appear to tally with each other.

2. During 7 weeks of electrolysis, the Pd-D_2O cell experienced three explosions, two of which lifted the cell lid.

3. The amount of D_2 gas released by the palladium electrode after the termination of the electrolysis, as well as that obtained by heating the electrode to 800°C, was used to calculate the deuterium-loading value expressed as D/Pd. It was

found to be not <2.2. The deuterium loading value is an important parameter for calculating the fusion rate per (*d-d*) pair. Since some D_2 absorbed by the palladium was lost to the atmosphere during the last explosion, the actual deuterium-loading value is probably close to 3.

Additional experiments are in progress using palladium sheet electrodes to study the cold fusion phenomena further.

ACKNOWLEDGMENTS

The authors wish to acknowledge the assistance rendered by G. Bharadwaj, M. D. Dharbe, M. P. Kini, and Jacob Joseph for the instrumentation and fabrication of the experimental setup. The authors also wish to thank their chemist colleagues for around-the-clock collection of experimental data.

9. TRITIUM ANALYSIS OF SAMPLES OBTAINED FROM VARIOUS ELECTROLYSIS EXPERIMENTS AT BARC

T. S. Murthy,* T. S. Iyengar,+ B. K. Sen,* and T. B. Joseph*

Introduction

The methodology and techniques used to determine the tritium content in various samples obtained during the initial experiments conducted at Bhabha Atomic Research Centre on the feasibility of "cold fusion" are summarized.

Sample Preparation Techniques

Sample preparation involved the use of the appropriate scintillation "cocktail," and, wherever applicable, the samples were distilled before use. Diluting the sample with double-distilled water, even though it reduced the number of signal pulses per unit volume, helped to reduce the pH as well as to quench impurities present in the sample. Alternately, the sample could be kept for "chemiluminescence cooling" so that the contribution from this, if any, would be reduced to a negligible level.

For low background 40 K free vials were used. Use of Dioxane for the solvent was avoided wherever direct counting was adopted, as it tends to show chemiluminescent properties in certain samples. The commercially available scintillation cocktail, Instagel (containing a surfactant such as Triton-X-100), was found to be suitable for counting in these situations.

Standardized procedures involved addition of 0.1 to 2 ml of sample to an appropriate volume of scintillator in cases where the count rates were high. Larger quantities were taken (8 to 12 ml) in the case of low-level samples.

Counting System

There are several liquid scintillation systems (LSSs) available to estimate low-energy beta emitters such as ^3H and ^{14}C. In the present case, the Packard Instrument Company model 4530 and the LKB model 1215 RACKBETA-II were used. (Some samples were also analyzed in an alternate Packard 4530 to confirm the reliability of the method.) These LSSs have facilities for automatic quench correction. The probable errors due to interference from chemiluminescence were avoided by adopting appropriate chemical counting methods.

The system stability was checked daily using sealed tritium standards and sealed background samples in a "calibration" mode, so that normalization was effected by the LSS adjusting the two photomultiplier tube (PMT) voltages automatically. The standardization and efficiency of each sample were determined by quench curves developed for each batch of experimental samples using quench standards of the appropriate chemical form.

The heavy water used in each set of electrolytic experiments was sampled initially and counted along with the samples drawn during the experiments. The rooms where the experiments are conducted were constantly monitored for tritium contamination from the air. In almost all the experiments, samples were drawn at appropriate intervals to follow the trend in tritium concentration values. In all the tritium measurements, the following factors were considered in determining the excess tritium content produced (if any):

1. initial tritium content in the heavy water used in each experiment
2. concentration of tritium content due to electrolysis
3. concentration effects due to makeup volumes of heavy water.

Materials and Method

Tritium Content in Heavy Water Before Electrolysis

Heavy water used for electrolysis experiments in the Analytical Chemistry and Reactor Operations Divisions was analyzed for tritium content. Almost all the experiments in these divisions were conducted using heavy water from these stock solutions.

Tritium Content in Palladium Cathodes

For the electrolysis experiments in the Analytical Chemistry Division, palladium metal in different shapes was generally used as the cathode. Before the cathodes were prepared, samples of palladium metal were collected for tritium assay. In

TABLE I

Tritium Content of Initial Heavy Water Used

Stock Number	Tritium Concentration (μCi/ml)
D_2O-1	1.16×10^{-3}
D_2O-2	0.489×10^{-3}
D_2O-3	0.845×10^{-3}
D_2O-4	0.076×10^{-3}
D_2O-5	0.117×10^{-3}
D_2O-6	0.27×10^{-3}
D_2O-7	0.045×10^{-3}
D_2O-8	0.055×10^{-3}

*Isotope Division.
+Health Physics Division.

addition, samples of palladium metal and palladium salts from the Radiation Technology Division were also collected and analyzed for tritium content.

The palladium metal was dissolved in aqua regia, while the palladium salts were dissolved in water and nitric acid. Suitable stock solutions were prepared from these solutions, including

1. acidic solutions
2. neutralized solutions
3. diluted solutions
4. diluted and neutralized solutions finally made for counting.

Dummy stock solutions were also made with the reagents used except palladium.

The counting continued for 1 week. The acidic solutions initially showed very high chemiluminescence; the diluted and neutralized samples showed that the palladium and palladium salts do not contain any tritium.

TABLE

Tritium Counting Data

Experiment	Initial Volume of D_2O (ml)	D_2O Added (ml)	Final D_2O Volume (ml)	A·h	Electrolyte
Analytical Chemistry Division					
Expt (i)	45	50	45	52.2	0.1 *M* LiOD
Expt (ii)	65	52.6	65	296	0.1 *M* LiOD
Expt (iii)	60	85	60	231	0.1 *M* NaOD
Expt (iii)a RC-2	75	55	75	174.08	0.1 *M* LiOD
Expt (iv) RC-II	75	326	75	844	0.113 *M* LiOD
TC-I	100	1113.2	100	2510.7	0.1 *M* LiOD
TC-II	100	40	100	61.83	0.1 *M* LiOD
RC-III	75	345	75	1032.9	0.1 *M* LiOD
Reactor Operations Division					
RCS-2	237	74	237	73.3	0.1 *M* LiOH
RCS-3	78	20	76	25.6	0.1 *M* LiOH

*Palladium metal cathodes and platinum anodes.

TABLE

Tritium Counting Data in Experiments

Experiment	Initial Volume of D_2O (ml)	D_2O Added (ml)	Final D_2O Volume (ml)	A·h	Electrolyte
Analytical Chemistry Division					
Expt (i)	45	50	45	52.2	0.1 *M* LiOD
Expt (ii)	65	52.6	60	296	0.1 *M* LiOD
Reactor Operations Division					
RCS-2	237	74	237	73.3	0.1 *M* LiOH
RCS-3	78	20	76	25.6	0.1 *M* LiOH
Heavy Water Division					
Expt (A)	250	50	250	360	5 *M* NaOD
Expt (B)	135	300	135	120	5 *M* NaOD
Expt (C)	1000	6000	1000	3120	5 *M* NaOD
Expt (D)	250	1296	250	3216	5 *M* NaOD

*Palladium metal cathodes and platinum anodes.

[a]These two values were given by the Heavy Water Division as the average values of initial tritium content in D_2O used for

Checking of Lithium Electrolyte

Generally, LiOD was used as the electrolyte (0.1 *M*) in the electrolysis experiments. In view of this, the lithium solutions were checked for

1. tritium contamination
2. chemical effects, including chemiluminescence.

Lithium deuteroxide solution (0.2 *M*) was prepared with known heavy water (D_2O) stock solution and analyzed for both.

From the counting data, the following observations were made:

1. Immediately after preparation, high chemiluminescence was observed. However, with passage of time, this chemiluminescence reduced to negligible amounts (in ~10 days). When these lithium stock solutions were neutralized, the chemiluminescence effect was greatly reduced.

2. When these samples were subjected to distillation and the water was collected and counted, no chemiluminescence was observed. The distilled samples showed the original tritium

II

in Experiments*

Tritium Data				
D_2O Used (μCi/ml)	Electrolysis End Sample (μCi/ml)	D_2O Activity After Volume Correction (μCi/ml)	Net Tritium Activity (μCi/ml)	Remarks
0.845×10^{-3}	0.45	1.78×10^{-3}	0.448	Excess tritium observed
0.489×10^{-3}	0.239	0.885×10^{-3}	0.238	Excess tritium observed
0.076×10^{-3}	0.1×10^{-3}	0.183×10^{-3}	---	Excess tritium *not* observed
0.076×10^{-3}	0.116×10^{-3}	0.131×10^{-3}	---	Electrolyte solution boiled off
0.076×10^{-3}	0.114×10^{-3}	0.406×10^{-3}	---	Black coating formed on electrode surface
0.076×10^{-3}	0.119×10^{-3}	0.922×10^{-3}	---	Stopped due to accident
0.076×10^{-3}	0.092×10^{-3}	0.106×10^{-3}	---	Excess tritium *not* observed
0.076×10^{-3}	0.239×10^{-3}	0.426×10^{-3}	---	Experiment continuing
0.076×10^{-3}	2.6×10^{-3}	0.1×10^{-3}	2.5×10^{-3}	Excess tritium observed
0.076×10^{-3}	6.83×10^{-3}	0.098×10^{-3}	6.73×10^{-3}	Excess tritium observed

III

Where Excess Tritium Was Observed*

Tritium Data				
D_2O Used (μCi/ml)	Electrolysis End Sample (μCi/ml)	D_2O Activity After Volume Correction (μCi/ml)	Net Tritium Activity (μCi/ml)	Remarks
0.845×10^{-3}	0.45	1.78×10^{-3}	0.448	Excess tritium observed
0.489×10^{-3}	0.239	0.885×10^{-3}	0.238	Excess tritium observed
0.076×10^{-3}	2.6×10^{-3}	0.1×10^{-3}	2.5×10^{-3}	Excess tritium observed
0.076×10^{-3}	6.83×10^{-3}	0.098×10^{-3}	6.73×10^{-3}	Excess tritium observed
0.045×10^{-3}	1.505	0.342×10^{-3}	1.503	Excess tritium observed
0.055×10^{-3}[a]	48.15×10^{-3}	0.177×10^{-3}	47.97×10^{-3}	Excess tritium observed
0.055×10^{-3}[a]	190.3×10^{-3}	0.385×10^{-3}	189.92×10^{-3}	Excess tritium observed
0.27×10^{-3}	121.0×10^{-3}	1.669×10^{-3}	119.33×10^{-3}	Excess tritium observed

experiments (B) and (C).

TABLE IV

Tritium Concentration Data in Other Electrolysis Experiments*

Division	Number of Experiments	Number of Samples Collected	Remarks
Physical Chemistry	2	20	Palladium-nickel system; 0.1 *M* LiOD; ionic membrane used between electrodes; volume and cell dimensions varied in different cells
Radiation Chemistry	2	14	Platinum-palladium system; 0.01 *M* LiOD; control experiment; with D_2SO_4
Water Chemistry	3	33	Platinum-palladium system; 0.1 *M* LiOD; electrode size varied; one cell exploded

*No apparent increase in tritium concentration was observed in these experiments.

content of the heavy water. Therefore, no tritium contamination was seen in the lithium salts used for the electrolysis.

3. The electrolyte samples that had been subjected to a few days of electrolysis showed small amounts of chemiluminescence compared to unelectrolyzed LiOD samples. The initial chemiluminescence observed in some of the electrolyzed samples was found to decay rapidly within 24 h.

4. The tritium content in the final samples from cells was confirmed by counting the D_2O distilled from these samples.

Quench Corrections

Due to the presence of chemical impurities, even in trace quantities, chemical quenching possibilities exist, which in turn reduce the pulse output. In impurity quench, the components that quench the sample do so either by competing with the fluors for energy transfer or by chemically interacting with the fluor molecules to make them less reactive to energy transfer. Oxidizing agents at high pH can alter oxygen atoms in many of the fluors so that the fluorescent properties are also changed.

In color quench, the quenching component absorbs the photons produced by the scintillation process before they can be detected by the PMTs. Color quench usually does not interfere with the scintillation process, but exerts its effect by preventing the photon from being seen by the LSS detector.

In both the above cases, the resultant effect is compression of the beta spectrum of tritium and reduction in pulse output, which reduces the efficiency of the LSS. Thus, it becomes necessary to correct for such quench errors and determine the efficiency of each sample.

Quench corrections are carried out by any one of the following methods:

1. The standard addition technique consists of a known amount of standard of appropriate concentration being added to the sample to determine the efficiency for that particular sample. In this "spike method," the sample is irretrievable.

2. The sample channel ratio method effectively takes the ratio of two preset channels of the beta spectrum for the sample and compares it with a calibration curve developed with a series of known quenchers of appropriate chemical form whose efficiencies have been determined previously. For very highly quenched samples, this technique is not quite as suitable because the ratio of the two channels does not reflect a true picture of the actual situations.

3. Many LSSs have a built-in automatic external standard channel ratio technique for quench corrections. The principle depends on pneumatically shooting a gamma-emitting pellet that occupies a place very near the counting vial for a very short period and produces Compton electrons that undergo quench effects similar to that of the sample. Here again, a calibration curve with a known set of quenched standards of appropriate chemical composition helps in determining the efficiency of the sample being counted.

Results

Table I gives the tritium content in the heavy water stock solutions used for the electrolysis experiments conducted by the Analytical Chemistry, Reactor Operations, and Heavy Water Divisions.

Table II gives the data pertaining to ten electrolysis experiments conducted by the Analytical Chemistry and Reactor Operations Divisions.

Data from experiments where excess tritium was observed in the electrolyte solution after electrolysis are summarized in Table III.

Information from various experiments that do not show any apparent increase in tritium values is given in Table IV.

10. MATERIAL BALANCE OF TRITIUM IN ELECTROLYSIS OF HEAVY WATER

S. K Malhotra, M. S. Krishnan, and H. K. Sadhukhan*

Introduction

Electrolysis of heavy water has acquired great importance during the last few months in view of the discovery of the

*Heavy Water Division.

phenomenon of cold fusion.[1,2] Though the initial reports presented measurements of neutron emission or heat only, tritium formation has lately been reported (see report A.1 of this technical note). However, any tritium measurements should be corrected for the isotopic enrichment of tritium during electrolysis since it is a well-known technique for hydrogen isotope separation. We attempt here to give a complete material balance of tritium escaping from the system in the form of deuterium-tritium (D-T) gas and as DTO vapor. Tritium produced in excess of what is predicted from this equation may be attributed to nuclear fusion reactions.

Basic Material Balance Equation

Consider an electrolyzer (Fig. 1), in which the deuterium gas formed is let out, D_2O vapor escapes along with the gases evolved, and heavy water is continuously added to maintain a constant level of electrolyte in the cell.

For low tritium concentrations, all the tritium in the liquid and gas phases is in the form of DTO and D-T, respectively. The rate of increase in the number of DTO moles in the electrolyzer per unit time can be written as

$$\frac{d}{dt} n_{\mathrm{DTO}}(EL) = \frac{d}{dt} n_{\mathrm{DTO}}(F) - \frac{d}{dt} n_{\mathrm{DTO}} - \frac{d}{dt} n_{\mathrm{DTO}}(V) \ , \tag{1}$$

where the term with (F) is the rate of addition of DTO in moles per second, the term with n_{DTO} is the rate of escape of D-T with gas, and the term with (V) is the rate of escape of DTO as vapor.

The rate of escape of D-T can be calculated from the electrolytic separation factor for tritium. Thus, if n_E mol/s are electrolyzed and α_E is the electrolytic separation factor, then for low tritium concentration, α_E can be defined as

$$\alpha_E = \frac{(\mathrm{T/D})_{liq}}{(\mathrm{T/D})_{gas}} \ . \tag{2}$$

The number of D-T moles escaping per second is

$$\frac{d}{dt} n_{\mathrm{DT}} = \frac{n_E \cdot x}{\alpha_E} \ , \tag{3}$$

where x is the mole fraction of DTO in the electrolyzer at time t.

The rate of escape of DTO as vapor can be calculated from vapor pressure P_v of heavy water at the temperature of electrolysis, pressure P in the electrolyzer, flow rate F_g of the gases evolving out of the electrolyzer, and the separation factor α_v for isotopic fractionation of tritium due to evaporation. Thus,

$$\frac{d}{dt} n_{\mathrm{DTO}}(V) = \frac{P_v}{P - P_v} F_g \frac{x}{\alpha_v} \ , \tag{4}$$

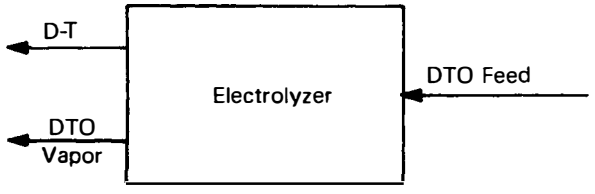

Fig. 1. Input and output of tritium in the electrolyzer.

where F_g is the flow of gases from the electrolyzer in moles per second.

The term due to the addition of fresh D_2O to the electrolyzer can be written as

$$\frac{d}{dt} n_{\mathrm{DTO}}(F) = F_L \cdot a \ , \tag{5}$$

where F_L is the feed rate of heavy water in moles per second and a is the mole fraction of DTO in the feed. Equation (1) can now be written as

$$\frac{d}{dt} n_{\mathrm{DTO}} = F_L \cdot a - \frac{n_E \cdot x}{\alpha_E} - \frac{P_v}{P - P_v} \cdot F_g \cdot \frac{x}{\alpha_v} \ . \tag{6}$$

If the electrolyzer contains N_t moles of heavy water at times t, then

$$x = \frac{n_{\mathrm{DTO}}}{N_t} \ . \tag{7}$$

Therefore,

$$\frac{dx}{dt} = \frac{1}{N_t} \cdot \frac{d}{dt} n_{\mathrm{DTO}} - \frac{n_{\mathrm{DTO}}}{N_t^2} \cdot \frac{d}{dt} N_t \tag{8}$$

or

$$\frac{dx}{dt} = \frac{1}{N_t} \cdot \left(\frac{d}{dt} n_{\mathrm{DTO}} - x \frac{d}{dt} N_t \right) \ . \tag{9}$$

Substituting $(d/dt)n_{\mathrm{DTO}}$ from Eq. (6) into Eq. (9),

$$\frac{dx}{dt} = \frac{1}{N_t} \left(F_L \cdot a - \frac{n_E \cdot x}{\alpha_E} - \frac{P_v}{P - P_v} F_g \frac{x}{\alpha_v} - x \cdot \frac{d}{dt} N_t \right) \ . \tag{10}$$

This is the basic differential equation that can be solved for x if all the other parameters are known. Some typical cases for application to different operational conditions are considered in the following sections.

Case 1: Diffusion-Type Electrolyzer with Automatic Level Maintainer

This case particularly refers to a Milton Roy electrolyzer used in experimental studies on cold fusion. In this electrolyzer, deuterium diffuses through the palladium cathode and is delivered in an absolutely dry condition. The level of electrolyte is automatically maintained. The total number of moles in the electrolyzer N_t is constant; therefore, $N_t = N$ and $(d/dt)N_t = 0$. The term F_g is the rate of evolution of oxygen; therefore,

$$F_g = \frac{1}{2} n_E \ . \tag{11}$$

The feed rate of heavy water is equal to the total of the rate of electrolysis and loss of heavy water due to evaporation. Therefore,

$$F_L = n_E + \frac{1}{2} n_E \cdot \frac{P_v}{P - P_v} \ . \tag{12}$$

Equation (10) now becomes

$$\frac{dx}{dt} = \frac{n_E}{N} \left\{ \left[1 + \frac{P_v}{2(P - P_v)} \right] a - \left[\frac{1}{\alpha_E} + \frac{P_v}{2\alpha_v (P - P_v)} \right] x \right\} \ . \tag{13}$$

Setting

$$\left[1 + \frac{P_v}{2(P - P_v)}\right] = A \tag{14}$$

and

$$\left[\frac{1}{\alpha_E} + \frac{P_v}{2\alpha_v(P - P_v)}\right] = B \ , \tag{15}$$

and rearranging Eq. (13),

$$\frac{dx}{aA - Bx} = \frac{n_E}{N}dt \ . \tag{16}$$

Integrating for $t = 0$ to t, we get

$$L_n \frac{aA - Bx_0}{aA - Bx} = B\frac{n_E}{N}t \ , \tag{17}$$

where x_0 is the mole fraction of DTO in the electrolyte initially. Equation (17) can be written as

$$x = a\frac{A}{B} - \left(a\frac{A}{B} - x_0\right)\exp\left(-\frac{Bn_E}{N}t\right) \ . \tag{18}$$

This equation gives the mole fraction of DTO in the electrolyte at time t. As x, x_0, and a have same units, Eq. (18) can be applied for any common units of these parameters.

It follows from Eq. (18) that x will increase or decrease with time, depending on the relative magnitudes of a and x_0. Thus, for $x_0 > aA/B$, the exponential term becomes positive and x increases with time; while for $x_0 < aA/B$, x decreases with time. In both cases, the tritium concentration in the cell tries to attain a steady-state value equal to aA/B, as shown by the asymptotic behavior of the tritium curves in the two cases (Fig. 2).

If the tritium concentration of the starting electrolyte and that of the feedwater are the same ($a = x_0$), then Eq. (18) becomes

$$x = x_0\left[\frac{A}{B} - \left(\frac{A}{B} - 1\right)\exp\left(-\frac{Bn_E}{N}t\right)\right] \ . \tag{19}$$

In this case also, x increases with time because it easily follows from Eqs. (14) and (15) that $A/B > 1$, rendering the exponential term negative.

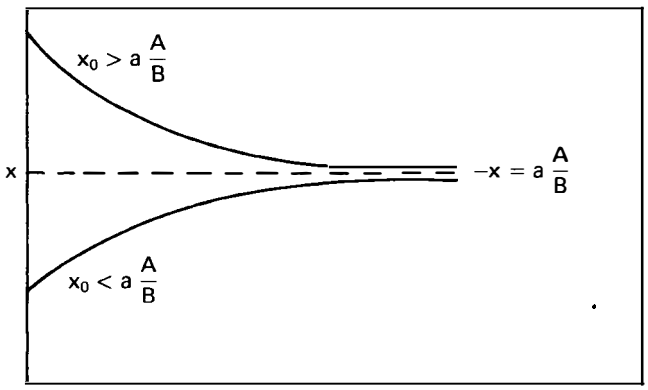

Fig. 2. Arbitrary plots of x versus t [Eq. (18)].

Case 2: Nondiffusion Batch Electrolyzers

In most of the electrolysis experiments, the mixed stream of deuterium and oxygen comes out of the electrolyzer and the cell is operated for a certain period without adding fresh heavy water. In this case, the first term in Eq. (10) is zero (as $F_L = 0$) and F_g is now equal to $\frac{3}{2}n_E$. Also N_t is no longer constant and is given as

$$N_t = N - \left(n_E + F_g\frac{P_v}{P - P_v}\right)t \tag{20}$$

or

$$N_t = N - n_E\left(1 + \frac{3}{2}\frac{P_v}{P - P_v}\right)t \ . \tag{21}$$

Therefore,

$$\frac{d}{dt}N_t = -n_E\left(1 + \frac{3}{2}\frac{P_v}{P - P_v}\right) \ . \tag{22}$$

Making these substitutions in Eq. (10) and simplifying, we get

$$\frac{dx}{dt} = \frac{n_E}{N - n_E\left(1 + \frac{3}{2}\frac{P_v}{P - P_v}\right)} \times \left(\frac{\alpha_E - 1}{\alpha_E} + \frac{3}{2}\frac{\alpha_v - 1}{\alpha_v}\cdot\frac{P_v}{P - P_v}\right)x \ . \tag{23}$$

Integrating and putting the condition $x = x_0$ at $t = 0$,

$$L_n\frac{x}{x_0} = -\frac{\frac{\alpha_E - 1}{\alpha_E} + \frac{3}{2}\frac{P_v}{P - P_v}\frac{\alpha_v - 1}{\alpha_v}}{1 + \frac{3}{2}\frac{P_v}{P - P_v}} \times L_n\left[1 - \frac{n_E}{N}\left(1 + \frac{3}{2}\frac{P_v}{P - P_v}\right)t\right] \ . \tag{24}$$

Equation (24) can be used to calculate the tritium enrichment during the electrolysis in terms of the time of electrolysis. Alternatively, this equation can also be written in terms of N_t. Thus,

$$L_n\frac{x}{x_0} = \frac{\frac{\alpha_E - 1}{\alpha_E} + \frac{3}{2}\frac{P_v}{P - P_v}\frac{\alpha_v - 1}{\alpha_v}}{1 + \frac{3}{2}\frac{P_v}{P - P_v}} L_n\frac{N_0}{N_t} \ . \tag{25}$$

Using Eq. (25), tritium enrichment can be calculated with the initial and final volumes of the electrolyte. Equation (26) is in fact similar to a well-known Rayleigh's equation[3]:

$$L_n\frac{N_t}{N_0} = (1 + H)\left(\frac{\alpha_E}{\alpha_E - 1}\right)\left(L_n\frac{x_0}{x_t} - \frac{1}{\alpha_E - 1}L_n\frac{1 - x_0}{1 - x_t}\right) \ , \tag{26}$$

where H is the humidity of the gases evolving. For low tritium concentrations, x_0 and $x_t \ll 1$; therefore, Eq. (26) becomes

$$L_n\frac{N_t}{N_0} = (1 + H)\left(\frac{\alpha_E}{\alpha_E - 1}\right)L_n\frac{x_0}{x_t} \ , \tag{27}$$

which is similar to Eq. (25) except that it does not include the term due to isotopic fractionation of tritium due to evaporation. A plot of x/x_0 against N_0/N_t as obtained from Eq. (25) is shown in Fig. 3.

Let us now consider the different parameters in Eqs. (18), (24), or (25). They are the electrolysis rate n_E, electrolytic separation factor α_E, distillation separation factor α_v, and vapor pressure of D_2O, P_v.

The rate of electrolysis n_E can be calculated from Faraday's laws of electrolysis, given the current. The electrolytic separation factor α_E depends on the temperature of electrolysis and on the electrode materials. Not many data are available for electrolytic tritium separation factors. Generally, a value of 2.0 is widely accepted.[4]

The distillation separation factor α_v can be calculated from the vapor pressure of D_2O and DTO. Thus,

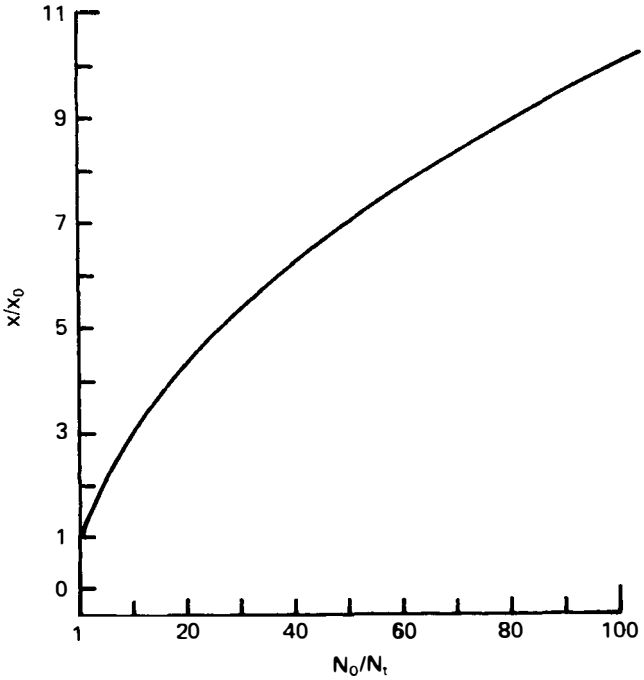

Fig. 3. Plot of x versus N_0/N_t [Eq. (25)].

TABLE I

Vapor Pressures (atm)

Temperature (°C)	P_{D_2O}	P_{DTO}	α_v
20	0.02013	0.01976	1.0187
30	0.03523	0.03472	1.0147
40	0.06566	0.06482	1.0130
50	0.10493	0.10381	1.0108
60	0.18210	0.18060	1.0083
70	0.27530	0.27360	1.0062
80	0.44210	0.44000	1.0048

$$\alpha_v = \frac{P_{D_2O}}{P_{DTO}} \quad . \tag{28}$$

The vapor pressures of D_2O and DTO have been computed and are available in the literature.[5] Table I gives the values of P_{D_2O} [P_v in Eqs. (18), (24), and (25)], P_{DTO}, and α_v at different temperatures.[5]

REFERENCES

1. M. FLEISCHMANN and S. PONS, "Electrochemically Induced Nuclear Fusion of Deuterium," *J. Electroanal. Chem.*, **261**, 301 (1989).

2. S. E. JONES et al., "Observation of Cold Nuclear Fusion in Condensed Matter," *Nature*, **338**, 737 (1989).

3. R. E. TREYBAL, *Mass Transfer Operations*, p. 308, McGraw-Hill, New Delhi (1968).

4. K. M. KALYANAM and S. K. SOOD, "A Comparison of Process Characteristics for the Recovery of Tritium from Heavy Water and Light Water Systems," *Fusion Technol.*, **14**, 524 (1988).

5. S. M. DAVE et al., "Tritium Separation Factors in Distillation and Chemical Exchange Processes," BARC-1168, Bhabha Atomic Research Centre (1982).

11. TECHNIQUE FOR CONCENTRATION OF HELIUM IN ELECTROLYTIC GASES FOR COLD FUSION STUDIES

K. A. Rao*

Introduction

In nuclear fusion reactions involving D_2, helium is one of the possible products. During electrolytic dissociation of D_2O with platinum or palladium electrodes, if any fusion reaction[1,2] takes place via the helium pathway with helium escaping to the gas phase, it should be possible to detect and estimate the yield quantitatively. Helium in excess of the background was reported in the electrolysis experiments conducted at the University of Utah.[1] The amount reported was of the order of 10^{12} atom/s (~0.013 μl/h).

In the presence of a large excess of D_2 and O_2 generated during electrolysis, detection of $^3He/^4He$ in the gas phase poses many problems. Among the methods available for the detection of small amounts of helium, gas chromatography and mass spectrometry are normally preferred. However, in this case, mass spectrometry is difficult as there is only a trace concentration of helium, and a large excess of D_2 interferes with the signal due to ^3He or ^4He ions unless a fractional mass difference method is adopted. To concentrate the helium in the gas phase, an experimental technique was devised wherein D_2 and O_2 generated by electrolysis are catalytically recombined *in situ*, facilitating gas collection over long periods of electrolysis. The results obtained by this technique, followed by gas chromatographic analysis, are given here. Though gas chromatography and mass spectrometry analyses of the enriched sample may be more conclusive, a suitable gas

*Chemistry Division.

inlet interface compatible with D_2 and helium is not commercially available.

Experimental

The electrolysis cell and the gas-handling system are shown schematically in Fig. 1. These consisted of a glass cell with a ground glass joint connected to a mercury manometer with a 20-ml expansion bulb at the bottom, a silicone septum with vacuumtight electrode leads, and a vacuum stopcock connecting the cell to a modified Toeppler pump with facilities to measure the gas pressure and volume and to pressurize and transfer the collected gas to a syringe sampling manifold through a threeway stopcock.[3] The third limb of this stopcock was connected to a rotary vacuum pump. The catalyst for the recombination of D_2 and O_2 at room temperature was a specially prepared platinum catalyst deposited on a thick synthetic fabric. It is freely suspended on the top inner side of the electrolysis cell.

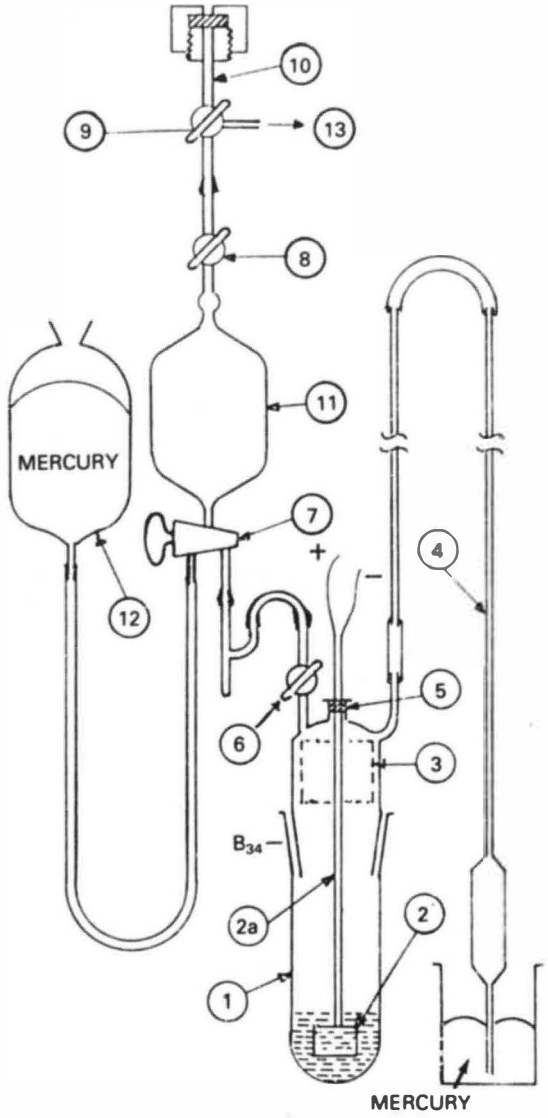

1 ELECTROLYTIC CELL
2 ELECTRODES
2a ELECTRODE LEADS
3 CATALYST FABRIC
4 MANOMETER
5 SILICONE SEPTUM
6-9 VACUUM STOPCOCKS
10 SAMPLING MANIFOLD WITH SEPTUM
11 EXPANSION BULB
12 MERCURY RESERVOIR
13 TO VACUUM PUMP

Fig. 1. Electrolysis cell and gas-handling system.

The catalyst was independently assessed for H_2/O_2 recombination efficiency and was found to have a half-life for H_2 reaction of <15 s in the presence of sufficient O_2 with gas volumes up to ~500 ml. The gaseous products were analyzed by gas chromatography using a thermal conductivity detector either on a 5-m × 3-mm-i.d. molecular sieve 5-A column at 25°C with argon carrier gas, which clearly separated helium and hydrogen for the analysis of trace amounts of helium in the sample, or on a 2-m × 4-mm-i.d. molecular sieve 5-A column at 25°C with helium carrier gas for the analysis of H_2 (or D_2), O_2, and N_2 in the sample. The smallest amount of helium detectable in the presence of a large excess of hydrogen under the experimental conditions was ~0.01 μl (or an ~1-ml sample with 10 ppm helium). The second column provided a reasonably good analysis of the major constituents of the residual gas.

The total volume of the electrolysis cell and the gas-handling system as well as the volume of each segment of the system facilitated computation of the gas volumes and composition at every stage of the experiment.

The electrolysis experiments were carried out in three stages. In these experiments, 20 ml of 0.1 *M* LiOH or LiOD was used as the electrolyte. Experiments I and II used a stainless steel cathode and anode mounted in a concentric tubular configuration with 1-mm electrode spacing. The electrodes were ~1.5 × 3 × 0.04 cm. These experiments were used to test leaktightness, gas recombination efficiency, trace helium recovery, and analysis. Experiments III to VI were carried out with palladium/platinum electrodes. In this case, a palladium plate (1 × 1.5 × 0.15 cm) was sandwiched between two platinum plates (1 × 1.5 × 0.05 cm).

Before starting the electrolysis, the entire system, including the cell with 20 ml of electrolyte, was evacuated through the threeway stopcock to thoroughly degas the electrolyte. After attaining a vacuum, the cell was isolated from the pump and rest of the system, and the electrolysis was started and continued for the required duration by connecting the electrodes to a dc power supply. At the end of the electrolysis, the power was turned off, and the system was allowed to stabilize until there was no further change in the mercury level of the manometer. At this stage, by suitable manipulation of the threeway stopcock and mercury reservoir gas transferring, compression, measurement of pressure and volume, and sampling for analysis were carried out. Whenever necessary, the desired reactant gas was introduced into the electrolysis cell through the silicone septum by means of a syringe. The electrolysis cell was found to retain the vacuum for >48 h (drop in mercury level ~0.5 cm). The results of the experiments with relevant details are given in Table I.

Conclusions

The following conclusions were drawn from these experiments:

TABLE I

Electrolysis Conditions and the Residual Gas Yields

	Experiment					
	I[a]	II[a]	III[b]	IV[b]	V[b]	VI[b]
Electrodes	Concentric stainless steel cathode and anode	Concentric stainless steel cathode and anode	Palladium cathode, platinum anode	Palladium cathode, platinum anode	Platinum cathode, palladium anode	Palladium cathode, platinum anode
Electrolyte	0.1 *M* LiOH in H_2O	0.1 *M* LiOD in D_2O	0.1 *M* LiOD in D_2O	0.1 *M* LiOD in D_2O	0.1 *M* LiOD in D_2O	0.1 *M* LiOD in D_2O
Electrolysis						
Voltage (V)	4.0	4.0	4.0	5.0	4.5	4.0
Current (mA)	~250	~250	~250	~500	~450	~275
Duration (h)	1 and 2[c]	2, 2, 4, 1, 6, 6	3	6	2	6
Residual gas volume (ml) and composition after electrolysis (25°C/76 cm of mercury)	~1 $H_2:O_2$ ~ 2:1	~1 to 3 $D_2:O_2$ ~ 2:1	26 ~90% O_2	16 ~90% O_2	48 ~94% D_2	28 ~94% O_2
Volume of reactant gas added (ml)	---	---	50 H_2	30 H_2	24 O_2	46 H_2
Final gas volume (ml) and composition	~1 $H_2:O_2$ ~ 2:1	~1 to 3 $D_2:O_2$ ~ 2:1	~3 ---[d]	~1.6 $D_2:O_2$ ~ 1:5[e]	~1.1 $D_2:O_2$ ~ 4:1	~5.6 $D_2:O_2$ ~ 1:8

[a]In experiments I and II, electrolysis was continued for varying times to ascertain the viability of the method and recombination efficiency of the catalyst.

[b]In experiments III through VI, initial evacuation of the system was done with dc potential for ~5 min, then continued with the potential off for ~5 min, with the system isolated and regular electrolysis (system purging). In these cases, the mercury level in the manometer showed a steady drop for the first 2.5 h, then slowed.

[c]In these cases, 150 μl of 1% helium in argon was added to the cell before electrolysis, and the residual gas at the end was analyzed for helium. Recovery was found to be better than 90%.

[d]In experiment III, the residual gas is used up in analyzing trace helium. Hence, D_2/O_2 composition was not determined.

[e]At the end of experiment IV, the electrolysis cell was maintained in the isolated mode overnight. The mercury level dropped by ~2 cm overnight, and the residual gas showed 90% D_2, indicating release of D_2 under vacuum.

1. In contrast to the stainless steel electrodes, the palladium cathode/platinum anode configuration resulted in D_2 deficient gas composition and the platinum cathode/palladium anode configuration showed O_2 deficient gas. In the initial stages of electrolysis, much of the hydrogen (or D_2) may be absorbed by palladium, reaching equilibrium in ~2.5 h as indicated by the steady pressure buildup.

2. Though all the released gas is contained and concentrated to a residual volume of 1 to 3 ml, no helium could be detected in any experiment.

3. Hydrogen (or D_2) absorbed on the electrode is slowly released under vacuum.

4. A platinum catalyst can be incorporated in the cell design to recombine the evolved gas, facilitating D_2O recovery and possible recovery of any tritium in the gas phase back into the aqueous phase.

5. In case independent proof for cold fusion via the helium pathway becomes available, this method can detect helium and substantiate the finding with the possibility of unambiguous evidence obtainable from gas chromatography and mass spectrometry analyses of the concentrated residual gas.

ACKNOWLEDGMENTS

The author is obliged to N. M. Gupta and A. D. Belapurkar of the Chemistry Division for providing the platinum catalyst. The author is also thankful to R. M. Iyer, director of the Chemical Group, and J. P. Mittal, head of the Chemistry Division, for their keen interest and helpful suggestions during the course of this work.

REFERENCES

1. M. FLEISCHMANN and S. PONS, "Electrochemically Induced Nuclear Fusion of Deuterium," *J. Electroanal. Chem.*, **261**, 301 (1989).

2. C. K. MATHEWS et al., "On the Possibility of Nuclear Fusion by the Electrolysis of Heavy Water," *Indian J. Technol.*, **27**, 229 (1989).

3. K. A. RAO and R. M. IYER, "Evaluation of Degradation of Insulating Oils in Power Transformers," *Indian J. Technol.*, **16**, 44 (1978).

PART B: D_2 GAS-LOADING EXPERIMENTS

1. SEARCH FOR NUCLEAR FUSION IN GAS-PHASE DEUTERIDING OF TITANIUM METAL

P. Raj,* P. Suryanarayana,* A. Sathyamoorthy,* and T. Datta+

Introduction

The possibility of deuterium-deuterium (D-D) nuclear fusion in some deuterium-metal systems, under ambient conditions, has aroused feverish worldwide interest. Most of the work reported thus far concerns deuterium charging of palladium metal through electrolysis of D_2O.

In the Chemistry Division, we have carried out some experiments on the deuteriding behavior of titanium metal, through the gaseous route, by absorption as well as desorption, to seek fusion products, neutrons in the present case. This kind of experiment has been reported by researchers at Frascati in Italy.[1] These authors detected neutron emission lasting for several hours.

Experiments

The experimental arrangement for deuteriding titanium metal is shown in Fig. 1. This setup is routinely used for high-pressure hydriding studies on several systems.[2-4] In some experiments, the deuterium pressure was cycled between high and low by simply changing the temperature of the cell housing the sample. Most of the experiments were done in the desorption mode. Titanium metal pieces (cut from a sheet) were surface cleaned and subjected to activation treatment before D_2 loading and subsequent desorption treatment.

The neutron counting setup consists of an array of 24 ^{3}He counters arranged in a well-like geometry. These counters (each 50 cm long × 2.5-cm diam and filled with ^{3}He at 4 atm) are housed in paraffin moderators and are connected in parallel to a single preamplifier. The counting efficiency of this system was found to be ≈10%. The counts are recorded in 8192 channel multiscalers. In the experiments reported here, a dwell time of 40 s was fixed, so that each point in Fig. 2 represents the number of counts per 40 s. The background counts collected for ~10 days before the start of these deuteriding experiments were found to be quite steady at 60 count/40 s. This background count rate continued to be the same well after our experiments.

Results

In the first set of experiments, starting on June 3, 1989, after activating the titanium metal pieces, D_2 gas contacted the sample at a pressure of ~10 atm while keeping the sample at low temperature (~77 K). After soaking for ~20 min, the sample temperature was raised gradually, while simultaneous evacuation was started. Within ~15 min, the neutron counter registered an increase in count rate, reaching a maximum of 3900 count/40 s (as compared to background counts of ~60), as shown in Fig. 2a. On withdrawing the reactor from the counting well, a considerable reduction in the counts was observed. On reintroducing the reactor after background counts

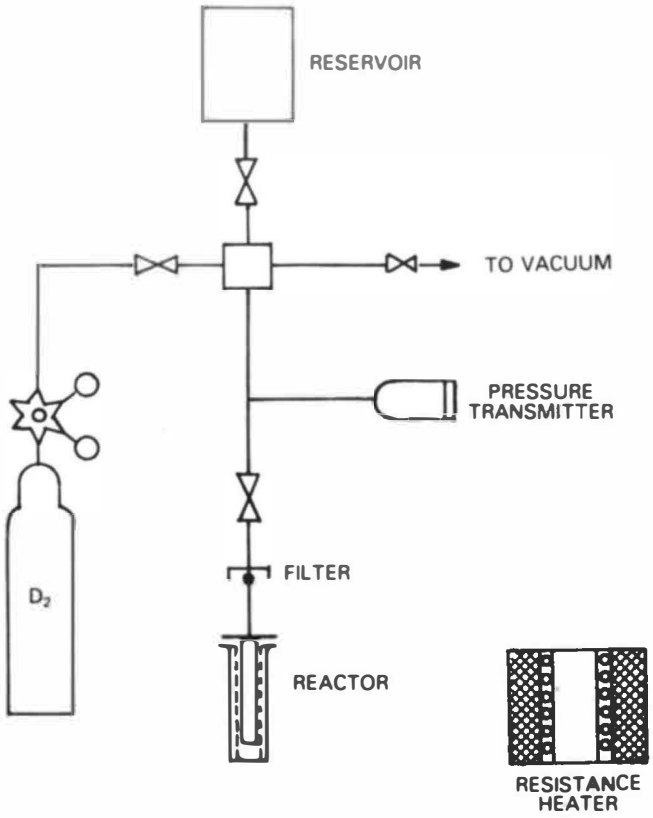

Fig. 1. Schematic of the hydriding/dehydriding unit.

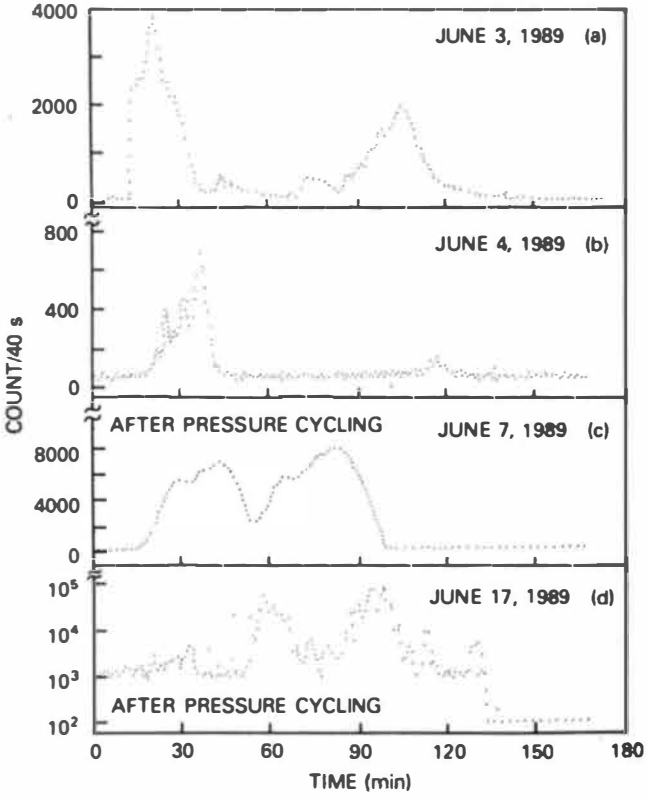

Fig. 2. Desorption mode experiments.

*Chemistry Division.
+Radiochemistry Division.

were restored, an additional peaklike structure was observed. Although evacuation was continued, no further increase in count rate over the background was seen over the next 20 h.

The next experiment on the same charge was carried out by repeating the conditions of the first experiment. The results of this experiment, on June 4, 1989, are shown in Fig. 2b. Again, two peaklike structures, each lasting for ~30 min and separated by 50 min, were seen. However, the intensities of both these structures are greatly reduced, as compared to the first experiment, the maximum count being ~700 count/40 s.

In the third experiment, with the same charge of titanium pieces, D_2 gas pressure was cycled between ~50 and ~13 atm by changing the reactor temperature from room temperature to 77 K. In this case, large changes in counts as a function of time were noticed. The increase of counts initiated at ~2330 h on June 4, 1989, lasted for almost 7 h with an estimated integral count of $\sim 6.5 \times 10^5$. After this long burstlike structure, additional peaks were observed on June 5, 1989. When no further structures were observed over the next few hours, desorption was carried out after loading the sample with D_2 gas at a sample temperature at ~77 K. By raising sample temperature gradually and simultaneously evacuating, a much bigger structure lasting for ~2 h (from ~1830 to 2030 on June 7, 1989) was seen (Fig. 2c). An approximate estimate of the integrated count over this period is 7×10^5. Further experiments with this charge, involving D_2 loading followed by prolonged periods of evacuation at temperatures up to a maximum of ~200°C, showed no further structures.

The second series of experiments on a fresh charge of titanium from the same source did not show identical behavior. However, one set of experiments on June 17, 1989 (see Fig. 2d), involving pressure cycling followed by evacuation exhibited an increase in count rate over a period of ~100 min. In this case, the scatter in the count was found to be rather large, and maximum counts up to 10^5/40 s were observed, as compared to the background count of ~60/40 s. This charge showed no further increase in count rate even after various treatments.

Further experiments are planned to study all possible parameters relating to the observed increase in the count rates, to identify the source of these extra counts, and to investigate the energy and time structure of the radiation responsible for the observed peaklike structures.

ACKNOWLEDGMENTS

The authors are indebted to R. M. Iyer, director of the Chemical Group, and J. P. Mittal, head of the Chemistry Division, for helpful discussions and encouragement. Sincere thanks are due to P. R. Natarajan, head of the Radiochemistry Division; H. K. Sadhukhan, head of the Heavy Water Division; C. K. Gupta, head of the Metallurgy Division; and their colleagues for providing the neutron counting facility, deuterium gas, and titanium metal, respectively.

REFERENCES

1. A. De NINNO et al., "Evidence of Emission of Neutrons from a Titanium-Deuterium System," *Europhys. Lett.*, **9**, 221 (1989).

2. P. RAJ, A. SATHYAMOORTHY, P. SURYANARAYANA, and R. M. IYER, "Nickel Substituted FeTi Hydrides: A Critical Study of the β-Region," *J. Less-Common Metals*, **123**, 145 (1986).

3. P. RAJ, A. SATHYAMOORTHY, P. SURYANARAYANA, A. J. SINGH, and R. M. IYER, "Hydriding Behaviour of FeTi and $FeTi_{1-15}$: Ease of Activation and Skipping of β-Region," *J. Less-Common Metals*, **130**, 139 (1987).

4. P. RAJ, P. SURYANARAYANA, A. SATHYAMOORTHY, and R. M. IYER, "α-Hydride $(Fe_{0.8}Ni_{0.2})TiH_x$: The Distribution and Manifestation of Dissolved Hydrogen," *Mat. Res. Bull.*, **24**, 717 (1989).

2. DEUTERATION OF MACHINED TITANIUM TARGETS FOR COLD FUSION EXPERIMENTS

V. K. Shrikhande* and K. C. Mittal+

Introduction

Cold fusion experiments were initiated with solid targets made of titanium loaded with deuterium gas following reports of the successful Frascati experiments.[1] The absorption of deuterium by titanium is a reversible process, and when titanium is heated in a deuterium atmosphere, the reaction continues until the concentration of deuterium in the metal attains an equilibrium value.[2] This equilibrium value depends on the specimen temperature and the pressure of the surrounding deuterium atmosphere. Any imposed temperature or pressure change causes rejection or absorption of deuterium until a new equilibrium state is achieved. If the surface of the titanium is clean, the rate of absorption increases rapidly with temperature. At temperatures >500°C, equilibrium is achieved in a few seconds. However, deuterium absorption is considerably reduced if the surface of the titanium is contaminated with oxygen. Keeping these facts in mind, a procedure was evolved for titanium target preparation and subsequent deuteration.

Preparation of the Targets

Titanium targets of different sizes and shapes (planar, conical, etc.) were prepared. They were typically a fraction of a gram in mass and were machined from a titanium rod using tungsten carbide tools with a continuous cooling arrangement. Care was taken to avoid overheating during machining because any overheating could harden the titanium and thereby inhibit its capacity to absorb H_2/D_2.

The machined targets were first ultrasonically degreased in trichloroethylene. Then the oxide layer, if any, was removed by immersing the targets in a 1:1:1 mixture of water, nitric acid, and sulfuric acid. They were then rinsed in water and dried in acetone. This was followed by HCl treatment to form an adherent hydride layer on the surface. Targets thus prepared were preserved in a moisture-free environment before deuterium absorption.

Degassing and Deuteration of Targets

The chemically cleaned targets were first degassed by heating to ≈900°C in a glass vacuum chamber using a 3-kW, 2-MHz induction heater. Degassing was continued until a vacuum of $<10^{-5}$ Torr was achieved. Targets were then

*Technical Physics and Prototype Engineering Division.
+Plasma Physics Division.

heated to ≃600°C in an H_2 atmosphere at a few Torr pressure and allowed to cool. The H_2 was absorbed into the targets while cooling. The absorbed H_2 was released again by heating to 900°C. At least three cycles of H_2 absorption and desorption were done to create active sites for D_2 absorption.

After release of all the H_2, the targets were heated to ≃600°C in a D_2 atmosphere at few Torr pressure and allowed to cool by switching off the induction heater. The D_2 gas was absorbed while cooling. At least three cycles of D_2 absorption and desorption were done, similar to the H_2 absorption and desorption. Decrease in pressure recorded by an oil manometer was the measure of the quantity of D_2 absorbed. It was found that the quantity of gas absorbed increased in each new cycle and tended to saturate in the third or fourth cycle. Table I shows the maximum absorption of hydrogen and deuterium in different titanium targets.

Targets could typically absorb $\simeq 10^{19}$ molecules of D_2. Considering that mass of titanium is a few hundred milligrams, this corresponds to an overall deuterium/titanium ratio of only $\simeq 10^{-3}$. However, if most of the absorption is restricted to the surface, as we suspect, it is likely that the deuterium/titanium ratio is >0.001 in the near surface region.

While preparing the targets, we found that successful deuteration depends on various experimental factors:

1. Initial sandblasting of the targets for cleaning and roughening of the surface leads to better absorption of D_2.

2. Impurity content (such as O_2, N_2, etc.) in D_2 should be <0.1%.

3. Since the glass vacuum chamber is isolated from the pumping system during D_2 absorption, it is important that the vacuum chamber be leaktight. Small air leaks may contaminate the D_2.

TABLE I

Maximum Absorption of H_2/D_2 in Different Titanium Targets

	Target Shape	Mass (g)	H_2 Absorption		D_2 Absorption	
			Oil (mm)	Mercury (mm)	Oil (mm)	Mercury (mm)
1	Disk	0.980	35	2.8	22.5	1.8
2	Cone	0.198	16	1.28	5	0.4
3	Cone	0.206	16	1.28	5	0.4
4	Kite	0.610	36	2.88	34	2.72
5	Cone	0.200	18	1.44	15	1.20
6	Disk	0.875	54	4.32	46	3.68
7	Cone	0.460	41	3.28	34	2.72
8	Disk	0.875	46	3.68	33.5	2.68
9	Sponge	0.350	108.5	8.68	85	6.80
10	Pellet	1.025	1000	80.0	955	76.40
11	Cone	0.200	10.5	0.84	11	0.88
12	Cone	0.203	23.5	1.88	29.5	2.36
13	Disk	2.837	208	16.64	372	29.76
14	Cone	0.460	53	4.24	35	2.80
15	Cone	0.203	14	1.12	7	0.56
16	Pellet	1.02	1010	80.8	970	77.60
17	Disk	0.860	57	4.56	40	3.20
18	Cone	0.190	22	1.76	15	1.20
19	Kite	0.605	60	4.80	45.5	3.64

The deuterated targets were then sent to the Neutron Physics Division for analysis in quest of evidence for cold fusion. See reports A.3 and B.3 for those results.

As mentioned earlier, the deuteration of the titanium targets was carried out using a 3-kW induction heater operating at a 2-MHz frequency. The power supply of this heater became defective in July 1989 following failure of the main driver tube. Since then, gas loading of targets could not be carried out in this division. Similar experiments were thereafter commenced by the Heavy Water Division using a resistance furnace. However, although the loading procedure adopted there was such that very large quantities of D_2 gas (≃6 ℓ at 1 kg/cm^2) could be successfully absorbed in titanium pieces (≃5-g mass), none of the titanium samples have shown any evidence of tritium so far. It is possible that use of high-frequency (2-MHz) induction heating may have had some role in causing the detectable levels of cold fusion.

When a metallic object is heated by induction heating, the current distribution within the object is nonuniform with the current density decreasing exponentially from the surface to the center of the metallic work load.[3] The characteristic penetration or skin depth δ is defined as that distance over which the current density is reduced to $1/e$ times the surface value:

$$\delta = (\rho/f\pi\mu)^{1/2} ,$$

where

ρ = resistivity

μ = permeability of the workload

f = frequency of the applied alternating magnetic field.

For a 2-MHz induction heater, the skin depth in titanium works out to be ≃0.1 mm. It is believed that most of the absorbed D_2 gas is accumulated in the near surface region even though the entire sample would have reached high temperatures due to conduction. Hence, it is likely that D_2 density is very much higher in the near surface region, although the gross deuterium/titanium ratio is hardly 0.001.

Further investigations to confirm these conjectures are under way.

ACKNOWLEDGMENTS

The authors wish to acknowledge the significant spade work done by S. K. H. Auluck in arriving at the optimum conditions for loading of H_2/D_2 in machined titanium targets. We are also grateful to V. G. Date of the Atomic Fuels Division for fabrication of the machined targets.

REFERENCES

1. A. De NINNO et al., "Evidence of Emission of Neutrons from a Titanium-Deuterium System," *Europhys. Lett.*, **9**, 221 (1989).

2. "Preparation of Hydride Configurations and Reactive Metal Surfaces—Silver G.L.," U.S. Patent Report 6-611, p. 773 (1985).

3. E. J. DAVIES and P. G. SIMPSON, *Induction Heating Handbook*, McGraw-Hill Book Company, New York (1979).

3. AUTORADIOGRAPHY OF DEUTERATED TITANIUM AND PALLADIUM TARGETS FDR SPATIALLY RESOLVED DETECTION OF TRITIUM PRODUCED BY COLD FUSION

R. K. Rout, M. Srinivasan, and A. Shyam*

Introduction

During the last few months, hectic experiments have been under way in various laboratories to study the cold fusion phenomenon. De Ninno et al.[1] reported emission of neutrons from titanium metal loaded with deuterium gas under pressure. Similar experiments have been conducted at Bhabha Atomic Research Centre (BARC). We report here evidence of cold fusion in D_2 gas-loaded titanium and palladium targets through the use of autoradiography for spatially resolved detection of tritium. Our study used three different techniques to observe tritium:

1. autoradiography using X-ray films
2. characteristic X-ray measurement of titanium, excited by the tritium beta
3. liquid scintillation for tritium beta counting.

Loading of Deuterium

Titanium and palladium metal samples of various shapes and sizes were loaded with deuterium in two different ways. In the first method, an individual titanium target was radio-frequency heated to a maximum temperature of ≃900°C in vacuum and then in a deuterium gas atmosphere to absorb deuterium (see report B.2). In the second method, palladium-silver foil was heated (by ohmic heating) to a temperature of 600°C in vacuum (10^{-5} mm of mercury) and then in D_2 gas (see report B.4). The deuterium gas used for loading had a tritium content of $\leq 5.5 \times 10^{-4}$ Bq/ml, corresponding to a tritium/deuterium ratio of $\sim 4 \times 10^{-14}$.

Autoradiography

Autoradiography is a simple and elegant technique to detect the presence of radiation-emitting zones. This technique is free of electromagnetic interference (pickups, discharge pulses, etc.), has relatively high sensitivity as it can integrate over long exposure times, and can give very useful information in the form of space-resolved images. To achieve good image resolution, the sample was kept very close to the X-ray film. Standard medical X-ray film of medium grain size (10 to 15 μm in diameter) on a cellulose triacetate base was used. The exposure time used for the deuterated samples varied from 18 h to a few days. At times, a stack of several films was used. In other cases, films were placed on both sides of the sample. For latent image formation, we used India Photographic Company 19B developer and fixer. The developing time was typically 4 to 5 min. Out of the many samples that had absorbed D_2 gas, only a few showed a latent image. The results are tabulated in Table I.

A radiograph (Fig. 1) of some of the deuterated titanium disk targets showed several spots randomly distributed within the sample boundary. The occurrence of spots all along the rim of the machined target is very intriguing. Repeated measurements over a period of 1 month, with the same sample and varying exposure times, gave an almost identical pattern and relative intensity distribution of spots, indicating that the radiation-emitting regions were well entrenched in the face of the titanium lattice. The second film of a stack exposed to the target also indicates similar though less intense spots, ruling out the possibility of any kind of a chemical reduction reaction caused by the deuterium or hydrogen in the target being responsible for causing the spots. The X-ray image (Fig. 2) of a conical target showed a diffused projection of the cone.

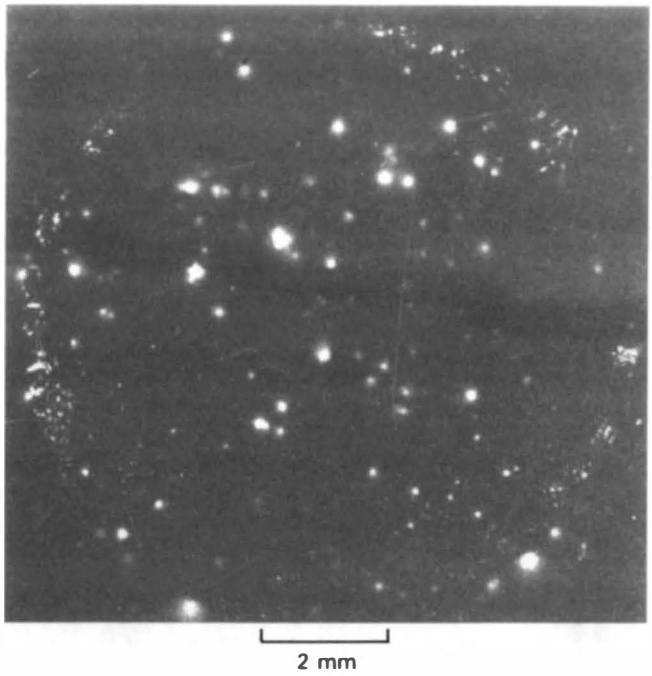

Fig. 1. Radiograph of titanium disk target.

The images of palladium-silver foils (Fig. 3) were more uniform. They did, however, indicate variation in intensity and some spots, but the fogging was more or less uniform. Unlike the deuterated titanium targets, the intensity of the fogging of the deuterated palladium foils reduced very rapidly, within a couple of days, the activity fell below measurement levels.

Measurements of X-Ray Emission

The characteristic X rays emitted from the deuterated titanium and palladium were studied with the help of a silicon/lithium-drifted detector by the Nuclear Physics Division. The detector had a 75-μm-thick beryllium window. Titanium X rays ($K\alpha$ = 4.5 keV, $K\beta$ = 4.9 keV) were observed in the conical (Fig. 4) and disk (Fig. 5) samples. The count rate of the conical sample was much greater than that of the disk sample. Some of the deuterated palladium-silver foils indicated X-ray peaks (Fig. 6) corresponding to titanium, presumably because of a small amount of titanium impurity picked up by the foils from the D_2 loading chamber, which had earlier been used for loading of titanium samples. We did not observe L X rays of palladium or silver.

Liquid Scintillation Counting

This was carried out at the Health Physics Division using the facilities described in report A.9. The sample was simply

*Neutron Physics Division.

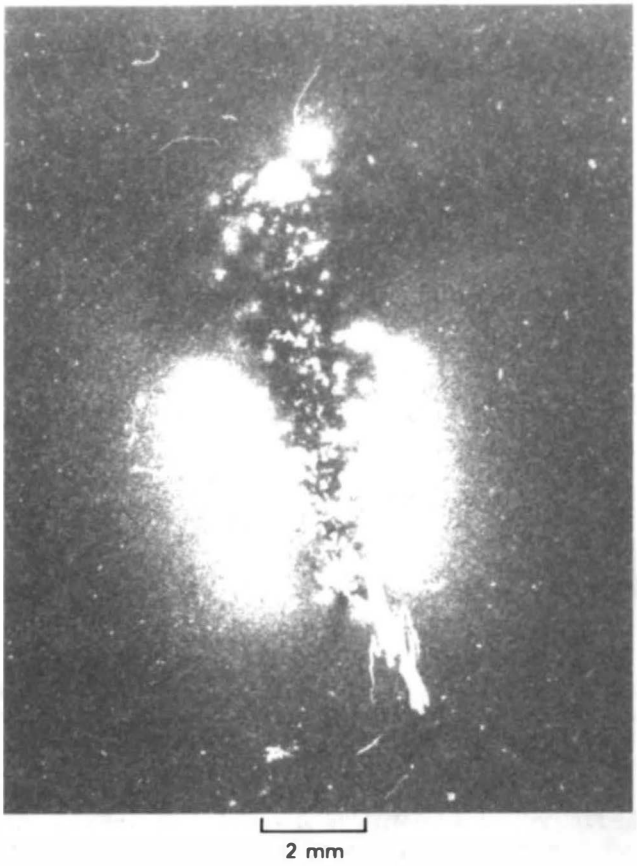

Fig. 2. Radiograph of conical titanium target.

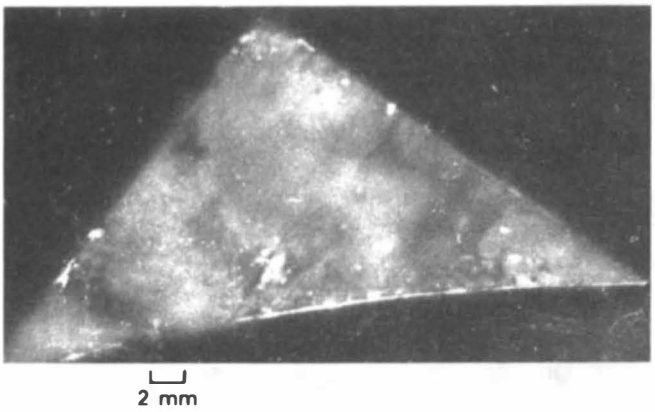

Fig. 3. Radiograph of palladium-silver foil target.

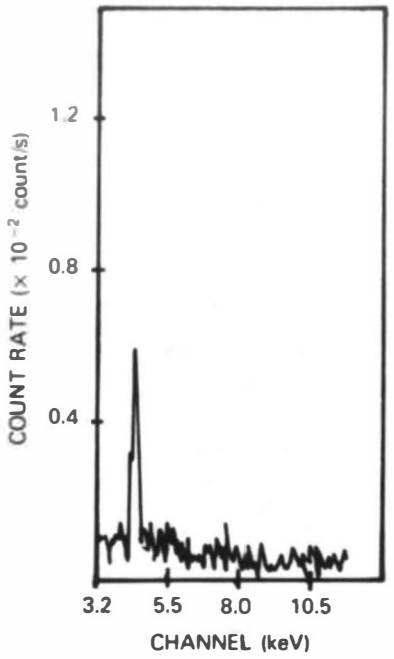

Fig. 4. Count rate in conical titanium target.

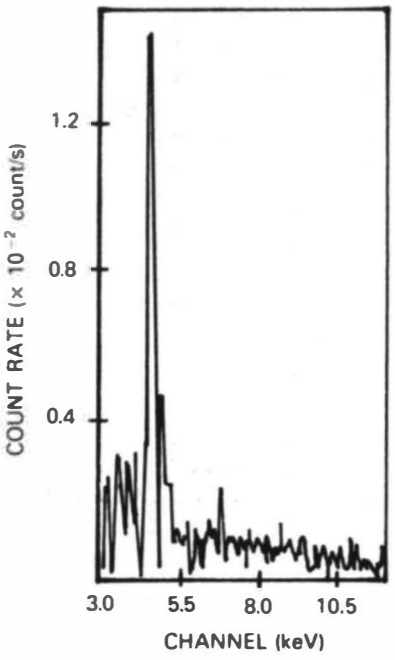

Fig. 5. Count rate in titanium disk target.

dropped into a vial containing a liquid scintillator cocktail, and the tritium activity was counted by two photomultiplier tubes in coincidence. The typical activities were 50 to 1000 Bq, compared to a background of <0.2 Bq. No correction was applied for possible quenching or shadowing effects.

Results and Discussion

The fogging observed in the autoradiographs is the combined effect of tritium betas and characteristic X rays of the host material. The radiograph of the disk sample (Fig. 1) indicates tritium localized in the form of microstructures. The spots are unevenly distributed on the face of the titanium, with a total of ~60 to 70 spots. On correlating the X-ray counts under the peak (*K* X-ray peak) and the liquid scintillation counting results, it was found that each emitting spot corresponds roughly to 10^9 to 10^{10} atoms of tritium. In comparison, the total number of deuterium atoms loaded in the disk sample was 10^{19} to 10^{20}. The X-ray images (Fig. 3) of

TABLE I

Sample Number	DS001	CS003	PS001
Material	Titanium	Titanium	Palladium-silver
Shape of sample	Disk	Cone	Foil
Sample mass (mg)	980	206	110
D_2 absorbed (mg)	0.42	0.07	0.73
Date of D_2 loading	June 14, 1989	July 9, 1989	August 22, 1989
Date of exposure	June 23, 1989	June 14, 1989	August 24, 1989
Exposure duration (h)	66	24	88
Number of repetitions	9	3	4
Silicon/lithium result (Bq)	290	1300	2960[a]
Date of measurement	June 16, 1989	June 16, 1989	August 24, 1989
Total tritium atoms	$\simeq 1.5 \times 10^{11}$	$\simeq 6.5 \times 10^{11}$	$\simeq 1.5 \times 10^{12}$
Tritium/deuterium ratio	$\simeq 1.2 \times 10^{-9}$	$\simeq 3.2 \times 10^{-8}$	$\simeq 7 \times 10^{-9}$
Liquid scintillation result (Bq)	28	850	---
Date of measurement	June 26, 1989	June 15, 1989	---

[a]Estimated from titanium (present as impurity) X rays; may be inaccurate.

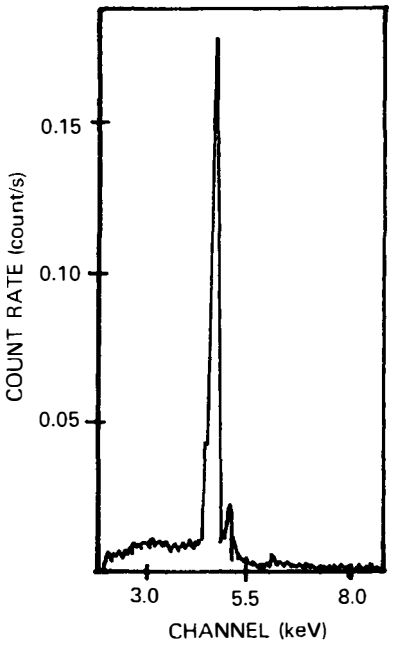

Fig. 6. Count rate in palladium-silver foil target.

the palladium-silver foils were uniformly fogged and the intensity of the fogging reduced very rapidly with time, unlike with the titanium. This type of loss in image may be attributed to the high mobility of tritium in palladium compared to titanium.

Observation of K X-ray peaks of titanium (Figs. 4, 5, and 6) was the result of excitation of the K-shell by tritium betas. No L X rays of palladium ($\simeq$3.6 keV) or silver ($\simeq$3.8 keV) were observed because of low fluorescent yield for L X rays, and the detector window was too thick (75 μm) to allow observable quantity of L X rays. Liquid scintillation counting further confirms the presence of tritium in the samples. The quantity of tritium observed on the surface of the samples exceeded the total quantity of tritium initially contained in the deuterium gas used to load the samples; hence, the gaseous tritium, even if preferentially absorbed by the samples, cannot explain this phenomenon. Undeuterated metallic targets machined out of the same titanium rods did not indicate any detectable tritium, ruling out any contamination during target fabrication or handling.

Summary and Conclusions

The evidence presented here seems to indicate cold fusion reactions occurring in some of the deuterium-loaded titanium and palladium targets. It has not been possible to conclusively establish whether the fusion reactions occur during the deuteration process or subsequently. It is also not clear whether the reactions occur in sporadic bursts or continuously. However, one of the disk targets, which gave an impressive spotty radiograph, did give rise to a significant neutron burst that produced 10^6 neutrons over a period of 85 min.

ACKNOWLEDGMENTS

The authors sincerely wish to express their gratefulness to P. K. Iyengar, director of BARC, for his keen interest and constant guidance in the present work. We are also thankful to M. S. Krishnan, S. K. Malhotra, S. Shrikhande, and K. C. Mittal for supplying the deuterated targets. We are also grateful to V. S. Ramamurthy and Madan Lal for the X-ray spectral measurements. The authors would like to express their thanks to T. S. Iyengar for carrying out the liquid scintillation counting of the targets.

REFERENCE

1. A. DE NINNO et al., "Evidence of Emission of Neutrons from a Titanium-Deuterium System," *Europhys. Lett.*, **9**, 221 (1989).

4. EVIDENCE FOR PRODUCTION OF TRITIUM VIA COLD FUSION REACTIONS IN DEUTERIUM-GAS-LOADED PALLADIUM

M. S. Krishnan, S. K. Malhotra, D. G. Gaonkar,
V. B. Nagvenkar, and H. K. Sadhukhan*

Introduction

After the first announcement of cold fusion,[1,2] further evidence has appeared in the literature, although many groups have failed to obtain positive results. Electrolytically loaded palladium and titanium[1,2] and titanium loaded directly with deuterium gas[3] have been reported to emit neutrons. Interestingly, gas-loading experiments involving palladium-deuterium targets have not yet been reported. Such experiments were therefore conducted recently by us. Tritium measurements in gas-loaded palladium-deuterium targets have been carried out. The results obtained thus far to ascertain whether cold fusion reactions occur in gas-loaded palladium are summarized here.

Preparation of Palladium Samples

For loading deuterium gas in palladium two types of samples were used. One was palladium-silver alloy directly used as manufactured without further surface treatment. The other sample used was palladium black powder prepared from $PdCl_2$. Absorption of deuterium by palladium black was very fast and readily gave a deuterium/palladium ratio of 0.6 as deduced from the drop in gas pressure during loading. In the palladium-silver alloy, however, absorption was rather slow and the amount of deuterium absorbed was much less than that corresponding to a deuterium/palladium ratio of 0.6.

O_2-Gas-Loading Procedure

The D_2 gas used for gas loading was prepared from D_2O. This D_2O had a tritium activity of 0.075 nCi/ml. The gas generated from it by reducing with sodium in a vacuum system under stringent conditions was stored in a stainless steel cylinder under pressure and liquid N_2 cooling in the presence of activated charcoal. The D_2 gas thus produced was not further analyzed for tritium as it was expected to contain not more than 0.038 nCi/ℓ activity. This corresponds to a tritium/deuterium isotopic ratio of 3×10^{-14}.

A schematic of the experimental setup used for gas loading is given in Fig. 1. It essentially consists of a vacuum system equipped with a rotary pump and an oil diffusion pump giving a vacuum of 10^{-6} Torr. The stainless steel reaction vessel containing the palladium sample is connected to the vacuum system through stainless steel buffer tank. A deuterium cylinder is connected to the vacuum system through a needle valve. The system is also equipped with a pressure gauge and a manometer/pressure gauge. The entire system was tested for a vacuum of 10^{-6} Torr and pressure of 100 kg/cm^2. A weighed amount of palladium black or palladium-silver alloy was placed in the vessel and heated to 600°C for 2 h under a vacuum of $>10^{-5}$ mm. After cooling to room temperature, deuterium gas was filled at 1-atm pressure, and the system was sealed off to attain equilibrium.

After completion of gas loading, the vessel containing the palladium sample was isolated from the filling system and transferred into a closed glass container in a dry enclosure, free of moisture and oxygen and kept for equilibrium for several hours. Adequate precautions were taken to avoid inadvertent exposure to air since this would lead to catalytic recombination of absorbed D_2 gas with O_2, accompanied by a considerable increase in temperature. The entire deuterium absorbed in the palladium would be lost if these precautions are not taken. This was confirmed in one set of experiments where the loaded sample was accidentally exposed to air and the resultant equilibrated water sample did not show any activity.

Tritium Analysis

To measure the tritium, if any, produced due to cold fusion reactions, the deuterated palladium samples were kept in contact with distilled water for a few hours to extract the tritium by isotopic exchange into the water. The water samples containing tritium were later sent to the tritium group of the Health Physics Division for liquid scintillation counting.

In converting the measured tritium activity in the distilled water to a calculated tritium activity originally present in the palladium samples, a conversion factor is used that is computed as follows:

Taking into consideration the exchange reaction

$$T_{abs} + H_2O = H_{abs} + HTO \quad (1)$$

and applying the laws of chemical equilibrium, one obtains the following relation for low tritium concentration:

$$Y_i n_g = n_l[X_e(1/K + 1) - X_i] \ , \quad (2)$$

where

X, Y = tritium atom fraction in the liquid and the absorbed phases, respectively,

i, e = initial and equilibration conditions, respectively

n_g, n_l = gram moles of gas absorbed in metal and of water taken for equilibration, respectively

K = equilibrium constant for reaction (1), taken to be the same as for exchange of tritium between hydrogen and water, since at equilibrium the system consists mainly of hydrogen both in the absorbed and the liquid phases. The value[4] of K is 6.128 at 30°C.

Y_i = number of tritium atoms produced for every deuterium atom absorbed in the metal.

The tritium atom fraction under equilibrium conditions X_e can now be calculated from the measured tritium activity of the water as follows:

$$X_e = \frac{A}{d \times 3200} \ , \quad (3)$$

where

A = activity (Ci/ml)

d = density of water (g/ml) ($d = 0.996542$ at 27°C).

Results and Discussion

Table I summarizes the results of the tritium measurements on the four samples studied. The tritium/deuterium ratio is about two or three times more in the palladium-silver

*Heavy Water Division.

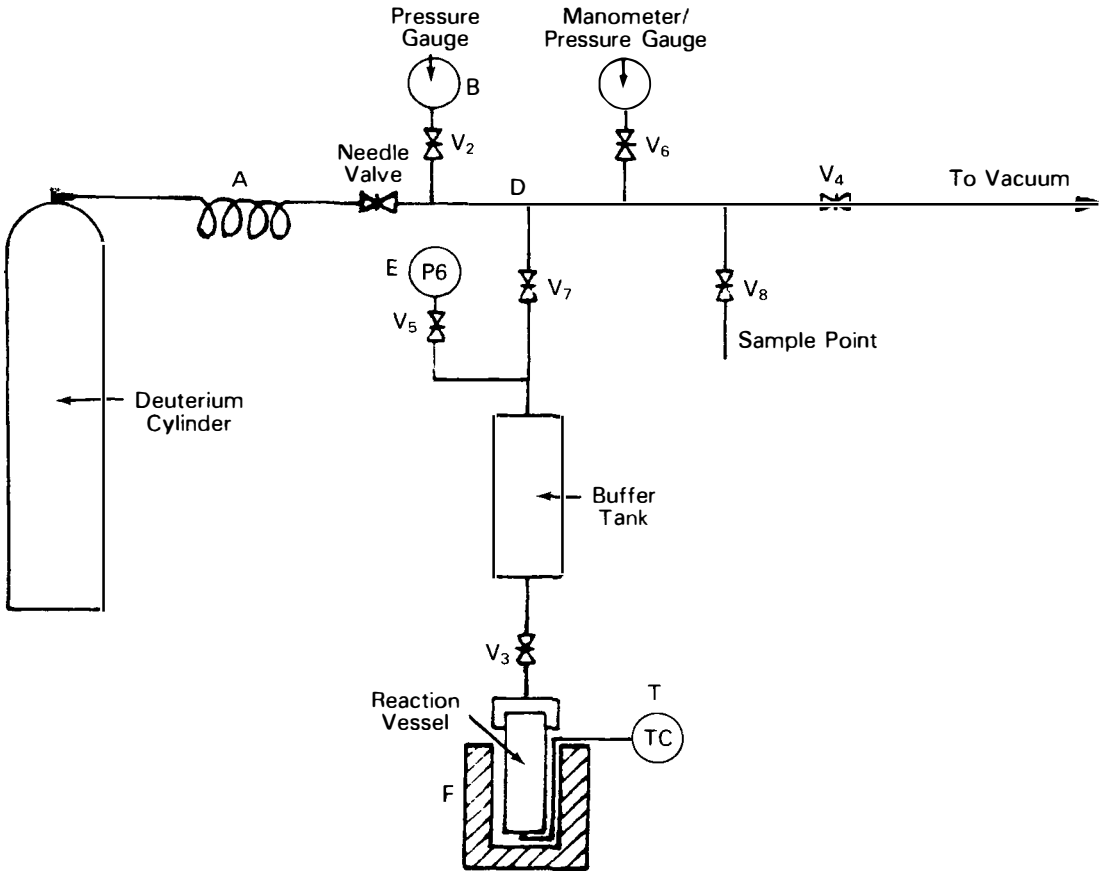

Fig. 1. Schematic of equilibration system.

TABLE I

Summary of Tritium Measurements

Nature of Sample	Palladium Black Powder	Palladium-Silver Foil[a]	Palladium-Silver Foil[a]	Silver Foil[b] (Single Foil)
Mass (g)	20.0	0.96	0.43	10.9
Volume of D_2 gas absorbed (ml)	1325	34.5	20.2	518.4
Deuterium-palladium ratio	0.63	0.46	0.45	0.45
Time of equilibrations (h)	16	16	240	240
Volume of water used for isotopic exchange (ml)	50	6	5	50
Tritium activity of water after equilibration (nCi/ml)	0.22	0.16	0.88	0.23
Tritium-deuterium ratio in palladium	3.24×10^{-12}	1.08×10^{-11}	8.31×10^{-11}	8.67×10^{-12}
Absolute tritium activity (nCi)	11.05	0.97	4.32	11.58
Number of tritium atoms in palladium	2.31×10^{11}	2.02×10^{10}	8.96×10^{10}	2.4×10^{11}

[a]These were the triangular foils also studied by autoradiography.
[b]This was a single 11.5-cm-diam foil, same as the cathode used in the cell of report A.2.

foils as compared to palladium black. Note that the tritium/deuterium ratio in the targets is in the range of 10^{-12} to 10^{-11}, which is more than two orders of magnitude higher than that in the initial deuterium gas used for loading. It is also seen that more tritium production is observed with longer equilibration time.

The method of isotopic exchange for extraction of tritium from metal to water phase is less cumbersome and the

tritium/deuterium ratio obtained from Eq. (1) gives at least a conservative estimate of tritium produced.

Autoradiography of Samples

The palladium-silver foils were also subjected to autoradiography to obtain images of tritium distribution as described in report B.3. It essentially consists of keeping the gas-loaded sample on X-ray film and developing it after allowing adequate exposure time. The palladium black samples could not be subjected to autoradiography as the powder got stuck to the film. But in case of palladium-silver foils, there was unmistakable fogging of X-ray film corresponding to the geometrical shape of the foils, indicating the emission of some radiation. The only possible radiation being emitted from these foils is the beta rays from tritium and the characteristic X rays of the metal excited by tritium betas.

Summary and Conclusions

Gas-loaded palladium samples have provided evidence for the first time of the presence of tritium, strongly suggesting the occurrence of cold fusion reactions. The palladium-deuterium system does not require high pressure of D_2 gas and also no external perturbation is required to create non equilibrium conditions as suggested by De Ninno et al.[3] Although no quantitative comparisons can be made between electrolytically loaded and gas-loaded palladium experiments, the present results confirm that electrolysis is not the only approach to inducing cold fusion in a palladium lattice. Unfortunately, no neutron measurements were carried out in the present work. A correlation between neutron production, if any, and tritium production would contribute significantly toward understanding the mechanism of cold fusion.

ACKNOWLEDGMENTS

The authors sincerely wish to express their gratefulness to P. K. Iyengar, director of the Bhabha Atomic Research Centre for his keen interest and constant guidance in the present work. We are thankful to M. Srinivasan for critically reading the manuscript and offering many suggestions. We also thank A. Shyam and R. K. Rout for carrying out the autoradiography of the samples. This work would not have been possible but for the unstinted cooperation of T. S. Iyengar, Health Physics Division, who carried out the tritium counting of all the water samples. The authors also wish to thank V. H. Patil, Heavy Water Division, who has been of great assistance in the experimental work.

REFERENCES

1. M. FLEISCHMANN and S. PONS, "Electrochemically Induced Nuclear Fusion of Deuterium," *J. Electroanal Chem.*, **261**, 301 (1989).

2. S. E. JONES et al., "Observation of Cold Nuclear Fusion in Condensed Matter," *Nature*, **338**, 737 (1989).

3. A. DE NINNO et al., "Evidence of Emission of Neutrons from a Titanium-Deuterium System," *Europhys. Lett.*, **9**, 221 (1989).

4. S. M. DAVE, S. K. GHOSH, and H. K. SADHUKHAN, "Tritium Separation Factors in Distillation and Chemical Exchange Processes," BARC-1168, Bhabha Atomic Research Centre (1982).

5. OBSERVATION OF HIGH TRITIUM LEVELS IN AGED DEUTERATED TITANIUM TARGETS AS POSSIBLE EVIDENCE OF COLD FUSION

M. Srinivasan,* R. K. Rout,* S. C. Misra,+ M. Lal,† A. Shyam,* P. S. Rao,+ and P. K. Iyengar†

Introduction

A number of groups have reported the occurrence of cold fusion reactions in D_2-gas-loaded titanium samples.[1-3] Although both neutrons and tritium have been detected in these measurements, it is tritium that is the main product of cold fusion reactions. At Bhabha Atomic Research Centre (BARC), the presence of tritium in titanium and palladium targets was first detected through the technique of autoradiography.[2,4] While tritium was found to be firmly entrenched in the body of the titanium lattice, it tended to easily diffuse out of palladium samples. The autoradiograph of the tritium-containing titanium target was reproducible even after a lapse of several months, in spite of the samples being exposed to atmosphere.

In this context, it was recently learned that the Radiological Protection Division had procured a number of deuterated titanium targets (on copper disk backing) during 1972 to 1981 for dosimetry studies with accelerator-based (*d-d*) neutron sources. It was therefore conjectured that cold fusion reactions might have occurred in these targets during the past 9 to 18 yr; if so, the targets should contain considerable amounts of tritium. We discuss here the measurement of tritium levels in these "aged" targets by a variety of techniques and comment on the significance of the results in the context of the cold fusion phenomenon.

Description of Targets

Twelve aged deuterium targets were available for tritium measurements. Nine of these (S4 to S12) were procured in 1981 and the remaining three (S1, S2, and S3) during 1972–1975. These targets were fabricated by coating titanium on 28.4-mm-diam × 0.25-mm-thick copper disks. Titanium is deposited within a 25.4-mm-diam region. The detailed specifications of the targets are summarized in Table I. Target S1 is the oldest, having been procured in January 1972. The titanium thickness in these targets is in the 2.26 to 3.39 mg/cm^2 range, except for S10, S11, and S12, in which it is approximately a factor of 10 lower. The amount of deuterium absorbed in these targets, as certified by the manufacturers, is in the 0.32- to 5.6-ml range. The corresponding gross deuterium/titanium atomic ratios are seen to vary in the 0.51 to 1.34 range, with targets S4 to S6 having the highest loading ratios.

Autoradiography

Autoradiography is a simple technique to establish the presence of radiation-emitting zones. This technique is free from any electromagnetic interference (pickups, discharge pulses, etc.), has relatively high sensitivity as it can integrate over long exposure times, and can give very useful information in the form of space-resolved images. To achieve a good

*Neutron Physics Division.
+Radiological Protection Division.
†Nuclear Physics Division.

TABLE I

Specifications of the Aged Deuterium Targets

Target	Target Identification	Date of Supply of Target	Titanium Layer Thickness (mg/cm^2)	Deuterium Gas Loading		Deuterium/Titanium Atomic Ratio
				ml	Atoms ($\times 10^{20}$)	
S1	CuT 60	January 1972	3.15	2.1	1.12	0.51
S2	CuT 367	February 1975	2.90	3.9	2.08	1.04
S3	CuT 86	February 1975	3.06	3.9	2.08	0.98
S4	Cdx 713	April 1981	2.72	4.6	2.46	1.30
S5	Cdx 715	April 1981	3.39	5.6	3.00	1.28
S6	Cdx 712	April 1981	3.13	5.4	2.90	1.34
S7	Cdx 999	September 1981	2.51	3.2	1.72	1.00
S8	Cdx 998	September 1981	2.26	3.2	1.72	1.10
S9	Cdx 997	September 1981	2.84	3.2	1.72	087
S10	Cdx 996	September 1981	0.39	0.32	0.172	0.64
S11	Cdx 994	September 1981	0.39	0.32	0.172	0.64
S12	Cdx 995	September 1981	0.45	0.32	0.172	0.55

image resolution, the sample was kept in contact with the X-ray film. Standard medical X-ray film of medium grain size (10 to 15 μm in diameter) on a cellulose triacetate base was used. The exposure time ranged between 16 h to a few days. At times, a stack of several films was used, and in some cases, films were placed on both sides of the sample.

Autoradiographs of all the 12 aged deuterium targets indicate a clear image of the central titanium-coated region. Two typical images are shown in Figs. 1 and 2. The fogging of the photographic films is presumably due to the combined effect of tritium betas and the characteristic X rays excited in the host titanium lattice. The second film in a stack of X-ray films exposed to the deuterated target gives a similar but fainter image, ruling out the possibility that image formation is due to pressure or chemical reduction effects. The autoradiographs show almost uniform distribution of tritium in the titanium zone and a faint outer ring corresponding to the bare copper region. The optical density of the autoradiographs was measured with the help of a computer-controlled microdensitometer. The autoradiograph of a standard tritium-loaded titanium target was used as reference for intensity calibration. The absolute tritium activity of the target estimated from the autoradiographs is tabulated in Table II. While three targets (S1, S2, and S3) indicate a tritium content in the 22- to 36-MBq region, the other targets indicate somewhat lower

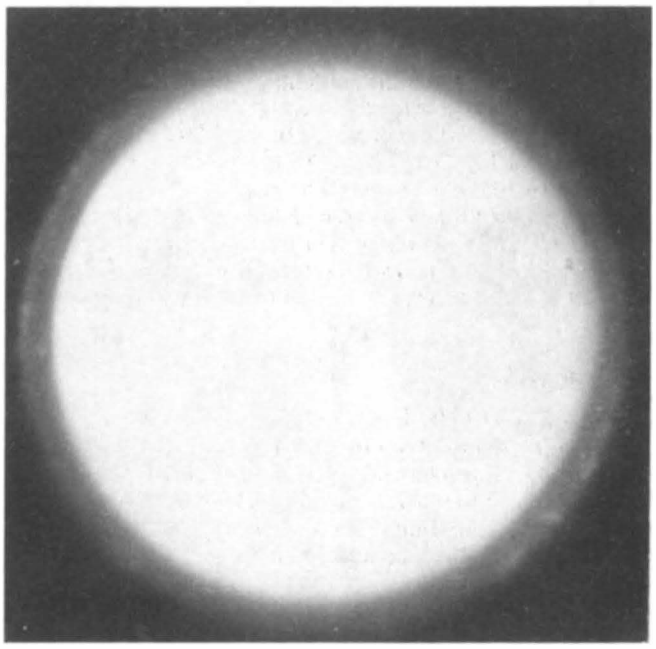

Fig. 1. Autoradiograph of target S4.

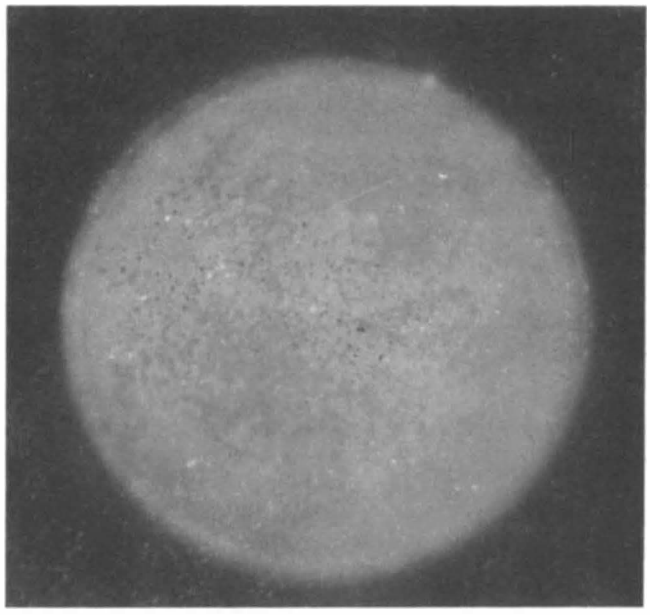

Fig. 2. Autoradiograph of target S3.

TABLE II

Autoradiography Measurements

Target	Relative Fogging Intensity[a]	Tritium Content	
		MBq	Atoms ($\times 10^{15}$)
S1	7.9	35.2	20.0
S2	6.1	27.4	15.0
S3	5.2	22.9	12.3
S4	19.4	86.2	48.0
S5	1.8	8.9	5.0
S6	2.0	8.1	4.5
S7	4.2	18.9	10.4
S8	2.7	12.2	6.9
S9	1.4	6.3	3.5
S10	2.7	12.2	6.9
S11	1.0	4.4	2.5
S12	0.5	2.2	1.2

[a]Arbitrary units, normalized to a standard exposure time.

TABLE III

NaI(Tl) Detector Measurements

Target	Titanium K X-Ray Count Rate (count/s)	Tritium Content[a]	
		MBq	Atoms ($\times 10^{15}$)
S1	70.6	25.9	14.5
S2	77.6	28.5	15.9
S3	86.8	31.8	17.8
S4	538.5	199.0	111.4
S5	49.2	18.1	10.1
S6	48.3	17.8	10.0
S7	22.2	8.1	4.6
S8	11.7	4.4	2.5
S9	8.6	3.2	1.8
S10	3.8	1.4	0.8
S11	1.8	0.67	0.4
S12	1.6	0.59	0.3

[a]Conversion factor (0.37 ± 0.1) MBq/count·s^{-1}.

tritium levels, in the 2.2- to 18.9-MBq range, except for target S4, which shows a very high value of 86.2 MBq. The high-activity targets (S1 to S4) also gave a faint but clearly visible image from the copper backing side.

Scintillation Counting by NaI(Tl) Detector

The first instrument used to count the activity of the samples was a standard thin-window NaI(Tl) scintillation detector system coupled to a multichannel analyzer. The NaI crystal used is 1 mm thick and 25 mm in diameter, with a 125-μm-thick beryllium window. The energy resolution of the detector is 55% at 6-keV X-ray energy. The output of the multichannel analyzer was processed by a personal computer. Figure 3 presents the typical X-ray spectrum observed. A tritiated titanium target of known activity, (2.8 ± 0.6) × 10^9 Bq, was used as reference for calibration. The count rate above the background under the peak was used to compute the absolute activity of the targets. The counting time was 600 s for each sample. From Table III, which summarizes the results, it is seen that the activity of the samples as measured by the NaI system is in the 0.59- to 31.8-MBq range, except for target S4, which shows a high activity of 199 MBq.

X-Ray Measurements by Germanium Detector

The second method of counting of tritium activity[5] was by means of a 100-mm^2-area × 10-mm-thick planar intrinsic germanium detector with a 0.075-mm-thick beryllium window, coupled to a low-noise cryogenic preamplifier, main amplifier with pileup rejecter, real-time corrector, and multichannel analyzer. The energy resolution of this detector is 170 eV for 5.9-keV X-ray energy. The samples to be counted were mounted coaxially 15 mm away from the front of the germanium detector. The counting time was in the 1000- to 4000-s range. Figure 4 shows the typical X-ray spectrum of

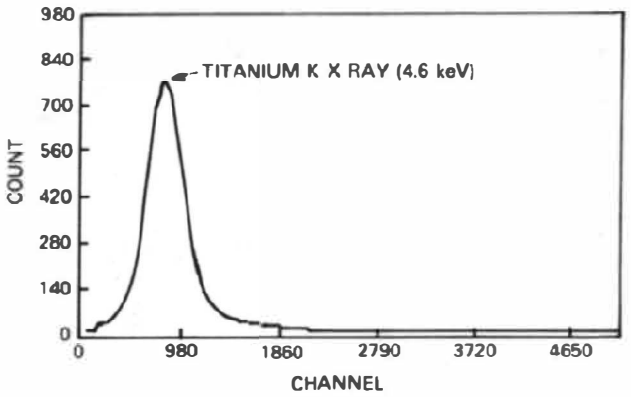

Fig. 3. Typical X-ray spectrum of target S4, by NaI detector.

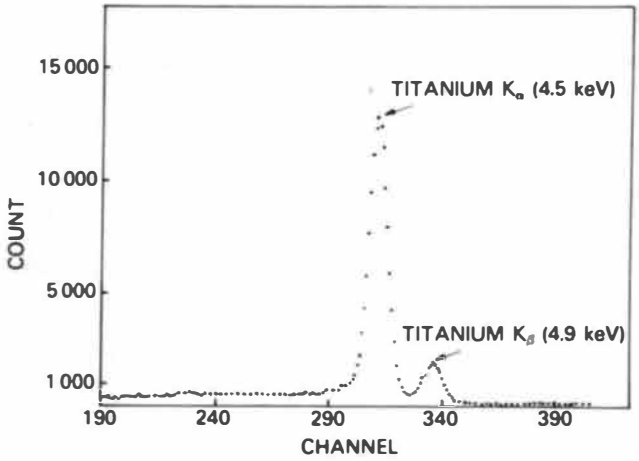

Fig. 4. Typical X-ray spectrum of target S3, by germanium detector.

the aged targets. The characteristic X-ray peaks of titanium ($K\alpha = 4.5$ keV, $K\beta = 4.9$ keV) and the bremsstrahlung X-ray background are clearly seen in the spectrum. To deduce the absolute tritium content corresponding to the observed titanium K X-ray counts, four tritiated titanium ($\simeq 3.0$ mg/cm^2) targets of known tritium content were used for calibration. The average calibration factor of (1.46 ± 0.4) MBq/count·s^{-1} deduced from these was used to compute the absolute tritium activity of the aged targets. The scatter of ~30% in the calibration factor is due to the uncertainty associated with the measurement of the quantity of tritium gas absorbed. Table IV presents the results of tritium activity of the D_2-gas-loaded targets obtained by this method. Target S4 shows the highest tritium level (236.8 MBq) and target S12 the lowest (0.59 MBq). Since the titanium layer thickness is much larger than the range of the average energy of the tritium betas (0.3 mg/cm^2) but less than the mean-free-path for X-ray absorption ($\simeq 10$ mg/cm^2) in titanium, the difference, if any, in the titanium thickness between the calibration sources and the test samples would not affect the results significantly.

Ion Chamber Current Measurements

A cylindrical graphite ion chamber with a central graphite anode was used to measure the ionization current produced by the radiation emanating from the targets. The ion chamber has a 42-mm o.d., 34-mm i.d., and overall length of 27 mm. The tip of the central anode is 10 mm from the target surface giving a clear air gap of 1.3 mg/cm^2, sufficient to absorb the tritium beta particles of energy ≤ 18.6 keV (the range of 18.6-keV electrons in aluminum, for example, is $\simeq 0.9$ mg/cm^2). The sensitive zone of the detector subtends a solid angle of 2π sr on the target.

The chamber current was measured by observing the time rate of rise of voltage across a condenser of known capacitance. The current was found to agree within 1% for positive and negative polarities. The background or leakage current was $<10^{-2}$ pA. It was confirmed that the current reduced to the background level when an aluminum foil of 5 mg/cm^2 thickness was inserted between the target and the sensitive volume of the chamber. The results are summarized in Table V. The currents with the aged deuterium targets were in the 0.2- to 2.5-pA range, except for target S4, which gave a high current of 15.6 pA.

Measurements were made separately with the titanium side as well as the copper side facing the sensitive volume. The ratio of currents from copper and titanium sides varied between 0.05 and 0.30, the highest ratio being 0.30 for target S4. The back surface currents could be attributed to the migration of tritium over the years.

2π Beta Counter

A pillbox-type 2π geometry proportional counter with burshane as the counting gas was the fourth method for counting the tritium activity. The gas counter has two compartments, with the particles in the lower and upper compartments being counted separately. The voltage applied was set in the plateau region, between 2.6 and 2.8 kV. The count rates with the titanium side were in the range of 7.7×10^3 to 4.5×10^4 count/s. The observed count rates, corrected for the circuit dead time of 6.5 μs, are presented in Table VI. The ratio of chamber current to beta counts is reasonably constant (see Fig. 5) and varies in the range of 2.5 to 3.0×10^{-5} pA/beta·s^{-1}. This is in good agreement with the value of 2.7×10^{-5} pA/beta·s^{-1} expected on the basis of an average beta-particle energy of 5.7 keV and energy required to produce one ion pair in air of 33.85 eV. This suggests that the radiation primarily responsible for ionization within the chamber is beta particles of ~5.7-keV average energy. The simple method of calibration by means of a standard source adopted for X-ray counting results does not work here since only betas from the top layer of thickness less than the range of betas in titanium would be leaking out. To estimate the total activity, we assume that the tritium in titanium is distributed uniformly over the whole volume of titanium. Hence, the total number of beta particles emitted from the target can be taken as $2\mu t/[1 - \exp(-\mu t)]$ times the count rate observed in 2π solid angle, where μ is the absorption coefficient

TABLE IV

Germanium Detector Measurements

Target	Titanium K X-Ray Count Rate (count/s)	Tritium Content[a]	
		MBq	Atoms ($\times 10^{15}$)
S1	25.4	37.0	20.7
S2	22.9	33.3	18.6
S3	24.9	37.0	20.7
S4	156.3	236.8	132.4
S5	16.1	25.9	14.5
S6	13.3	18.5	10.4
S7	6.2	9.6	5.4
S8	3.4	5.2	2.9
S9	2.3	3.7	2.0
S10	0.92	1.5	0.8
S11	0.54	0.74	0.4
S12	0.4	0.59	0.3

[a]Conversion factor (1.46 ± 0.4) MBq/count·s^{-1}.

TABLE V

Ion Chamber Current Measurements

Target	Chamber Current (pA)	Conversion Factor (MBq/pA)	Tritium Content	
			MBq	Atoms ($\times 10^{15}$)
S1	1.6	1.31	2.1	1.2
S2	2.5	1.24	3.1	1.8
S3	2.1	1.33	2.8	1.6
S4	15.6	1.16	18.2	10.2
S5	1.0	1.5	1.5	0.81
S6	1.3	1.3	1.7	1.0
S7	0.66	1.07	0.71	0.4
S8	0.37	1.0	0.36	0.2
S9	0.22	1.23	0.27	0.15
S10	0.62	0.19	0.12	0.07
S11	0.32	0.19	0.06	0.03
S12	0.21	0.19	0.04	0.02

TABLE VI

2π Beta Counter Measurements

Target	Count Rate ($\times 10^4$ count/s)	Conversion Factor (Bq/count·s^{-1})	Tritium Content	
			MBq	Atoms ($\times 10^{15}$)
S1[a]	---		---	---
S2[a]	---		---	---
S3[a]	---		---	---
S4[a]	---		---	---
S5[a]	---		---	---
S6	4.5	37.8	1.7	0.93
S7	2.18	29.4	0.64	0.34
S8	1.22	26.2	0.32	0.18
S9	0.77	33.8	0.26	0.14
S10	2.12	5.2	0.11	0.06
S11	1.12	5.3	0.06	0.03
S12	0.84	6.0	0.05	0.03

[a]Activity too high for measurement by counter.

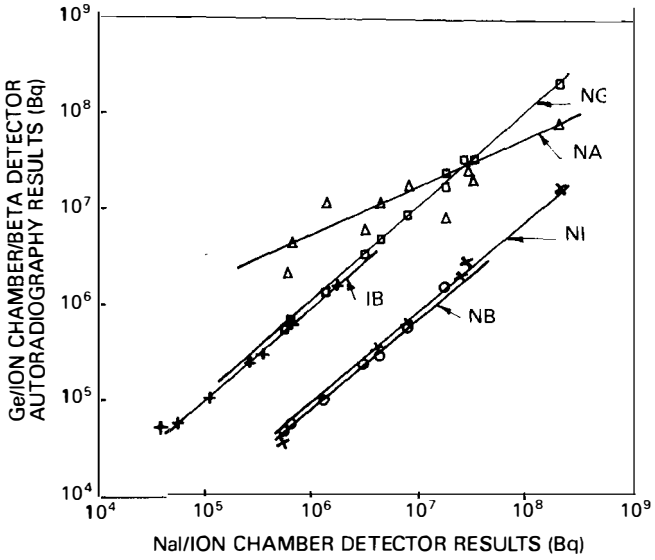

Fig. 5. Relative variation in tritium activities measured by five different methods.

(5844 cm^2/g) for the beta particles in titanium and t is the titanium thickness. The conversion factors so computed as well as the absolute tritium activity values deduced therefrom are given in Table VI.

Results, Discussion, and Conclusions

Table VII summarizes the tritium activities measured by the five different methods, and Fig. 5 shows logarithmic plots of the data. Lines NG, NI, and NB represent the activities measured by germanium, ion chamber, and beta detectors, respectively, against the NaI activity, while line IB corresponds to the beta counter data plotted against ion chamber data. The fact that all the plots display a slope of 45 deg confirms simple proportionality among these four results. Considering that absolute activities from NaI and germanium X-ray counts are derived using a standard tritium source for calibration disregarding titanium coating thickness variations, whereas ion chamber and beta counter values are obtained using computed conversion factors accounting for titanium thickness differences, it is gratifying to note that we still get good linearity. However, line NA between NaI and autoradiographic activities displays a slope distinctly different from 45 deg, suggesting the existence of nonlinear effects in autoradiographic results. This is also evident from the ratio of the maximum (target S4) to minimum (target S12) activities,

TABLE VII

Summary of Tritium Results by Five Methods

Target	Tritium Content (MBq)					
	Autoradiography	NaI	Germanium	Ion Chamber	2π Beta Counter	Average Value[a]
S1	35.2	25.90	37.00	2.10	---	21.7
S2	27.4	28.50	33.30	3.10	---	21.6
S3	22.9	31.80	37.00	2.80	---	23.8
S4	86.2	199.00	236.80	18.20	---	151.3
S5	8.9	18.10	25.90	1.50	---	15.2
S6	8.1	17.80	18.50	1.70	1.70	10.0
S7	18.9	8.10	9.60	0.71	0.64	4.8
S8	12.2	4.40	5.20	0.36	0.32	2.6
S9	6.3	3.20	3.70	0.27	0.26	1.9
S10	12.2	1.40	1.50	0.12	0.11	0.8
S11	4.4	0.67	0.74	0.06	0.06	0.4
S12	2.2	0.59	0.59	0.04	0.05	0.3

[a]Autoradiography result not considered.

which is hardly 40 in the case of autoradiography, whereas the other techniques give values in the 330 to 500 range. The behavior of the autoradiographic data can be ascribed to possible saturation characteristics of film fogging. Hence, the autoradiographic results are disregarded and for computing the average activity for each target (given in the last column of Table VII) only the X-ray and beta measurements are taken into consideration.

It may, however, be observed from Table VII that the absolute tritium activities deduced from the titanium X-ray counts (NaI and germanium data) are an order of magnitude higher than those obtained from the beta measurements. To understand this discrepancy, it must be remembered that whereas the X rays originate from the entire bulk of titanium, only the betas emanating from the outermost layers succeed in leaking out and giving counts and current. The formation of a thin oxide layer or loss of tritium from the surface due to evaporation during the aging period could account, at least in part, for the lower absolute activity values given by the beta measurements. In fact, it was observed that the beta to X-ray counts given by an old tritium source were indeed smaller than that given by a tritium target procured ~1 yr ago. Part of this discrepancy can be explained on the basis of possible differences in the depthwise distribution of tritium. In other words, our assumption that the specific tritium activity in the inner layers is the same as that near the surface may not be valid. Hence, while the relative variation of the tritium levels indicated by the average values given in the last column of Table VII is reliable, there is possibly an overall uncertainty to the extent of almost 50% in the absolute tritium values.

Table VIII presents the specific tritium levels in terms of the tritium/deuterium isotopic ratios, taking into consideration the initial deuterium atom loading in the targets. The tritium/deuterium ratios are seen to vary in the 0.07 to 3.5 $\times$ 10^{-4} range. Note that the three older targets indicate higher tritium/deuterium ratios as compared to the other targets, except for target S4, whose absolute tritium content and tritium/deuterium isotopic ratio is the highest among the 12 aged targets.

There does not appear to be any overall correlation between the tritium/deuterium ratios and the deuterium loading of each target given by the deuterium/titanium ratio. However, target S4, which has the maximum tritium level, does happen to have the highest deuterium loading (along with targets S5 and S6).

It is worth pointing out here that the specific tritium activity of the D_2O moderator in a Canada deuterium-uranium power reactor is at most $\simeq$30 Ci/ℓ, corresponding to a tritium/deuterium ratio of $\simeq 10^{-5}$. In practice, however, due to the health hazards involved, the tritium level in the moderator is seldom permitted to exceed ~10 Ci/ℓ, corresponding to tritium-deuterium ratios in the range of 3×10^{-6}. Thus, the tritium-deuterium values of 10^{-5} to 10^{-4} observed in the aged deuterium targets cannot be attributed to the initially loaded D_2 gas having been produced using reactor irradiated heavy water.

It is indeed conceivable that manufacturers of these targets may have carried out the deuterium gas loading using gloveboxes and gas-filling systems used normally for producing tritium targets, resulting in a high level of tritium contamination during the fabrication process. On enquiry regarding this possibility, however, the manufacturers indicated "these targets were not checked for tritium activity before dispatch. However, we would not normally expect to find any traces of tritium." Our discussions with the manufacturers of the BARC targets also indicate that while tritium contamination in the range of a hundred bequerels is in principle a likely possibility, inadvertent tritium contamination of the order of megabequerels is difficult to explain.

We are therefore inclined to speculate that cold fusion reactions over the years could be a plausible explanation for the unexpectedly high tritium levels observed in these 9- to 18-yr-old deuterated titanium targets. Assuming that a typical target containing 10^{20} (*d-d*) pairs supports cold fusion reactions uniformly and continuously over a period of a few years ($\simeq 10^9$ s) producing $\simeq 10^{15}$ tritium atoms, the fusion reaction probability works out to be $\simeq 10^{-14}$ fusion/(*d-d*)/s, which is remarkably close to the value deduced from the BARC electrolysis and D_2-gas-loading experiments.[2]

TABLE VIII

Tritium to Deuterium Isotopic Ratios

Target	Date of Supply of Target	D_2 Gas Loading ($\times 10^{20}$ atom)	Deuterium/Titanium Loading Ratio	Average Tritium Content ($\times 10^{15}$ atom)	Average Tritium/Deuterium Ratio ($\times 10^{-5}$)
S1	January 1972	1.12	0.51	12.2	11.0
S2	February 1975	2.08	1.04	12.1	5.9
S3	February 1975	2.08	0.98	13.3	6.4
S4	April 1981	2.46	1.30	84.8	35.0
S5	April 1981	3.00	1.28	8.5	2.8
S6	April 1981	2.90	1.34	5.6	1.5
S7	September 1981	1.72	1.00	2.6	1.6
S8	September 1981	1.72	1.10	1.4	0.9
S9	September 1981	1.72	0.87	1.1	0.7
S10	September 1981	0.17	0.64	0.5	2.6
S11	September 1981	0.17	0.64	0.3	2.6
S12	September 1981	0.17	0.55	0.2	1.0

If indeed cold fusion reactions are the cause of high tritium levels, then one may argue that even now it could be occurring, in which case the reaction rate would be as high as $\simeq 10^6$ fusion/s. The corresponding neutron production rate would be $\geq 10^{-2}$ n/s, assuming the neutron-to-tritium yield ratio of 10^{-8} as reported in Ref. 2. To verify this, we looked for energetic protons using a surface barrier detector, but without any success. Neither could any neutron production nor any other signature of on-line fusion reactions be observed. Further investigations are continuing.

The main objective of this report is to alert experimentalists in other laboratories who may have in their possession similar "aged" deuterium targets, so that they may also carry out similar investigations to confirm whether they also find high tritium levels and, if so, whether cold fusion could be the root cause.

ACKNOWLEDGMENTS

The authors wish to thank S. S. Kapoor and T. S. Murthy for offering many valuable suggestions and critical comments throughout these investigations, and H. K. Sahoo and P. K. Srivastav for their help in measurements with the 2π beta counter.

REFERENCES

1. A. De NINNO et al., "Evidence of Emission of Neutrons from a Titanium-Deuterium System," *Europhys. Lett.*, **9**, 221 (1989).

2. P. K. IYENGAR, "Cold Fusion Results in BARC Experiments," *Proc. 5th Int. Conf. Emerging Nuclear Energy Systems*, Karlsruhe, FRG, July 3-6, 1989, World Scientific, Singapore (1989).

3. T. N. CLAYTOR, P. A. SEEGER, R. K. ROHWER, D. G. TUGGLE, and W. R. DOTY, "Tritium and Neutron Measurements of a Solid State Cell," *Proc. Workshop Anomalous Effects in Deuterated Materials*, Washington, D.C., 1989.

4. P. K. IYENGAR and M. SRINIVASAN, Eds., "BARC Studies in Cold Fusion," BARC-1500, Bhabha Atomic Research Centre (Dec. 1989).

5. M. LAL, R. K. CHOUDHURY, V. S. RAMAMURTHY, and S. S. KAPOOR, *Bull. Radiation Protection*, **13**, 79 (1990).